Aus der

Klinik und Poliklinik für Psychiatrie und Psychotherapie

Klinikum der Ludwig-Maximilians-Universität München

Interleaved TMS-fMRI of Clinical iTBS Protocols: A Novel Approach to Exploring Dosing and Target Involvement

Dissertation

zum Erwerb des Doctor of Philosophy (Ph.D.)

an der Medizinischen Fakultät

der Ludwig-Maximilians-Universität München

vorgelegt von

Kai-Yen Chang

aus

Taipei / Taiwan

Jahr

2025

Mit Genehmigung der Medizinischen Fakultät der
Ludwig-Maximilians-Universität München

Erstes Gutachten:	Prof. Dr. Frank Padberg
Zweites Gutachten:	Dr. Daniel Keeser
Drittes Gutachten:	Prof. Dr. Sophia Stöcklein
Viertes Gutachten:	Prof. Dr. Olaf Dietrich

Dekan: Prof. Dr. med. Thomas Gudermann

Tag der mündlichen Prüfung: 25.03.2025

Affidavit

LMU LUDWIG-MAXIMILIANS-UNIVERSITÄT MÜNCHEN

Dean's Office Medical Faculty
Faculty of Medicine

Affidavit

Chang, Kai-Yen

Surname, first name

I hereby declare, that the submitted thesis entitled

Interleaved TMS-fMRI of Clinical iTBS Protocols: A Novel Approach to Exploring Dosing and Target Involvement

is my own work. I have only used the sources indicated and have not made unauthorised use of services of a third party. Where the work of others has been quoted or reproduced, the source is always given.

I further declare that the dissertation presented here has not been submitted in the same or similar form to any other institution for the purpose of obtaining an academic degree.

Munich, 11.04.2025
Place, Date

Kai-Yen Chang
Signature doctoral candidate

Confirmation of congruency

LMU LUDWIG-MAXIMILIANS-UNIVERSITÄT MÜNCHEN

Dean's Office Medical Faculty
Doctoral Office

Confirmation of congruency between printed and electronic version of the doctoral thesis

Chang, Kai-Yen

Surname, first name

I hereby declare that the electronic version of the submitted thesis, entitled

Interleaved TMS-fMRI of Clinical iTBS Protocols: A Novel Approach to Exploring Dosing and Target Involvement

is congruent with the printed version both in content and format.

Munich, 11.04.2025

Place, Date

Kai-Yen Chang

Signature doctoral candidate

Table of content

List of abbreviations

BOLD	blood-oxygen-level-dependent
DLPFC	dorsolateral prefrontal cortex
E-field	electric field
EMG	electromyography
fMRI	functional magnetic resonance imaging
HRF	hemodynamic response function
ICA	independent component analysis
M1	primary motor cortex
MDD	major depressive disorder
MT	motor threshold
ROI	region of interest
sgACC	subgenual anterior cingulate cortex
rTMS	repetitive transcranial magnetic stimulation
TMS	transcranial magnetic stimulation
tSNR	temporal signal-to-noise ratio

List of publications

Subject of this PhD thesis

Chang, K. Y*., Tik, M*., Mizutani-Tiebel, Y., Schuler, A. L., Taylor, P., Campana, M., Vogelmann, U., Huber, B., Dechanstreiter, E., Thielscher, A., Bulubas. L., Padberg. F*., Keeser, D*. (2024). Neural response during prefrontal theta burst stimulation: Interleaved TMS-fMRI of full iTBS protocols. *NeuroImage*, 120596. https://doi.org/10.1016/j.neuroimage.2024.120596

Chang, K. Y., Tik, M., Mizutani-Tiebel, Y., Taylor, P., van Hattem, T., Falkai, P., Padberg, F., Bulubas, L*., Keeser, D*. (2024). Dose-Dependent Target Engagement of a Clinical Intermittent Theta Burst Stimulation Protocol: An Interleaved Transcranial Magnetic Stimulation-Functional Magnetic Resonance Imaging Study in Healthy People. *Biological psychiatry. Cognitive neuroscience and neuroimaging*, S2451-9022(24)00244-1. Advance online publication. https://doi.org/10.1016/j.bpsc.2024.08.009

Mizutani-Tiebel, Y., Tik, M., **Chang, K. Y**., Padberg, F., Soldini, A., Wilkinson, Z., Voon, C., Bulubas, L., Windischberger, C., Keeser, D. (2022). Concurrent TMS-fMRI: technical challenges, developments, and overview of previous studies. *Frontiers in Psychiatry*, *13*, 825205. https://doi.org/10.3389/fpsyt.2022.825205

(*these authors contributed equally)

1. Candidate's contribution to the publications

1.1 Paper I – Neural response during prefrontal theta burst stimulation: Interleaved TMS-fMRI of full iTBS protocols

This publication represents a significant milestone for our research group as it showcases our first concurrent TMS-fMRI study (MRstim). The candidate led the initial technical setup and the progressive establishment of concurrent TMS-fMRI for this study, which involved configuring MR-compatible neuronavigation and EMG systems. In collaboration with MT from the University of Vienna, the candidate established the first interleaved iTBS-fMRI sequence at the Department of Psychiatry, University Hospital LMU. Furthermore, the candidate collaborated with YM-T to design the study and collect the pioneering MRstim data using interleaved iTBS-fMRI.

Subsequently, the candidate undertook the preprocessing and analysis of fMRI data, utilizing MT's established automated pipelines for concurrent TMS-fMRI analysis. Additionally, the candidate independently structured the dataset according to the Brain Imaging Data Structure (BIDS) standard, conducted comprehensive MRI quality control, assessed motion and tSNR, and performed visual inspections through various software packages such as SPM, FSL, and MRIQC. Moreover, the candidate also performed E-field simulation analyses using SIMNIBS 4.0, comparing the results with fMRI findings for the final publication.

While preparing the first publication, the candidate regularly discussed the conception and findings of fMRI analysis with MT, FP, LB, and DK. The candidate then drafted the manuscript, created all tables and figures, and incorporated revisions from co-authors. Additionally, the candidate led the submission process and ensured the manuscript complied with all relevant guidelines.

Authorship was shared among the candidate, MT, FP, and DK, acknowledging their significant contributions and intellectual input. The candidate also presented the results of this study at various international and national conferences, sharing and communicating the findings within the scientific community.

1.2 Paper II – Dose-dependent target engagement of a clinical iTBS protocol: An interleaved TMS-fMRI study in healthy subjects

This study expands upon the MRstim dataset by analyzing additional experimental conditions. The candidate developed a novel analysis pipeline by incorporating ICA denoising into the fMRI preprocessing, building upon MT's established TMS-fMRI preprocessing pipelines.

In addition to analyzing each interleaved iTBS-fMRI condition and investigating activation in several ROIs, the candidate also performed correlation analyses between simulated E-field magnitudes and fMRI HRF beta values. This investigation aimed to determine whether E-field magnitude could be a reliable indicator of the BOLD response during TMS.

Throughout the preparation of this second publication, the candidate regularly discussed the conception, interpretation, and analysis of fMRI results with FP, LB, and DK. Subsequently, the candidate independently drafted the manuscript, created all tables and figures with TH, and incorporated co-author revisions. Furthermore, the candidate handled the submission process, ensuring compliance with all relevant guidelines. All authors contributed to revising the manuscript, providing essential intellectual content, and approving the final version. Finally, the candidate presented study results at various international and national conferences, fostering communication within the scientific community.

1.3 Paper III (Appendix) – Concurrent TMS-fMRI: Technical Challenges, Developments, and Overview of Previous Studies

This systematic review offers insights into the methodologies in concurrent TMS-fMRI studies, focusing on the techniques summarized in the first and second MRstim papers. The candidate, AS and YM-T contributed significantly by collecting a complete list of previous concurrent TMS-fMRI studies and categorizing each publication for further discussion and writing.

Moreover, the candidate was pivotal in establishing the first concurrent TMS-fMRI setup at the Department of Psychiatry, University Hospital LMU. Although the significant efforts for this publication were led by YM-T, the candidate's contributions were critical to successfully implementing the study's methodology and subsequent writing.

2. Introductory summary

2.1 Background

2.1.1 Transcranial Magnetic Stimulation (TMS)

Transcranial magnetic stimulation (TMS) stands out as one of the most promising non-invasive brain stimulation techniques, offering safe and well-tolerated treatment options for psychiatric disorders, particularly major depressive disorder (MDD) (O'Reardon et al., 2007). The earliest documentation of electrical stimulation in medical practice dates back to 46 AD when a physician observed the potential pain-relieving effects of electric eels on gout (Tsoucalas et al., 2014). In the 18th century, an Italian scientist observed that a frog's leg twitched when applied to electric stimulation (Cajavilca et al., 2009). Later, Michael Faraday discovered electromagnetic induction, the phenomenon wherein an electric current can be induced in a circuit by changing the magnetic field (Vidal-Dourado et al., 2014). Based on these findings, an English physicist, Anthony Barker, introduced the first modern TMS application in 1985. This breakthrough technology could generate a sufficiently powerful magnetic field to stimulate the human cortex in a contactless and non-invasive manner, thereby inducing contractions in hand muscles through motor cortex stimulation (Barker et al., 1985). Since the end of the 20th century, significant growth has been made in utilizing TMS applications. This expansion results from the increasing number of laboratories using TMS for neuroscientific or therapeutic purposes, aiming to identify optimal paradigms for clinical applications and the potential neural circuit why TMS could improve neuropsychiatry symptoms. Today, standardized application guidelines regarding stimulation parameters, localization of stimulation targets, and subject/patient inclusion and exclusion criteria have been set to ensure the safe use of TMS in both clinical practice and research (Rossi et al., 2009).

There are various significant parameters for TMS, and one of them is the motor threshold (MT), defined as the minimal intensity needed to provoke a response in the hand muscle during stimulation of the primary motor cortex (M1). This measurement assumes that excitability in the non-motor target cortex, such as the dorsolateral prefrontal cortex (DLPFC), is similar to that measured in M1 (Westin et al., 2014); however, there is still insufficient evidence to support this assumption. Nevertheless, MT determination has become the standard method for determining TMS dosage due to its reproducibility and ease of measurement in M1 (Westin et al., 2014). MT can be defined through visual observations or electromyograph (EMG) recording. The former method is popular in clinical settings as it is simpler to measure. It involves determining the minimum TMS intensity at which more than 5 out of 10 stimuli result in observable hand movement (Pridmore et al., 1998). In the EMG method, electrodes are commonly attached over the abductor pollicis brevis (APB) or first dorsal interosseous (FDI) muscle during relaxation, with motor-evoked potentials (MEPs) defined as responses with amplitudes greater than 50 μV and at least 5 out of 10 MEPs surpassing the threshold (Rossini et al., 1994; Boroojerdi et al., 2001; Rossi et al., 2009).

Depending on the research interests, this MT intensity is applied over the DLPFC or other regions, with adjustments normally ranging from 80% to 120% of MT.

Another crucial parameter, the frequency of TMS protocols, is also widely discussed in research and clinical applications. It includes single and paired-pulse TMS, as well as various types of repetitive TMS (rTMS). For instance, the MT measurement mentioned earlier is based on single-pulse TMS, commonly used to investigate brain functioning in time and space (Robertson et al., 2003; Lee et al., 2006; Hoogendam et al., 2010; Klomjai et al., 2015). Conversely, rTMS is believed to induce long-lasting after-effects on brain activity. It is supported by the concept that it can induce plasticity, such as long-term potentiation (LTP) and long-term depression (LTD), with different rTMS protocols (Hoogendam et al., 2010; Klomjai et al., 2015). Consequently, TMS has emerged as an ideal therapy for certain neurological and psychiatric disorders.

2.1.2 rTMS for the treatment of depression

High-frequency 10 Hz rTMS and intermittent theta burst stimulation (iTBS) protocols have been categorized as effective treatments for MDD (Brunoni et al., 2017; Blumberger et al., 2018). ITBS offers the advantage of shorter treatment duration, with a session lasting only 3 minutes and 20 seconds (Huang et al., 2005; Suppa et al., 2016). Our study focuses on the standard clinical iTBS protocol (Figure 1A) with 600 pulses cleared by the FDA for depressive treatment. This protocol involves high-frequency stimulation with 3 pulses at 50 Hz, constituting a theta burst. Each theta burst is repeated with an inter-stimulus interval of 200 ms and delivered for 2 seconds (10 theta bursts with 30 stimuli each), followed by an 8-second pause and repeated 20 times (Huang et al., 2005; Klomjai et al., 2015; Blumberger et al., 2018). On the other hand, 10 Hz rTMS has various protocol paradigms, but the most conventional FDA-approved parameters involve a 4-second stimulus at 10 Hz frequency (Figure 1B), followed by a 26-second pause, repeated 75 times. Each session involves 3000 pulses, with a total duration of 37.5 minutes (O'Reardon et al., 2007; George et al., 2010).

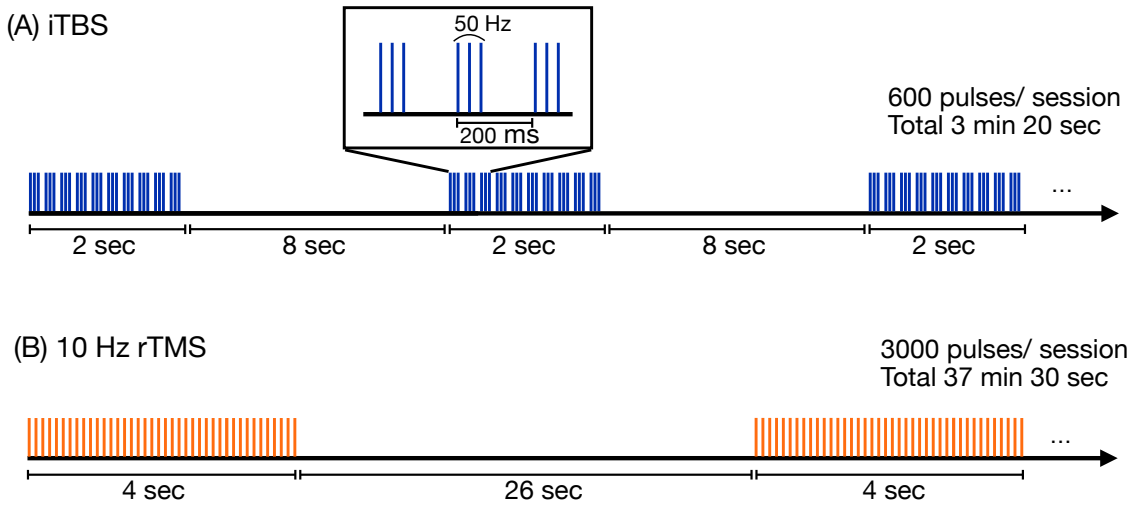

Figure 1. (A) The iTBS protocol consists of high-frequency stimulation with 3 pulses at 50 Hz, forming a theta burst. Each theta burst is repeated every 200 ms and delivered for 2 seconds (30

stimuli), followed by an 8-second pause, and repeated 20 times. Each session includes 600 pulses, with a total duration of 3 minutes and 20 seconds. (B) The FDA-approved 10 Hz rTMS protocol involves 4 seconds of stimulation at 10 Hz, followed by a 26-second pause, repeated 75 times. Each session delivers 3000 pulses, lasting 37 minutes 30 seconds.

Most rTMS treatments for depression have focused on targeting the left DLPFC for treating MDD, as it has been demonstrated to be an effective target for eliciting antidepressant therapeutic effects (George et al., 2010; Fox et al., 2012; Blumberger et al., 2018). Initially, clinical trial studies demonstrated that the 10 Hz rTMS protocol significantly improves symptoms in patients with medication-resistant depression (George et al., 1995; O'Reardon et al., 2007; Padberg & George, 2009). Subsequently, several pilot studies have evaluated the iTBS protocol in MDD and have noted it as a safe and well-tolerated treatment with antidepressant properties (Holzer & Padberg, 2010; Di Lazzaro et al., 2011; Chistyakov et al., 2015). In 2018, Blumberger and colleagues performed a large randomized, multicenter, non-inferiority clinical trial aimed at demonstrating the clinical effectiveness, tolerability, and safety of iTBS compared to the conventional FDA-approved 10 Hz rTMS protocol in adults with medication-resistant depression. Their findings provide evidence that iTBS was non-inferior to 10 Hz rTMS in terms of depressive treatment efficacy, with similar numbers of dropouts and side-effects observed in both groups. Moreover, implementing the shorter iTBS protocol increased efficiency without compromising clinical effectiveness, allowing more patients to be treated daily with current TMS devices (Blumberger et al., 2018).

To enhance TMS treatment efficacy, scientists have sought an optimal neuroimaging biomarker based on resting-state functional connectivity within and between networks to refine TMS targeting. Numerous studies have indicated that symptom reduction of rTMS may be associated with the individual functional connectivity between the prefrontal cortex regions and subgenual anterior cingulate cortex (sgACC) (Baeken et al., 2014, 2017; Liston et al., 2014; Salomons et al., 2014; Tik et al., 2017; Vink et al., 2018; Weigand et al., 2018; Ge et al., 2020; Tura & Goya-Maldonado, 2023). Building upon these findings, a recent accelerated iTBS protocol, Stanford Accelerated Intelligent Neuromodulation Therapy (SAINT), has been developed. SAINT is based on high-dose iTBS and defines individual left DLPFC targeting as selected based on its anticorrelation in functional connectivity with the sgACC region. They delivered a full 5-day course of 90% rMT iTBS, with 10 sessions per day, each consisting of 1800 pulses (3 times of standard iTBS protocol) for a total of 18000 pulses daily, with an inter-session interval of 50 minutes. With this high dose iTBS protocol and DLPFC-sgACC functional connectivity targeting, the SAINT protocol had a remission rate of approximately 90% after 5 days of treatment. Importantly, this protocol was also found to be more effective than the sham stimulation condition (Cole et al., 2020, 2022).

Previous studies have demonstrated the effectiveness of rTMS as a treatment for MDD, but the neural activity mechanisms underlying its therapeutic action remain unclear. The following section will introduce the combination of TMS with neuroimaging, specifically MRI, to investigate brain activity during TMS.

2.1.3 Concurrent TMS-fMRI

Concurrent or interleaved TMS-fMRI (Figure 2) is a promising method for studying the immediate effects of TMS on brain activation and connectivity. The first concurrent TMS-fMRI study, which demonstrated the feasibility of combining TMS and fMRI inside an MR scanner, dates back to 1998. In this study, Bohning and colleagues detected significant blood-oxygen-level-dependent (BOLD) fMRI changes under the TMS coil during M1 stimulation, compared to rest (Bohning et al., 1998). However, since then, the field of concurrent TMS-fMRI has experienced relatively slow growth, with studies often using single TMS pulses, limited rTMS pulses, or low-frequencies (e.g., 1 Hz) rTMS (Nahas et al., 2001; Li et al., 2004; Dowdle et al., 2018; Eshel et al., 2020; Bergmann et al., 2021; Mizutani-Tiebel et al., 2022; Tik, Vasileiadi, et al., 2023; Tik, Woletz, et al., 2023).

Interleaved TMS-fMRI studies have shown that TMS pulses over the DLPFC can induce BOLD signal changes not only in the targeted area but also in contralateral regions, subcortical structures, and the auditory cortex (Hanlon et al., 2013; Dowdle et al., 2018). Previous studies have also established a dose-response relationship between stimulation intensity and BOLD signal changes for both M1 and DLPFC targets (Bestmann et al., 2003, 2004; Navarro de Lara et al., 2017; Tik, Vasileiadi, et al., 2023). They found that using suprathreshold TMS intensities generally leads to higher BOLD activation patterns in the stimulated region and its connected networks (Bohning et al., 1999; Nahas et al., 2001; Navarro de Lara et al., 2017; Tik, Vasileiadi, et al., 2023). In addition, most studies have focused on healthy participants and primarily investigated the M1 (Bergmann et al., 2021; Mizutani-Tiebel et al., 2022). Data from patient cohorts or targeting the DLPFC to investigate the effects of TMS treatment are limited. However, these studies have yet to explore the acute brain response to complete therapeutic rTMS protocols with concurrent TMS-fMRI, presumably due to the restricted numbers of TMS pulses that the MR-compatible TMS coil can deliver. It was not until Chang et al., 2024, that a complete therapeutic rTMS protocol, such as iTBS, was established inside the MRI scanner and investigated across different targets and dosages (Chang, Tik, Mizutani-Tiebel, Taylor, et al., 2024).

One of the primary reasons for this slow progress is the high methodological demands associated with concurrent TMS-fMRI. Specifically, it requires specialized TMS equipment that can be safely used inside the MR scanner and a specially designed multi-channel MR radio frequency (RF) coil to enhance the signal-to-noise ratio (SNR) and provide flexibility in TMS positioning (Navarro de Lara et al., 2015, 2017). Previous studies have frequently faced challenges associated with low temporal SNR due to limitations in the number of channels of bird-cage MR receive coils, various sources of artifacts during TMS-fMRI data acquisition, and a lack of standardized data analysis methods for preprocessing concurrent TMS-fMRI data (Bergmann et al., 2021; Mizutani-Tiebel et al., 2022; Riddle et al., 2022). Despite numerous difficulties in establishing concurrent TMS-fMRI over the past two decades, the progressive maturing of TMS-fMRI technology has attracted many scientists to implement it in clinical research and cognitive neuroscience. Concurrent TMS-fMRI offers several advantages for investigating complex neural connectivity, such as capturing immediate BOLD responses during TMS and assessing functional engagement through cortico-cortical

or cortico-subcortical pathways to remote brain areas (Bergmann et al., 2021). Furthermore, clinical research can gain unique insights by investigating different TMS parameters with concurrent TMS-fMRI, such as TMS targeting, coil orientation, stimulation frequency and intensities. This approach can determine whether target selection or stimulation intensities effectively elicit neural responses at local stimulation sites and remote networks, thereby enhancing the understanding of therapeutic rTMS mechanisms.

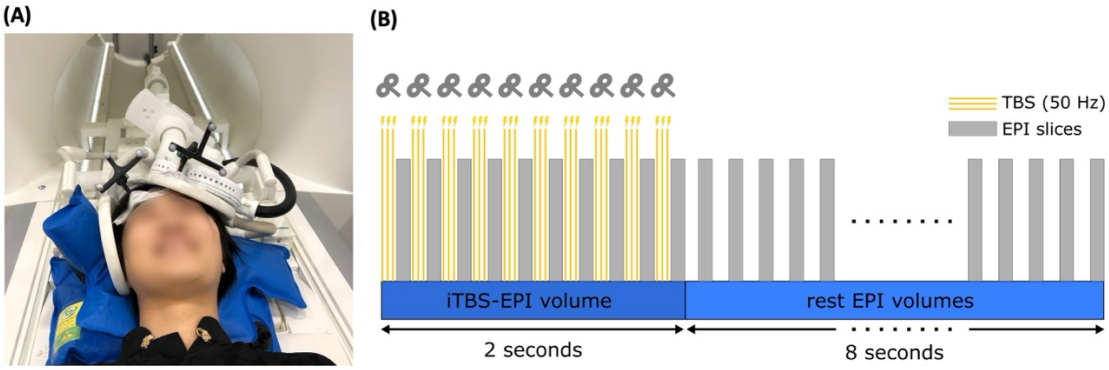

Figure 2. (A) Concurrent TMS-fMRI set-up with a MR-compatible TMS coil, two 7-channel RF coils, and neuronavigation trackers. The MR-compatible TMS coil was mounted on the left RF coil with a holder and vacuum cushion to stabilize two sides of coils. (B) The interleaved iTBS-fMRI sequence consisted of a standard 600 stimuli. A train of iTBS comprised 50 Hz triplets repeated 10 times at 5 Hz over 2 seconds, followed by 8 seconds of rest. This train was repeated 20 times for 3 minutes and 20 seconds, with multiband EPI acquired continuously throughout the stimulation paradigm.

2.2 Hypotheses

Targeting the DLPFC for TMS treatment of MDD has yielded promising outcomes. However, the therapeutic application of TMS involves numerous parameters such as stimulation target, intensity, frequency, and duration. The optimal parameters configuration tailored to each individual for effective treatment still needs to be completed.

Therefore, our study focuses on investigating a specific rTMS protocol – iTBS, which has gained widespread application as an accelerated rTMS protocol (Cole et al., 2020) and has demonstrated efficacy in ameliorating MDD symptoms (Holzer & Padberg, 2010; Blumberger et al., 2018). Given that this was the first investigation of the full 600 pulses iTBS protocol conducted inside an MRI scanner, our goal was to examine the immediate effects of iTBS on cortical activity during stimulation in healthy individuals and a long-term patient with bipolar depression, providing test-retest reliability to assess its potential clinical applicability. In addition, we included three interleaved iTBS-fMRI conditions: 80% rMT iTBS over the left DLPFC, serving as the standard therapeutic protocol; 40% rMT iTBS over the left DLPFC as a low-intensity control; and 80% rMT iTBS over left M1 as an active control at a different target region.

In this project, our primary aim was to assess the feasibility of interleaved TMS-fMRI using full 600 pulses iTBS protocols. Secondly, we aimed to investigate whether varying the intensities and targets of iTBS would induce different patterns of acute changes in neural activation within the stimulated regions and interconnected distant target areas. Thirdly, we sought to explore individual variability in the bilateral DLPFCs in response to low and high iTBS intensities. Lastly, we correlated simulated E-field magnitude with fMRI HRF beta values to assess its potential as an indicator for predicting motor threshold measurement on M1 and transferring it to the DLPFC.

We hypothesized that iTBS would induce acute activation in both the stimulated regions and interconnected distant target areas, with variations based on different intensities and stimulation targets. However, due to various potential sources of inter-individual variability, including factors such as gender, age, brain-state, and technical variability during the TMS-fMRI setup, we expected to experience some degree of variability in BOLD responses among individuals receiving iTBS. Additionally, considering the structural and functional complexity disparities between M1 and DLPFC (Frith & Dolan, 1996; Anderson et al., 2013), it is conceivable that the correlation between the E-field magnitude and fMRI might exhibit different patterns.

2.3 Conclusions

This Ph.D. project aims to demonstrate the feasibility of performing the standard clinical 600 stimuli iTBS with concurrent TMS-fMRI methodology and to understand its immediate neural effects. We observed different neural response patterns in both healthy subjects and a patient undergoing long-term iTBS treatment for bipolar depression. Specifically, in healthy subjects, increased BOLD activation during iTBS was localized to the stimulated target left DLPFC and spread to various connected regions. In the low-intensity 40% rMT DLPFC condition, less BOLD activation was observed in both cortical and subcortical regions, suggesting that decreasing the strength of TMS may influence not only the stimulation target but also remote areas. To delve deeper, we further explored the target effects between M1 and DLPFC using E-field simulations and their correlation with fMRI beta values during iTBS. As expected, only M1 showed a positive correlation between simulation E-field magnitude and fMRI BOLD activation, while no such correlation was observed in the DLPFC conditions, regardless of intensity. Although we noticed a positive trend suggesting that higher stimulation intensity induces higher beta values in the left DLPFC region of interest (ROI), there was significant inter-individual variability in DLPFC responses. Not all healthy subjects demonstrated higher beta values with increased TMS intensity.

The patient with long-term bipolar depression showed considerable intra-individual variability across the four interleaved iTBS-fMRI sessions. The brain regions responding to therapeutic iTBS varied, but a consistent pattern of reduced neural activity during iTBS was observed in all sessions. Several factors, including varying brain states, slight differences in TMS coil positioning, and medication adjustments, likely contributed to these variations. Moreover, our patient differed from our young, healthy control group in age, extensive TMS experience, and long-term pharmacological treatments, which may have influenced neural activity during iTBS. Therefore, further research is

needed to investigate the generalizability of these findings to broader healthy and clinical populations, which is crucial for future studies.

2.4 Perspectives

Our study demonstrated the feasibility of conducting a complete therapeutic iTBS protocol with concurrent TMS-fMRI despite the typical technical challenges in this field. While there is room for improvement in current methodologies, our findings offer valuable insights to guide the future development of clinical rTMS protocols within the scanner.

We also highlighted various inter- and intra-individual variability sources that may influence outcomes in concurrent TMS-fMRI research. Overall, we showed that this approach can enhance understanding of the acute effects of iTBS treatment, revealing dose-dependent target engagement. This methodology holds the potential for identifying neuroimaging biomarkers linked to iTBS therapeutic protocols, laying the groundwork for more personalized treatment strategies.

3. Paper I

Neural response during prefrontal theta burst stimulation: Interleaved TMS-fMRI of full iTBS protocols

NeuroImage 291 (2024) 120596

Contents lists available at ScienceDirect

NeuroImage

journal homepage: www.elsevier.com/locate/ynimg

Neural response during prefrontal theta burst stimulation: Interleaved TMS-fMRI of full iTBS protocols

Kai-Yen Chang [a,b,1], Martin Tik [c,d,1,*], Yuki Mizutani-Tiebel [a,b], Anna-Lisa Schuler [e], Paul Taylor [f], Mattia Campana [a,b], Ulrike Vogelmann [a], Barbara Huber [a], Esther Dechantsreiter [a], Axel Thielscher [g,h], Lucia Bulubas [a,b], Frank Padberg [a,b,1], Daniel Keeser [a,b,1,*]

[a] Department of Psychiatry and Psychotherapy, University Hospital, LMU Munich, Munich, Germany
[b] Neuroimaging Core Unit Munich - NICUM, University Hospital, LMU Munich, Munich, Germany
[c] High Field MR Center, Center for Medical Physics and Biomedical Engineering, Medical University of Vienna, Vienna, Austria
[d] Brain Stimulation Lab, Department of Psychiatry and Behavioral Sciences, Stanford University, Stanford, USA
[e] Lise Meitner Research Group Cognition and Plasticity, Max Planck Institute for Human Cognitive and Brain Sciences, Leipzig, Germany
[f] Department of Psychology, LMU Munich, Munich, Germany
[g] Department of Health Technology, Technical University of Denmark, Kgs. Lyngby, Denmark
[h] Danish Research Centre for Magnetic Resonance, Centre for Functional and Diagnostic Imaging and Research, Copenhagen University Hospital Amager and Hvidovre, Denmark

ARTICLE INFO

Keywords:
Functional MRI (fMRI)
Transcranial magnetic stimulation (TMS)
Concurrent TMS-fMRI
Interleaved iTBS-fMRI
Non-invasive brain stimulation
Neuromodulation

ABSTRACT

Background: Left prefrontal intermittent theta-burst stimulation (iTBS) has emerged as a safe and effective transcranial magnetic stimulation (TMS) treatment protocol in depression. Though network effects after iTBS have been widely studied, the deeper mechanistic understanding of target engagement is still at its beginning. Here, we investigate the feasibility of a novel integrated TMS-fMRI setup and accelerated echo planar imaging protocol to directly observe the immediate effects of full iTBS treatment sessions.

Objective/hypothesis: In our effort to explore interleaved iTBS-fMRI feasibility, we hypothesize that TMS will induce acute BOLD signal changes in both the stimulated area and interconnected neural regions.

Methods: Concurrent TMS-fMRI with full sessions of neuronavigated iTBS (i.e. 600 pulses) of the left dorsolateral prefrontal cortex (DLPFC) was investigated in 18 healthy participants. In addition, we conducted four TMS-fMRI sessions in a single patient on long-term maintenance iTBS for bipolar depression to test the transfer to clinical cases.

Results: Concurrent TMS-fMRI was feasible for iTBS sequences with 600 pulses. During interleaved iTBS-fMRI, an increase of the BOLD signal was observed in a network including bilateral DLPFC regions. In the clinical case, a reduced BOLD response was found in the left DLPFC and the subgenual anterior cingulate cortex, with high variability across individual sessions.

Conclusions: Full iTBS sessions as applied for the treatment of depressive disorders can be established in the interleaved iTBS-fMRI paradigm. In the future, this experimental approach could be valuable in clinical samples, for demonstrating target engagement by iTBS protocols and investigating their mechanisms of therapeutic action.

1. Introduction

In the field of non-invasive brain stimulation (NIBS) techniques, repetitive transcranial magnetic stimulation (rTMS) of the dorsolateral prefrontal cortex (DLPFC) has been developed into an effective treatment for depressive disorders (Brunoni et al., 2017; Kan et al., 2023). Intermittent theta-burst stimulation (iTBS) is a variant of rTMS and was originally introduced for motor cortex stimulation based on its capacity for inducing long-term potentiation-like plasticity effects through a coupling between gamma (circa 50 Hz) and theta rhythms (circa 5 Hz). More recently, iTBS has been applied over prefrontal cortex regions and established as therapeutic intervention for people with depressive

* Corresponding authors at: Department of Psychiatry and Psychotherapy, University Hospital, LMU Munich, Munich, Germany.
E-mail addresses: mtik@stanford.edu (M. Tik), daniel.keeser@med.uni-muenchen.de (D. Keeser).
[1] Contributed equally

https://doi.org/10.1016/j.neuroimage.2024.120596
Received 13 November 2023; Received in revised form 25 March 2024; Accepted 28 March 2024
Available online 29 March 2024

disorders (Grossheinrich et al., ; Huang et al., 2005; Suppa et al., 2016). Besides its potential superiority in inducing plasticity effects (Hermiller et al., 2020), iTBS has the clear advantage of shorter treatment duration, i.e. 3 min and 20 s as compared to 37.5 min for the standard 10 Hz protocol (Blumberger et al., 2018), and can easily be repeated in accelerated iTBS protocols (Cole et al., 2020).

Previous rTMS studies have shown changes in functional MRI connectivity within and between brain networks in MDD, and symptom reduction has been associated with individual connectivity patterns, e.g. with functional connectivity between subgenual anterior cingulate cortex (sgACC) and prefrontal cortex regions (Salomons et al., 2014; Liston et al., 2014; Baeken et al., 2014; Baeken et al., 2017; Tik et al., 2017; Vink et al., 2018; Weigand et al., 2018; Ge et al., 2020; Tura and Goya-Maldonado, 2023). However, disentangling mechanistic effects of rTMS protocols at the cortex level from non-specific network modulation due to auditory and somatosensory artefacts as well as intra-individual changes of brain states is challenging and demonstration of causality and target engagement difficult to achieve (Siebner et al., 2022). To fill this knowledge gap, researchers have combined magnetic resonance imaging (MRI) with TMS to investigate the immediate blood-oxygen-level-dependent (BOLD) response caused by TMS, a technique commonly known as combined or concurrent TMS-fMRI (Bohning et al., 1998; Bergmann et al., 2021; Mizutani-Tiebel et al., 2022). The first publication on combined TMS-fMRI was more than 20 years ago, but the field has shown relatively slow growth since (Bohning et al., 1998; Bohning et al., 1999), which may have been due to technical constraints. Early concurrent TMS-fMRI setups showed low signal-to-noise-ratio (SNR) and TMS-induced artifacts during fMRI acquisition (Bergmann et al., 2021; Mizutani-Tiebel et al., 2022; Riddle et al., 2022). As a result, only a few prior studies have explored the effects of rTMS on the left DLPFC (Vink et al., 2018; Hanlon et al., 2013; Li et al., 2004; Hawco et al., 2017; Oathes et al., 2021; Tik et al., 2023a,b; Nahas et al., 2001). Importantly, previous concurrent TMS-fMRI studies have investigated short rTMS sequences, but not full iTBS protocols (e.g. 600 pulses) as originally reported (Huang et al., 2005).

Given that iTBS protocols are used for clinical treatment of depressive disorders and other psychiatric conditions (Kan et al., 2023), there is a strong research interest in the acute effects of such protocols in health and disease. Thus, the main focus of the current study was the feasibility of interleaved iTBS-fMRI within an integrated TMS-fMRI setup and accelerated echo planar imaging (EPI) protocol. Our hypothesis was that iTBS leads to acute changes of BOLD signal in the iTBS target area as well as in interconnected regions. In order to investigate feasibility in a clinical context, we additionally applied our approach in a patient with bipolar depression during long-term iTBS maintenance treatment at four different time points.

2. Methods & materials

2.1. Samples

2.1.1. Healthy participants

We recruited 27 healthy right-handed adult participants who met the usual MRI and TMS inclusion criteria (incl. no history of psychiatric or neurological conditions). Six subjects dropped out after the baseline session due to high resting motor thresholds (rMT), DLPFC stimulation intolerance (after TMS test pulses), or incidental findings in the brain. Additionally, 2 subjects dropped out during the interleaved TMS-fMRI sessions due to either personal reasons and or the implantation of a new medical device. Finally, 19 participants completed all four sessions of the experiment (8 females, 11 males; ages 21–36 years, average age = 26.4 years, standard deviation = 3.2 years). All participants signed written informed consent approved by the LMU ethical committee in accordance with the Declaration of Helsinki.

2.1.2. Patient with bipolar depression

We recruited a 59-year-old male patient who has been undergoing long-term maintenance treatment at our department for recurrent major depressive episodes in bipolar disorder. The patient was first admitted to a psychiatric ward at the age of 24 (1986), and over the next 20 years, 5 further inpatient stays followed. He was finally diagnosed with bipolar disorder with predominantly depressive episodes. In 2009, after most available treatment options had failed, TMS treatment was offered to the patient, within a series of the first clinical iTBS applications in patients with depressive episodes (Holzer and Padberg, 2010). Following the start of iTBS, in addition to the continuation of the patient's medication and regular outpatient visits, the severity of symptoms decreased and no further inpatient treatment has been required since. However, minor to medium, rarely severe, depressive and occasionally hypomanic symptoms have occurred over the years, so that the maintenance iTBS treatment could not be phased out fully and was maintained at a varying frequency of 1–3 times per week, adapted to patient condition. To date, the patient has received almost 1500 rTMS sessions. He participated in 4 interleaved iTBS-fMRI treatment sessions, conceived as an initial exploration into the topic of test-retest reliability in a single-subject. The patient met the criteria for the TMS and MRI safety check and also participated in a baseline session before undergoing the concurrent TMS-fMRI. During the concurrent TMS-fMRI, the patient received 80% rMT stimulation of the DLPFC.

2.2. Experimental setup

For this study, all participants were requested to complete at least two experimental sessions. These sessions included a baseline assessment and an interleaved iTBS-fMRI 80% rMT DLPFC session, with a minimum of one week between each session. During the baseline session, participants were required to provide written informed consent and subsequently underwent structural and functional MRI scans for neuronavigation, rMT measurement inside the MR scanner, and test stimulation over the left DLPFC with 80% rMT intensity to assess their ability to tolerate discomfort caused by TMS. The second session involved a concurrent TMS-fMRI session. Photos illustrating an example of our TMS-fMRI setup are available in Mizutani-Tiebel et al. (2022) and Fig. 1C.

2.2.1. Magnetic resonance imaging

In the baseline session, we collected structural MRI and resting-state functional MRI (rsfMRI) using a 3T Siemens PRISMA scanner (Siemens, Erlangen, Germany) with a standard 64-channel head/neck coil. Structural images were acquired using a T1-weighted MPRAGE (Magnetization-Prepared Rapid Acquisition with Gradient Echo) sequence (TR = 2300 ms; TE = 2.26 ms; TI = 900 ms; flip angle = 8°; voxel size 1 × 1 × 1 mm; 256 mm FOV; number of slices = 192; scan duration 5 min 21 s), and a T2-weighted SPACE (Sampling Perfection with Application-optimized Contrasts) sequence (TR = 5000 ms; TE = 383 ms; TI =1800 ms; voxel size 1 × 1 × 1 mm; 256 mm FOV; number of slices = 176; scan duration 4 min 57 s).

2.2.2. Concurrent TMS-fMRI

For concurrent TMS-fMRI, an integrated system with two 7-channel surface RF coils (Navarro de Lara et al., 2015) and an MR-compatible TMS set-up (MagVenture A/S, Farum, Denmark). One RF coil was mounted with the TMS coil, while the other was placed over the contralateral hemisphere to ensure complete brain coverage. An MP2RAGE sequence (TR = 4000 ms, TE = 2.98 ms, TI1/TI2 = 700/2500 ms, flip angle 1/flip angle 2 = 4° / 5°, 160 slices, 1 mm slice thickness), was used to perform a structural scan in the concurrent TMS-fMRI sessions (Marques et al., 2010).

Interleaved iTBS-fMRI was performed continuously for 3 min and 32 s (12 s dummy scan included), using a multiband EPI sequence with an MB-factor of 4, TR = 2000 ms, TE = 30 ms, 40 slices, and voxel size of

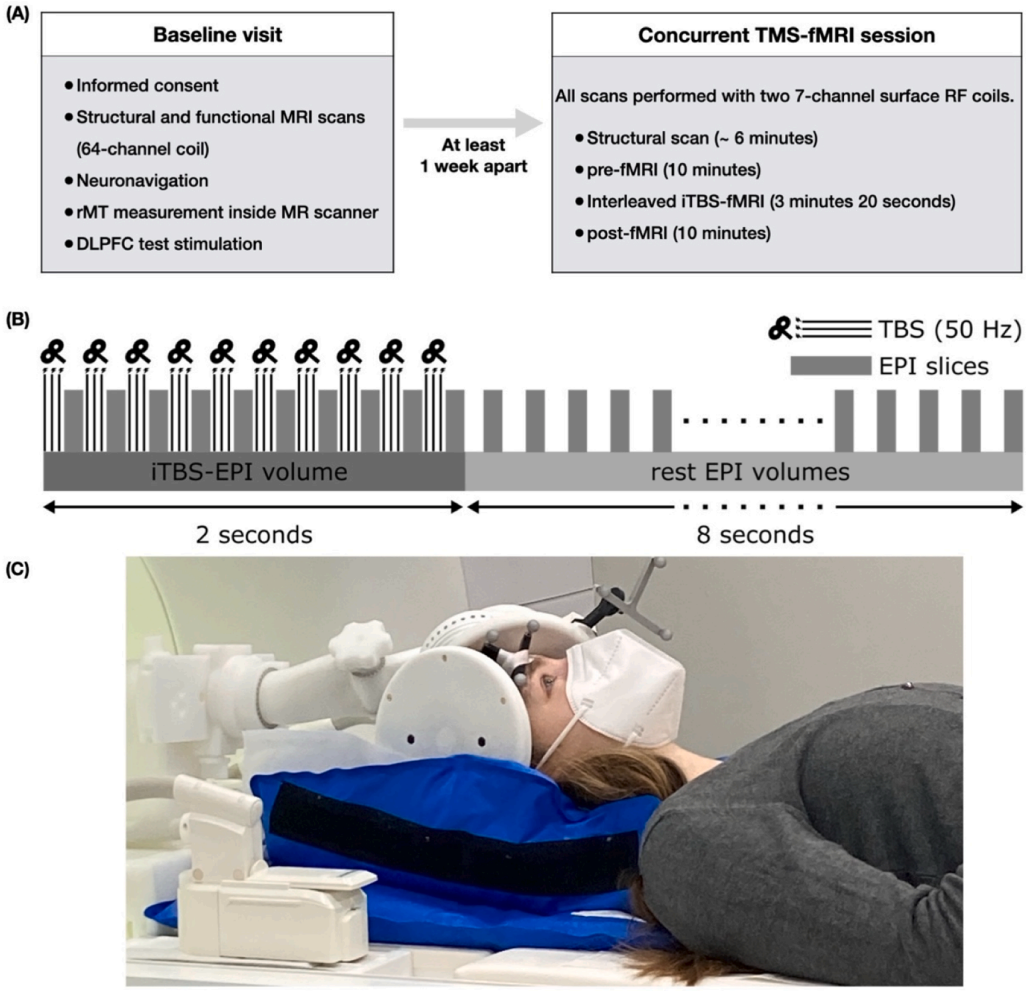

Fig. 1. (A)The experiment protocol on the baseline visit and concurrent TMS-fMRI session. (B)The interleaved iTBS-fMRI sequence. The standard clinical iTBS consisted of 50 Hz triplets repeated 10 times at 5 Hz over 2 s, followed by 8 s of rest. The train was repeated 20 times. EPIs were acquired continuously throughout the stimulation paradigm. (C)Concurrent TMS-fMRI set-up with two 7-channel surface RF coils positioned over the left and right anterior hemisphere. The MR-compatible TMS coil was mounted on top of the left RF coil and positioned over the stimulation target (left DLPFC). The mask was exclusively worn during the photo session.

3.3 × 3.3 × 3 mm. This protocol matches standard clinical iTBS protocols and consists of 50 Hz triplets repeated 10 times (at 5 Hz) within 2 s (Huang et al., 2005; Suppa et al., 2016), followed by 8 s inter train interval.

2.2.3. Neuronavigation

T1-weighted images from the baseline session (see above) were used for MR-compatible neuronavigation (Localite GmbH, Bonn, Germany) with a Polaris Vega camera (NDI, Waterloo, Canada) to target the left DLPFC. The left DLPFC target was determined using MNI (x,y,z) coordinates of −38, 44, 26 with the coil rotated at a 45° angle to midline. This targeting approach has been demonstrated to be clinically effective, safe, and as well-tolerated in iTBS as standard 10 Hz rTMS treatment of patients with treatment-resistant depression (Blumberger et al., 2018). To replicate the typical clinical setting, the clinical case utilized an EEG cap with 5 cm rules to locate the left DLPFC position (George et al., 1995), and stimulation location was recorded with neuronavigation.

2.2.4. TMS

All TMS was performed inside the MRI scanner room using an MRi-B91 MR-compatible TMS coil and MagProX100 stimulator (MagVenture A/S, Farum, Denmark). Biphasic pulses were used with a duration of approximately 290 μs. Maximum machine output is 180 A/μs (di/dt).

A 7-channel surface RF coil (Navarro de Lara et al., 2015) was mounted to the TMS coil throughout our concurrent TMS-fMRI sessions and motor threshold determination, which increased the distance between the TMS coil and skull, resulting in higher thresholds than usual. For motor threshold determination, participants were positioned lying down, and their hands relaxed on the MR scanner bed, using an MR-compatible electromyography (EMG) recorder (Brain Product, Gilching, Germany). EMG electrodes were attached over the right abductor pollicis brevis (APB), and a ground electrode was placed over the right ankle. Suprathreshold motor-evoked potentials (MEP) were defined as responses with amplitudes greater than 50 μV within 15 and 35 ms after each TMS pulse. The TMS intensity was reduced in steps of 2% of the stimulator output until such MEP responses were absent in 5 out of 10 trials.

2.2.5. MRI data preprocessing

Preprocessing was performed as described in Tik et al. (2023a) using Matlab, SPM12, AFNI and ANTS transformation of EPIs into MNI space (cat12) and spatial smoothing with a 6 mm FWHM Gaussian kernel (SPM12).

2.2.6. Statistical analyses

Both single-subject and group-level analyses were performed using SPM12. One subject was excluded due to showing excessive motion (more than 3 mm). For single-subject (first-level) analysis linear regression was performed on each voxel using generalized least squares with a global approximate AR (Brunoni et al., 2017) autocorrelation model and high-pass filter with a cutoff of 128 s. The regressors were 2-second blocks of theta burst volleys. The beta (β) map from first-level (theta burst block) generalized linear model (GLM) analyses were used for the group analysis in SPM12, performed with linear regression on each voxel and one-sample *t*-tests. Resulting single-subject beta map estimates of BOLD responses were used for group analyses. Linear regression was performed at each voxel, using generalized least squares with a global repeated measures correlation model.

2.2.7. E-field simulation

We utilized SimNIBS 4.0 (https://simnibs.github.io/simnibs/build/html/index.html), a free software package designed for electric field modeling in NIBS such as TMS. Prior to conducting the E-field simulation, it was necessary to generate a volume conductor model of each subject's head. This was accomplished using "charm", which uses anatomical MRI images (T1-weighted & T2-weighted) acquired from the baseline session. For the simulation of DLPFC TMS, we specified the MRi-B91 TMS coil file and set the stimulation intensity to the di/dt value recorded from the TMS stimulator during the iTBS protocol at 80% rMT for each subject. The first TMS marker saved during neuronavigation provided the location and orientation of the TMS coil.

The group-level analysis of peak electric field magnitude and focality included a total of 16 subjects from the MRI data analysis, because two subjects did not have TMS markers recorded during neuronavigation.

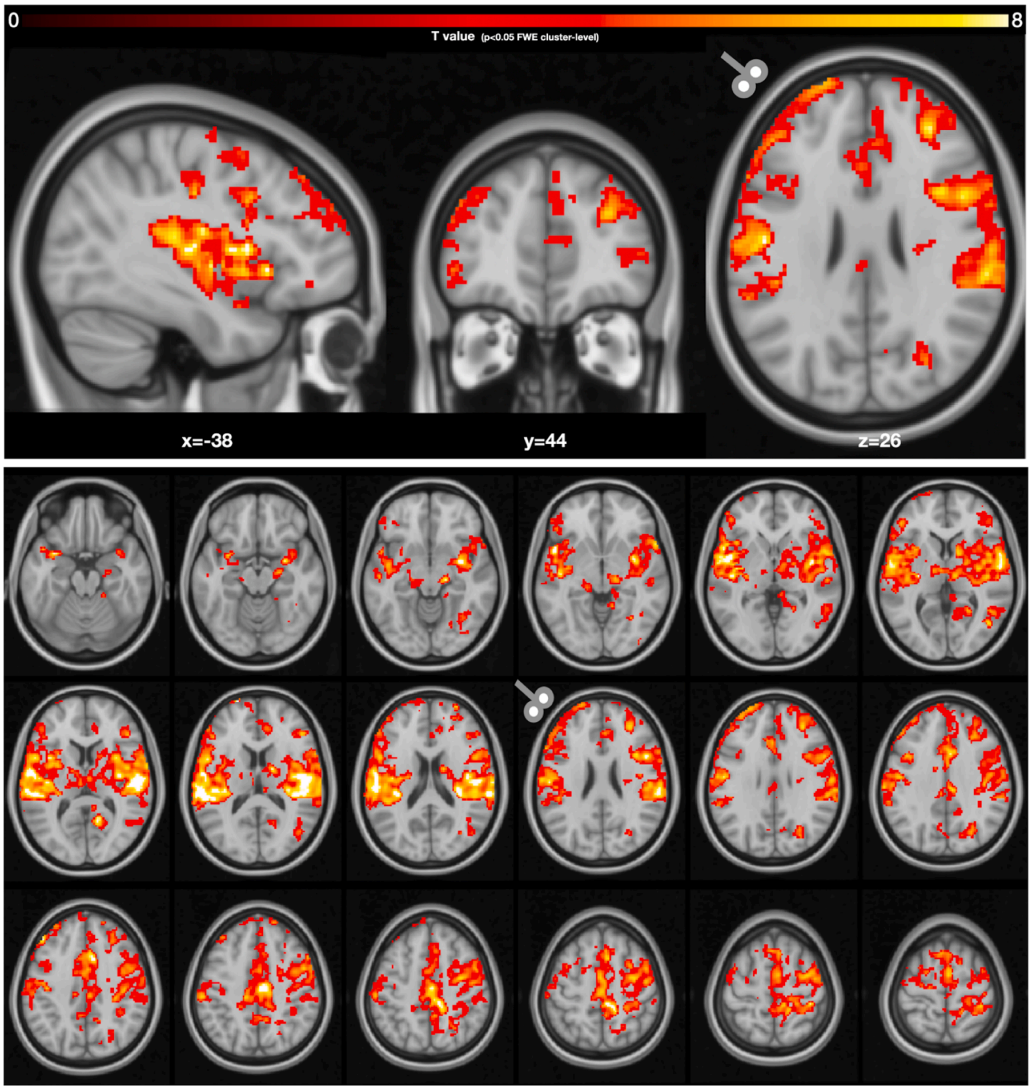

Fig. 2. Acute BOLD changes during interleaved iTBS-fMRI in healthy subjects. A full iTBS protocol (i.e. 600 pulses) resulted in increased brain activation, bilaterally in the DLPFC and auditory cortex regions as well as the right superior frontal gyrus.

We visualized the group results by transforming the individual simulation results from native space to MNI space in order to present the group peak electric field (Saturnino et al., 2019).

3. Results

3.1. Healthy controls

Mean rMT was 83% (sd = 12%) of maximum stimulator output, corresponding to the recorded dI/dt of 120 A/μs (sd = 19.1 A/μs). Note that the effective stimulation intensity is lower in the TMS-fMRI set-up compared to standard TMS settings because of several factors: (a) the cable length, (b) the hardware for suppressing leakages, and (c) an increased coil-to-brain distance due to the RF coil, where the TMS coil is mounted on.

Subjects were asked to self-report their pain levels during and after the TMS sessions (see Supplementary Fig. S1). This result suggests that the interleaved iTBS-fMRI procedure was generally tolerable, as the reported pain levels were tolerable, with a reasonable degree of variability among the participants.

3.1.1. Immediate BOLD changes during interleaved iTBS-fMRI in healthy subjects

As shown in Fig. 2 and Table 1, iTBS resulted in increased brain activation in the bilateral DLPFC (left DLPFC peak at −20, 68, 14 mm MNI, t = 10.3; right DLPFC peak at 32, 42, 26 mm MNI, t = 7.74), bilateral auditory cortex consistent with perception of the sound of TMS (left temporal region peak at −56, −8, 8 mm MNI, t = 12.3; right temporal region peak at 48, −12, 14 mm MNI, t = 12.3), and right superior frontal gyrus (28, 62, 18 mm MNI, t = 6.87).

3.1.2. Group results of SimNIBS based e-field models

We compared the patterns of BOLD response to interleaved iTBS-fMRI with the intensity and distribution of the iTBS induced electric field (e-field) (Fig. 3). Although the e-field was distributed around the primary target region, i.e. the left DLPFC, there was significant variability in positioning, attributable to variation in individual anatomy. Note that this simulation only models the acute effect of TMS on tissue and not any spreading across synapses to other brain areas.

3.2. Clinical case

3.2.1. Clinical information

During study participation, the patient continued his long-term medication (i.e. 20 (mornings) / 0 (evenings) mg citalopram, 25 / 250 mg quetiapine IR, 0 / 200 mg quetiapine XR, 300 / 300 mg pregabalin, and 100 / 200 mg lamotrigine daily, with additional 25 mg of quetiapine and 0,25 mg lorazepam to be taken as needed, on average twice per week). The interleaved iTBS-fMRI sessions were consistently conducted in the early afternoon, ensuring a consistent time gap between MRI scans and medication administration. Depression questionnaires (Hamilton rating scale for depression, Montgomery–Åsberg Depression Rating Scale) are being collected as part of the standard care of the patient and suggested mild depressive symptoms during study participation (HAMD 9–12, MADRS 9–10). While the clinical symptoms remained stable at less severe levels throughout our investigations, the patient underwent subtle mood changes from his bipolar disorder which resulted in dosage adaptations by the patient himself (i.e. citalopram increased at visit 4, lorazepam discontinued after visit 2). The patient was able to participate in the TMS-fMRI experiment without any adverse events.

Table 1
Peak BOLD activation results during interleaved iTBS-fMRI.

Peak activation during interleaved iTBS-fMRI						
Area	peak MNI (mm)			cluster size	t-value	Z
Left dorsolateral prefrontal region	−20	68	14	34,033	10.03	5.66
Left temporal region	−56	−8	8		12.3	6.17
Right temporal region	48	−12	14		14.52	6.52
Right dorsolateral prefrontal region	32	42	26	1036	7.74	5.00
Right superior frontal region	28	62	18		6.87	4.69

3.2.2. Interleaved iTBS-fMRI: results of a clinical case study

MRI quality control (see Supplementary Fig. S3) and visual inspection were performed before data analysis, and we had to exclude the results from the third session due to strong ghosting artifacts. We found considerable variance in activation pattern over the three sessions: During the first session, we found a statistically significant reduction of BOLD response in the left DLPFC region (peak at −24, 44, 38 mm MNI, t = −6.5) located at the stimulation site. In the second session, a significant BOLD reduction was observed in the sgACC region (peak at 6, 16, −14 mm MNI, t = −13.08). In the fourth session, we did not observe any statistically significant BOLD changes in the left DLPFC or sgACC regions.

4. Discussion

4.1. Feasibility of interleaved TMS-fMRI with full clinical iTBS protocols

This study shows that interleaved TMS-fMRI can be applied with 600 pulses of iTBS (Huang et al., 2005) as originally reported by Huang et al. (Huang et al., 2005) and clinically used for the treatment of depressive disorders (Holzer and Padberg, 2010; Blumberger et al., 2018). In addition, test-retest TMS-fMRI sessions were conducted in a single patient with a bipolar depression in order to test the transfer of this paradigm in a clinical case.

Previous concurrent TMS-fMRI studies have only used much shorter sequences of rTMS, e.g. TBS with 30 pulses in 2 s (Hermiller et al., 2020), but not full rTMS treatment protocols, due to restrictions from coil capacity and cooling in TMS-fMRI setting (see reviews by (Bergmann et al., 2021; Mizutani-Tiebel et al., 2022)). However, concurrent TMS-fMRI represents a promising approach in specialized settings for investigating effects of iTBS and other protocols, and allows studying acute and short-term effects of iTBS on regional BOLD activation and connectivity. None of the participants reported any adverse effects during or after the experiment, indicating a generally safe and well-tolerated procedure.

4.2. Neural response to iTBS in healthy individuals

In healthy subjects, we observed an increase in BOLD signals during iTBS (600 pulses) of the left DLPFC in several regions, including the bilateral DLPFC, bilateral auditory cortex, and contralateral frontal areas beyond DLPFC regions (Fig. 2). In contrast, the majority of previous concurrent TMS-fMRI studies has primarily used low-frequency (e.g., 1 Hz) rTMS, or single TMS pulses, or only applied high frequency protocols with a low number of pulses delivered (Nahas et al., 2001; Li et al., 2004; Dowdle et al., 2018; Eshel et al., 2020; M Tik et al., 2023; M Tik et al., 2023). Furthermore, most of these studies used suprathreshold intensity during TMS, and it has generally been observed that higher TMS intensity result in greater BOLD activation underneath the coil compared to subthreshold intensities (Bohning et al., 1999; M Tik et al., 2023; Nahas et al., 2001; Navarro de Lara et al., 2017). Despite utilizing an iTBS protocol at 80% rMT intensity, i.e. a protocol very close to the original iTBS protocol by Huang et al. (Huang et al., 2005), our study still yielded significant BOLD activations in both directly stimulated and remote areas. However, it is important to note that we observed changes in BOLD activation only in cortical, but not in subcortical regions. This finding differs from those of other TMS-fMRI studies targeting the left DLPFC, which also observed BOLD changes in subcortical regions, e.g.

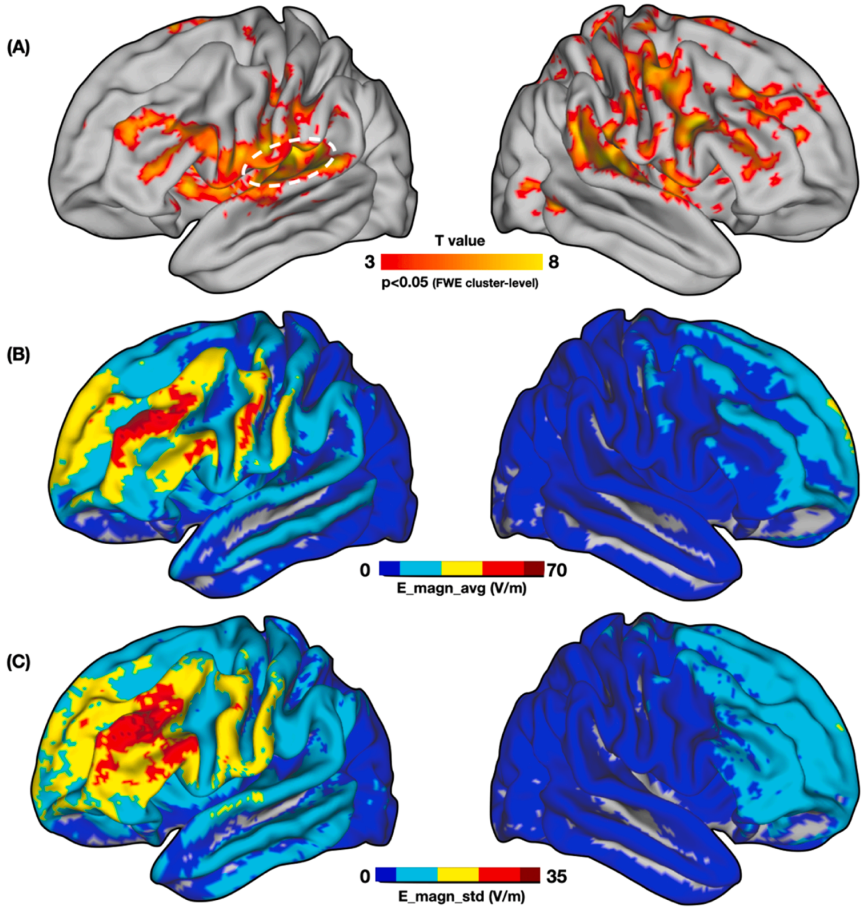

Fig. 3. (A) Acute BOLD changes during iTBS (i.e. 600 pulses) in the healthy control group. Auditory cortex activation is represented by the marked white dashed line. (B) E-field simulation group average peak electric field magnitude and focality in 16 subjects. (C) E-field simulation group standard deviation in magnitude value in 16 subjects.

sgACC (Vink et al., 2018; Hanlon et al., 2013; Oathes et al., 2021); however, Vink et al. (2018) noted that only half of their sample showed this activation pattern. This heterogeneity in findings may be attributed to several factors, such as different TMS and fMRI protocols, and the two RF coils used in this study, which were attached at the left and right frontal regions. This configuration may have resulted in limited tSNR in the subcortical and occipital regions (Supplementary Fig. S4). We believe that incorporating a third RF coil, particularly to cover the occipital region, could potentially enhance the tSNR across the whole brain.

Moreover, it is important to highlight that changes in BOLD activation in healthy subjects were not confined to the iTBS target region (i.e. the left DLPFC), but rather spread to other prefrontal areas. This distribution may be compared with our e-field modeling results, which also indicated non-focal DLPFC stimulation, which may be influenced by variability in DLPFC targeting. To analyze the change of BOLD activation over the course of an iTBS session, we conducted an investigation wherein the complete 20 iTBS trains were divided into four blocks, each consisting of 5 trains of iTBS (equivalent to 150 stimuli). Interestingly, in the initial block, the left stimulated DLPFC did not exhibit strong BOLD activation at the stimulated location, as the number of iTBS stimuli increased, we observed a cumulative effect, resulting in stronger BOLD activation in the left prefrontal region (see Supplementary Fig. S5). Given that this is the first complete iTBS protocol conducted inside MRI, our primary aim was to present the most straightforward and comprehensible analyses. We therefore provide fMRI results with minimal data preprocessing. However, it is important to mention that previous research has suggested the necessity of including independent component analysis (ICA) denoising in the preprocessing pipeline for concurrent TMS-fMRI data. The rationale behind this recommendation is that the TMS coil can induce vibrations and leakage currents, and these effects can persist for up to 8 s after TMS (Riddle et al., 2022). ICA analysis may be better at eliminating these and other artifacts, but at the cost that ICA may also eliminate biologically relevant information.

4.3. Neural response across three TMS-fMRI sessions in a single patient with bipolar depression

In a further step, we applied the concurrent TMS-fMRI protocol with full 600 pulse iTBS sessions in a patient who has undergone long-term iTBS treatment for bipolar depression. In a clinical setting, this approach allows monitoring the effects of iTBS on a patient during maintenance treatment. Despite the patient's prior experience with TMS, remaining inside the MRI for over thirty minutes posed a challenge and resulted in increased motion compared to healthy controls. We initially conducted quality control measures on motion, temporal signal to noise ratio (tSNR) calculation, and visual inspection (see supplementary materials). We noted that the third session showed strong

ghosting artifacts, and this dataset was consequently excluded from further analysis. Across the remaining three sessions, we observed a high degree of inter-session variability in BOLD effects. For example, we found reduced neural activity in the stimulated area, the left DLPFC (Fig. 4), during the first session. There are several possible reasons for this variability, e.g. intra-individual variation of brain states or differences in coil position/orientation in relation to target regions, i.e. DLPFC and interconnected sgACC areas (Fox et al., 2012; Fox et al., 2013; Dunlop et al., 2017; Weigand et al., 2018; Cash et al., 2019). Importantly, the distance between the TMS coil and the cortex was variable across sessions, which could have been due to differences in coil positioning; i.e. the coil-to-cortex distance was larger in the first (37 mm) and second (38 mm) sessions, while it was reduced in the third (25 mm) and fourth (28 mm) sessions. Taken together, we acknowledge that there are (at least) four of sources of variability in the measurement of target engagement with TMS-fMRI which are essential for future studies to investigate: (Brunoni et al., 2017) fluctuations in the tSNR; (Kan et al., 2023) variations in the coil position and hence distance between TMS coil and cortex; (Grossheinrich et al.,) intrinsic spontaneous fluctuation in resting functional connectivity between sessions; and (Huang et al., 2005) the subjectś psychopathological status (i.e. healthy volunteers or patient population).

4.4. Limitations

While piloting this approach, our study does not allow the interpretation of BOLD signal changes as being specific to iTBS of the DLPFC, as auditory and somatosensory effects were not controlled for in our experiment, and could significantly contribute to large scale network activation (Siebner et al., 2019), for example through activating auditory cortex. Additionally, our experiment lacks sham iTBS or other active sites for comparison. Including a sham or other active site

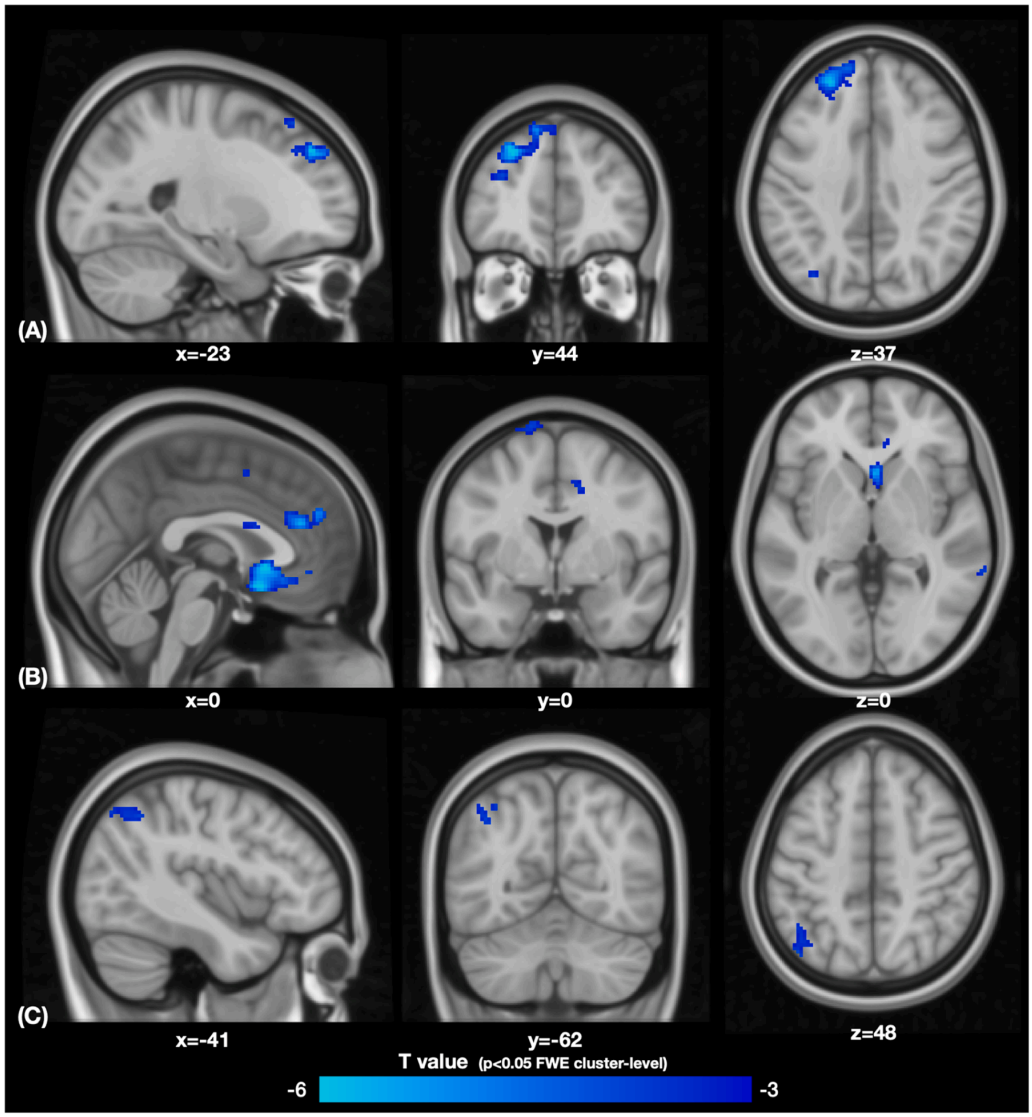

Fig. 4. Acute BOLD changes in a patient with bipolar depression. (A) First session: Negative BOLD response in the left DLPFC during iTBS. (B) Second session: Negative BOLD response in the sgACC during iTBS (C) Fourth session: No statistically significant BOLD changes in the DLPFC or sgACC. The third session was not included in the analysis due to strong ghosting artifacts.

condition is crucial for disentangling the effects of cortex stimulation from peripheral sensory or auditory effects of TMS and other non-specific sources (e.g., parameters of the experimental setting) (Siebner et al., 2022). It is essential to note that implementing a sham control in concurrent TMS-fMRI studies poses inherent challenges. Although future should always consider sham conditions as controls, TMS sham controls are far from ideal (Duecker and Sack, 2015), particularly in the concurrent TMS-fMRI field. To address this limitation, we performed e-field simulations to simulate the potential TMS effect over the left DLPFC, resulting in a similar pattern of the BOLD activation. Thirdly, while our design notably deviates from the Food and Drug Administration approved iTBS treatment protocol at 120% rMT (Blumberger et al., 2018), several other trials suggest that iTBS at the 80% rMT poses an effective strategy for treating MDD (Bulteau et al., 2022). Due to increased pain levels at higher stimulation intensities, we decided to apply the lower intensity in this feasibility study. Fourthly, MR imaging coils used for concurrent TMS-fMRI studies have fewer channels (i.e. two 7-channel coils) than standard MR head coils (i.e. 64-channel coils), which may affect the accuracy and reliability of TMS-fMRI BOLD signal measurements, especially in the deep subcortical regions. Additionally, while facing challenges such as a complicated technical setup, a large amount of experimental time, and personnel requirements, the sample size of our TMS-fMRI study is small, and we included only one clinical case. Finally, while we were able to show the feasibility of this approach in one participant from the clinical population, the generalizability of these findings to larger healthy and clinical cohorts needs further investigation in future studies. In particular, this patient is older than the young healthy control group and may differ from the clinical population included in many TMS clinical trials, having had previous TMS experience and having major depressive episodes with high chronicity levels based on the diagnosis of bipolar disorder. The patient has received pharmacological and rTMS treatment for many years, thus potentially affecting neuronal responses to the acute interventions applied in our study. Thus, future work is necessary to investigate whether the high intraindividual variability of BOLD effects we observed is representative of individuals with major depressive episodes.

5. Conclusions

In conclusion, we were able to establish a full iTBS treatment protocol in the concurrent TMS-fMRI setting and could disentangle several sources of variability relevant for this approach. We propose that this experimental paradigm could reveal acute effects of clinical iTBS treatment at the single session level, and may not only be used to demonstrate the immediate target engagement, but could also provide deeper insights into putative mechanisms of action.

Funding information

PT's work is funded by the DFG (TA 857/3-2). The procurement of the Prisma 3T MRI scanner was supported by the Deutsche Forschungsgemeinschaft (DFG, INST 409/193-1 FUGG). LB's work is part of the funding program of the Medical Faculty of LMU (FöFöLe Plus, Munich Clinician Scientist Program).

CRediT authorship contribution statement

Kai-Yen Chang: Writing – review & editing, Writing – original draft, Visualization, Software, Project administration, Methodology, Investigation, Formal analysis, Data curation, Conceptualization. **Martin Tik:** Investigation, Formal analysis, Conceptualization, Methodology, Software, Supervision, Validation, Writing – review & editing. **Yuki Mizutani-Tiebel:** Conceptualization, Data curation, Methodology, Investigation, Project administration. **Anna-Lisa Schuler:** Writing – review & editing. **Paul Taylor:** Writing – review & editing. **Mattia Campana:** Methodology. **Ulrike Vogelmann:** Methodology, Data curation. **Barbara Huber:** Writing – review & editing. **Esther Dechantsreiter:** Resources, Project administration, Funding acquisition. **Axel Thielscher:** Writing – review & editing, Validation, Software. **Lucia Bulubas:** Writing – review & editing, Supervision, Software, Resources, Project administration, Methodology, Investigation, Funding acquisition, Formal analysis, Conceptualization. **Frank Padberg:** Writing – review & editing, Visualization, Validation, Supervision, Resources, Project administration, Methodology, Conceptualization, Funding acquisition, Investigation. **Daniel Keeser:** Writing – review & editing, Visualization, Validation, Supervision, Software, Resources, Project administration, Methodology, Investigation, Funding acquisition, Formal analysis, Conceptualization.

Declaration of competing interest

This work is a part of K-YC's Ph.D. program at Munich Medical Research School. YM-T received remuneration from neuroCare Group AG as a part-time office worker. FP is a member of the European Scientific Advisory Board of Brainsway Inc., Jerusalem, Israel, and the International Scientific Advisory Board of Sooma, Helsinki, Finland. He has received speaker's honoraria from Mag&More GmbH, the neuroCare Group, Munich, Germany, and Brainsway Inc. His-lab has received support with equipment from neuroConn GmbH, Ilmenau, Germany, Mag&More GmbH and Brainsway Inc. MT, A-LS, PT, MC, UV, BH, ED, AT, LB, & DK reported no potential conflicts of interest.

Data availability

Data will be made available on request.

Acknowledgments

We want to thank Linda Schuster, Zane Wilkinson, and Cuici Voon for assisting TMS-fMRI data collection and Larissa Behnke for E-field simulation data preprocessing. We would like to thank Christian Windischberger (Center for Medical Physics and Biomedical Engineering at the Medical University of Vienna, Austria) for providing his comprehensive expertise in concurrent TMS-MRI, as well as Patrik Kunz (Localite GmbH, Bonn, Germany) and Matthias Kienle (MagVenture A/S, Farum, Denmark) for their kind support with the technical setup.

Supplementary materials

Supplementary material associated with this article can be found, in the online version, at doi:10.1016/j.neuroimage.2024.120596.

References

Baeken, C., Duprat, R., Wu, G.R., De Raedt, R., Van Heeringen, K., 2017. Subgenual anterior cingulate–medial orbitofrontal functional connectivity in medication-resistant major depression: a neurobiological marker for accelerated intermittent theta burst stimulation treatment? Biol. Psychiatry. Cogn. Neurosci. Neuroimag. 2 (7), 556–565.

Baeken, C., Marinazzo, D., Wu, G.R., Van Schuerbeek, P., De Mey, J., Marchetti, I., et al., 2014. Accelerated HF-rTMS in treatment-resistant unipolar depression: insights from subgenual anterior cingulate functional connectivity. World. J. Biol. Psychiatry 15 (4), 286–297.

Bergmann, T.O., Varatheeswaran, R., Hanlon, C.A., Madsen, K.H., Thielscher, A., Siebner, H.R., 2021. Concurrent TMS-fMRI for causal network perturbation and proof of target engagement. Neuroimage 237, 118093.

Blumberger, D.M., Vila-Rodriguez, F., Thorpe, K.E., Feffer, K., Noda, Y., Giacobbe, P., et al., 2018. Effectiveness of theta burst versus high-frequency repetitive transcranial magnetic stimulation in patients with depression (THREE-D): a randomised non-inferiority trial. Lancet 391 (10131), 1683–1692.

Bohning, D.E., Shastri, A., McConnell, K., Nahas, Z., Lorberbaum, J., Roberts, D., et al., 1999. A combined TMS/fMRI study of intensity-dependent TMS over motor cortex. Biol. Psychiatry 45 (4), 385–394.

Bohning, D.E., Shastri, A., Nahas, Z., Lorberbaum, J.P., Andersen, S.W., Dannels, W.R., et al., 1998. Echoplanar BOLD fMRI of brain activation induced by concurrent transcranial magnetic stimulation. Invest. Radiol. 33 (6), 336–340.

Brunoni, A.R., Moffa, A.H., Sampaio-Junior, B., Borrione, L., Moreno, M.L., Fernandes, R. A., et al., 2017. Trial of electrical direct-current therapy versus escitalopram for depression. N. Engl. J. Med. 376 (26), 2523–2533.

Bulteau, S., Laurin, A., Pere, M., Fayet, G., Thomas-Ollivier, V., Deschamps, T., et al., 2022. Intermittent theta burst stimulation (iTBS) versus 10 Hz high-frequency repetitive transcranial magnetic stimulation (rTMS) to alleviate treatment-resistant unipolar depression: a randomized controlled trial (THETA-DEP). Brain. Stimulat. 15 (3), 870–880.

Cash, R.F.H., Zalesky, A., Thomson, R.H., Tian, Y., Cocchi, L., Fitzgerald, P.B., 2019. Subgenual functional connectivity predicts antidepressant treatment response to transcranial magnetic stimulation: independent validation and evaluation of personalization. Biol. Psychiatry 86 (2), e5–e7.

Cole, E.J., Stimpson, K.H., Bentzley, B.S., Gulser, M., Cherian, K., Tischler, C., et al., 2020. Stanford accelerated intelligent neuromodulation therapy for treatment-resistant depression. Am. J. Psychiatry 177 (8), 716–726.

Dowdle, L.T., Brown, T.R., George, M.S., Hanlon, C.A., 2018. Single pulse TMS to the DLPFC, compared to a matched sham control, induces a direct, causal increase in caudate, cingulate, and thalamic BOLD signal. Brain. Stimulat. 11 (4), 789–796.

Duecker, F., Sack, A.T., 2015. Rethinking the role of sham TMS. Front. Psychol. 6, 210.

Dunlop, B.W., Rajendra, J.K., Craighead, W.E., Kelley, M.E., McGrath, C.L., Choi, K.S., et al., 2017. Functional connectivity of the subcallosal cingulate cortex and differential outcomes to treatment with cognitive-behavioral therapy or antidepressant medication for major depressive disorder. Am. J. Psychiatry 174 (6), 533–545.

Eshel, N., Keller, C.J., Wu, W., Jiang, J., Mills-Finnerty, C., Huemer, J., et al., 2020. Global connectivity and local excitability changes underlie antidepressant effects of repetitive transcranial magnetic stimulation. Neuropsychopharmacology. 45 (6), 1018–1025.

Fox, M.D., Buckner, R.L., White, M.P., Greicius, M.D., Pascual-Leone, A., 2012. Efficacy of transcranial magnetic stimulation targets for depression is related to intrinsic functional connectivity with the subgenual cingulate. Biol. Psychiatry 72 (7), 595–603.

Fox, M.D., Liu, H., Pascual-Leone, A., 2013. Identification of reproducible individualized targets for treatment of depression with TMS based on intrinsic connectivity. Neuroimage 66, 151–160.

Ge, R., Downar, J., Blumberger, D.M., Daskalakis, Z.J., Vila-Rodriguez, F., 2020. Functional connectivity of the anterior cingulate cortex predicts treatment outcome for rTMS in treatment-resistant depression at 3-month follow-up. Brain. Stimulat. 13 (1), 206–214.

George, M.S., Wassermann, E.M., Williams, W.A., Callahan, A., Ketter, T.A., Basser, P., et al., 1995. Daily repetitive transcranial magnetic stimulation (rTMS) improves mood in depression. Neuroreport. Int. J. Rapid. Commun. Res. Neurosci. 6 (14), 1853–1856.

Grossheinrich, N., Rau, A., Pogarell, O., Hennig-Fast, K., Reinl, M., Karch, S., et al., 2009. Theta burst stimulation of the prefrontal cortex: safety and impact on cognition, mood, and resting electroencephalogram. Biol. Psychiatry 65 (9), 778–784.

Hanlon, C.A., Canterberry, M., Taylor, J.J., DeVries, W., Li, X., Brown, T.R., et al., 2013. Probing the frontostriatal loops involved in executive and limbic processing via interleaved TMS and functional MRI at two prefrontal locations: a pilot study. Wang F., editor PLoS ONE 8 (7), e67917.

Hawco, C., Armony, J.L., Daskalakis, Z.J., Berlim, M.T., Chakravarty, M.M., Pike, G.B., et al., 2017. Differing time of onset of concurrent TMS-fMRI during associative memory encoding: a measure of dynamic connectivity. Front. Hum. Neurosci. 11, 404.

Hermiller, M.S., Chen, Y.F., Parrish, T.B., Voss, J.L., 2020. Evidence for immediate enhancement of hippocampal memory encoding by network-targeted theta-burst stimulation during concurrent fMRI. J. Neurosci. 40 (37), 7155–7168.

Holzer, M., Padberg, F., 2010. Intermittent theta burst stimulation (iTBS) ameliorates therapy-resistant depression: a case series. Brain. Stimulat. 3 (3), 181–183.

Huang, Y.Z., Edwards, M.J., Rounis, E., Bhatia, K.P., Rothwell, J.C., 2005. Theta burst stimulation of the human motor cortex. Neuron 45 (2), 201–206.

Kan, R.L.D., Padberg, F., Giron, C.G., Lin, T.T.Z., Zhang, B.B.B., Brunoni, A.R., et al., 2023. Effects of repetitive transcranial magnetic stimulation of the left dorsolateral prefrontal cortex on symptom domains in neuropsychiatric disorders: a systematic review and cross-diagnostic meta-analysis. Lancet Psychiatry 10 (4), 252–259.

Li, X., Nahas, Z., Kozel, F.A., Anderson, B., Bohning, D.E., George, M.S., 2004. Acute left prefrontal transcranial magnetic stimulation in depressed patients is associated with immediately increased activity in prefrontal cortical as well as subcortical regions. Biol. Psychiatry 55 (9), 882–890.

Liston, C., Chen, A.C., Zebley, B.D., Drysdale, A.T., Gordon, R., Leuchter, B., et al., 2014. Default mode network mechanisms of transcranial magnetic stimulation in depression. Biol. Psychiatry 76 (7), 517–526.

Marques, J.P., Kober, T., Krueger, G., van der Zwaag, W., Van de Moortele, P.F., Gruetter, R., 2010. MP2RAGE, a self bias-field corrected sequence for improved segmentation and T1-mapping at high field. Neuroimage 49 (2), 1271–1281.

Mizutani-Tiebel, Y., Tik, M., Chang, K.Y., Padberg, F., Soldini, A., Wilkinson, Z., et al., 2022. Concurrent TMS-fMRI: technical challenges, developments, and overview of previous studies. Front. Psychiatry 13, 825205.

Nahas, Z., Lomarev, M., Roberts, D.R., Shastri, A., Lorberbaum, J.P., Teneback, C., et al., 2001. Unilateral left prefrontal transcranial magnetic stimulation (TMS) produces intensity-dependent bilateral effects as measured by interleaved BOLD fMRI. Biol. Psychiatry 50 (9), 712–720.

Navarro de Lara, L.I., Tik, M., Woletz, M., Frass-Kriegl, R., Moser, E., Laistler, E., et al., 2017. High-sensitivity TMS/fMRI of the human motor cortex using a dedicated multichannel MR Coil. NeuroImage 150, 262–269.

Navarro de Lara, L.I., Windischberger, C., Kuehne, A., Woletz, M., Sieg, J., Bestmann, S., et al., 2015. A novel coil array for combined TMS/fMRI experiments at 3 T. Magn. Reson. Med. 74 (5), 1492–1501.

Oathes, D.J., Zimmerman, J.P., Duprat, R., Japp, S.S., Scully, M., Rosenberg, B.M., et al., 2021. Resting fMRI-guided TMS results in subcortical and brain network modulation indexed by interleaved TMS/fMRI. Exp. Brain. Res. 239 (4), 1165–1178.

Riddle, J., Scimeca, J.M., Pagnotta, M.F., Inglis, B., Sheltraw, D., Muse-Fisher, C., et al., 2022. A guide for concurrent TMS-fMRI to investigate functional brain networks. Front. Hum. Neurosci. 16, 1050605.

Salomons, T.V., Dunlop, K., Kennedy, S.H., Flint, A., Geraci, J., Giacobbe, P., et al., 2014. Resting-state cortico-thalamic-striatal connectivity predicts response to dorsomedial prefrontal rTMS in major depressive disorder. Neuropsychopharmacology 39 (2), 488–498.

Saturnino, G.B., Puonti, O., Nielsen, J.D., Antonenko, D., Madsen, K.H., Thielscher, A., 2019. SimNIBS 2.1: a comprehensive pipeline for individualized electric field modelling for transcranial brain stimulation. *Brain and Human Body Modeling: Computational Human Modeling at EMBC 2018*, pp. 3–25.

Siebner, H.R., Conde, V., Tomasevic, L., Thielscher, A., Bergmann, T.O., 2019. Distilling the essence of TMS-evoked EEG potentials (TEPs): a call for securing mechanistic specificity and experimental rigor. Brain. Stimulat. 12 (4), 1051–1054.

Siebner, H.R., Funke, K., Aberra, A.S., Antal, A., Bestmann, S., Chen, R., et al., 2022. Transcranial magnetic stimulation of the brain: what is stimulated? – A consensus and critical position paper. Clin. Neurophysiol. 140, 59–97.

Suppa, A., Huang, Y.Z., Funke, K., Ridding, M.C., Cheeran, B., Di Lazzaro, V., et al., 2016. Ten years of theta burst stimulation in humans: established knowledge, unknowns and prospects. Brain. Stimulat. 9 (3), 323–335.

Tik, M., Hoffmann, A., Sladky, R., Tomova, L., Hummer, A., Navarro de Lara, L., et al., 2017. Towards understanding rTMS mechanism of action: stimulation of the DLPFC causes network-specific increase in functional connectivity. Neuroimage 162, 289–296.

Tik, M., Vasileiadi, M., Woletz, M., Linhardt, D., Schuler, A.L., Williams, N., et al., 2023a. Concurrent TMS/fMRI reveals individual DLPFC dose-response pattern. Neuroimage, 120394.

Tik, M., Woletz, M., Schuler, A.L., Vasileiadi, M., Cash, R.F.H., Zalesky, A., et al., 2023b. Acute TMS/fMRI response explains offline TMS network effects – An interleaved TMS-fMRI study. Neuroimage 267, 119833.

Tura, A., Goya-Maldonado, R., 2023. Brain connectivity in major depressive disorder: a precision component of treatment modalities? Transl. Psychiatry 13 (1), 196.

Vink, J.J.T., Mandija, S., Petrov, P.I., van den Berg, C.A.T., Sommer, I.E.C., Neggers, S.F. W., 2018. A novel concurrent TMS-fMRI method to reveal propagation patterns of prefrontal magnetic brain stimulation. Hum. Brain. Mapp. 39 (11), 4580–4592.

Weigand, A., Horn, A., Caballero, R., Cooke, D., Stern, A.P., Taylor, S.F., et al., 2018. Prospective validation that subgenual connectivity predicts antidepressant efficacy of transcranial magnetic stimulation sites. Biol. Psychiatry 84 (1), 28–37.

4. Paper II

Dose-Dependent Target Engagement of a Clinical Intermittent Theta Burst Stimulation Protocol: An Interleaved Transcranial Magnetic Stimulation-Functional Magnetic Resonance Imaging Study in Healthy People

ARTICLE IN PRESS

Archival Report

Biological Psychiatry: CNNI

Dose-Dependent Target Engagement of a Clinical Intermittent Theta Burst Stimulation Protocol: An Interleaved Transcranial Magnetic Stimulation–Functional Magnetic Resonance Imaging Study in Healthy People

Kai-Yen Chang, Martin Tik, Yuki Mizutani-Tiebel, Paul Taylor, Timo van Hattem, Peter Falkai, Frank Padberg, Lucia Bulubas, and Daniel Keeser

ABSTRACT

BACKGROUND: Intermittent theta burst stimulation (iTBS) of the dorsolateral prefrontal cortex (DLPFC) is widely applied as a therapeutic intervention in mental health; however, the understanding of its mechanisms is still incomplete. Prior magnetic resonance imaging (MRI) studies have mainly used offline iTBS or short sequences in concurrent transcranial magnetic stimulation (TMS)–functional MRI (fMRI). This study investigated a full 600-stimuli iTBS protocol using interleaved TMS-fMRI in comparison with 2 control conditions in healthy subjects.

METHODS: In a crossover design, 18 participants underwent 3 sessions of interleaved iTBS-fMRI: 1) the left DLPFC at 40% resting motor threshold (rMT) intensity, 2) the left DLPFC at 80% rMT intensity, and 3) the left primary motor cortex (M1) at 80% rMT intensity. We compared immediate blood oxygen level–dependent (BOLD) responses during interleaved iTBS-fMRI across these conditions including correlations between individual fMRI BOLD activation and iTBS-induced electric field strength at the target sites.

RESULTS: Whole-brain analysis showed increased activation in several regions following iTBS. Specifically, the left DLPFC, as well as the bilateral M1, anterior cingulate cortex, and insula, showed increased activation during 80% rMT left DLPFC stimulation. Increased BOLD activity in the left DLPFC was observed with neither 40% rMT left DLPFC stimulation nor left M1 80% rMT iTBS, whereas activation in other regions was found to overlap between conditions. Of note, BOLD activation and electric field intensities were only correlated for M1 stimulation and not for the DLPFC conditions.

CONCLUSIONS: This interleaved TMS-fMRI study showed dosage- and target-specific BOLD activation during a 600-stimuli iTBS protocol in healthy individuals. Future studies may use our approach for investigating target engagement in clinical samples.

https://doi.org/10.1016/j.bpsc.2024.08.009

Theta burst stimulation (TBS) is a repetitive transcranial magnetic stimulation (rTMS) protocol and is frequently applied to treat psychiatric disorders due to its shorter duration as compared to standard clinical rTMS protocols. TBS was initially developed by translating burst-patterned stimulation, known to induce long-term potentiation and long-term depression in animal brain slices (1–3), into rTMS protocols in humans to identify protocols that more effectively modulate cortical excitability (4,5). Based on a milestone study by Huang *et al.* (5), 2 main TBS protocols emerged early in the field, i.e., intermittent TBS (iTBS) and continuous TBS, and both protocols originally used 50-Hz rTMS bursts at 5 Hz (theta) frequency with up to 600 total pulses and an intensity of 80% of the active motor threshold (MT). Interestingly, these protocols differ primarily in the intervals for iTBS (i.e., 2 seconds on and 8 seconds off), leading to a facilitation of motor evoked potentials (MEPs) and a reduction of short intracortical inhibition, whereas continuous TBS has the opposite effects. Comprehensive studies in animals and humans suggest that these effects are mediated by the differential interaction of TBS protocols with various neuronal subpopulations including modulation of GABAergic (gamma-aminobutyric acidergic) circuits and glutamatergic neurotransmission (6–12).

Current therapeutic TBS variants are essentially based on the original TBS protocols. For clinical use, these protocols are often extended (e.g., up to 1800 stimuli per session) or are applied as accelerated iTBS with multiple iTBS sessions per day (13). Stimulation intensities have similarly varied across clinical iTBS studies. For instance, major depressive disorder is the most common application of iTBS in psychiatry to date

ISSN: 2451-9022

(14), with intensities ranging from 80% resting MT (rMT) to 120% rMT across studies (15–19). In contrast to the rapid spread of iTBS in clinical applications, there is comparably scarce preclinical research on specific protocols, their mechanistic understanding is limited, and dose-response relationships need to be established. Moreover, therapeutic effects vary largely among individuals, partially influenced by differences in their structural and functional brain connectivity (20–22).

One method to study the acute effects of rTMS protocols is interleaved (or concurrent) TMS–functional magnetic resonance imaging (TMS-fMRI) in which the blood oxygen level–dependent (BOLD) response is measured during rTMS in an MRI scanner. Most interleaved TMS-fMRI studies have focused on the primary motor cortex (M1) (23–28), while fewer studies investigated its effects on the dorsolateral prefrontal cortex (DLPFC) (29–34). Generally, interleaved TMS-fMRI paradigms have typically used short rTMS bursts or single pulses, rather than full rTMS protocols (27–34). To investigate clinical iTBS protocols in terms of their mechanistic action, we have recently implemented a full 600-stimuli iTBS of the left DLPFC in the interleaved TMS-fMRI approach and have shown its feasibility in healthy individuals and a patient with bipolar depression (35). To extend these findings and to test the dose and target specificity of acute iTBS effects in healthy subjects, we investigated the BOLD effects of 600-stimuli iTBS of the left DLPFC in comparison with a 40% rMT iTBS of the left DLPFC and an 80% rMT intensity iTBS of the M1 region in the interleaved TMS-fMRI paradigm. We expected a maximum BOLD effect in the iTBS target region and connected brain areas. To assess the iTBS neural response in specific regions across subjects, we reported the hemodynamic response function (HRF) beta values to indicate the strength of the BOLD responses to TMS. A larger fMRI-BOLD response, evoked by neural activity, is reflected by a higher beta value estimate. The beta value is widely reported in the concurrent TMS-fMRI field as a method for quantifying the HRF induced by TMS (32,36,37). In addition, we used computational modeling of TMS-induced electrical field (E-field) to explore E-field intensity as a further proxy for iTBS dosing (38). In sum, this interleaved TMS-fMRI study investigates first-level hypotheses (i.e., dose and target specificity) on the acute effects of left DLPFC iTBS to establish more specific hypotheses regarding the action of iTBS on brain connectivity, modulation, and function.

METHODS AND MATERIALS

Healthy Participants

The recruitment criteria of healthy adult participants and the detailed procedures are described in the Supplement. A total of 19 healthy participants (8 female, 11 male; ages 21–36 years, average age = 26.4 years, SD = 3.2 years) completed all sessions in this study. One subject was excluded from the group-level analysis due to excessive motion exceeding 3 mm even after motion correction, leaving 18 subjects included in the fMRI analysis. All subjects signed informed consent as approved by the LMU Munich ethical committee prior to participation, and all procedures adhere to the principles outlined in the Declaration of Helsinki.

Experimental Setup

Participants completed 4 experimental sessions, comprising a baseline session without TMS and 3 interleaved iTBS-fMRI sessions. Each subject underwent interleaved iTBS-fMRI sessions with a randomized order of stimulated conditions, including 80% rMT left DLPFC, 40% rMT left DLPFC, and 80% rMT left M1. There was a minimum of 1 week between each session (Figure 1A). The baseline session was performed using a 64-channel standard head coil. In the TMS-fMRI sessions (Figure 1B), we utilized 2 TMS-compatible 7-channel MR coils (39) to cover the whole brain. Neuronavigation (Localite GmbH) was precisely employed to target the predefined anatomical region over the left DLPFC, based on a previous study (16) and individual measured M1 hotspot (Figure 1D). The detailed baseline MRI sequences and neuronavigation setup are described in the Supplement.

Transcranial Magnetic Stimulation. All TMS procedures were conducted inside the MRI scanner room using an MRi-B91 MR-compatible TMS coil and MagProX100 stimulator (MagVenture A/S). A 7-channel surface radiofrequency coil (39) was affixed between the scalp and the MR-compatible TMS coil during MT determination to ensure a matching intensity during interleaved iTBS-fMRI sessions. MT determination was measured exclusively during the baseline session. Participants were lying down with their hands relaxed on the MR scanner bed. An MR-compatible electromyography recorder (Brain Products) was used, with electromyography electrodes placed over the right abductor pollicis brevis, while a ground electrode was positioned over the right ankle. MEPs were identified as responses with amplitudes exceeding 50 μV within 15 to 35 ms following each TMS pulse. The rMT was determined at the optimal coil position for eliciting MEPs in the right abductor pollicis brevis using the standard method (40).

Concurrent TMS-fMRI. The concurrent TMS-fMRI sessions utilized two 7-channel surface radiofrequency coils (39). Structural imaging was performed using a magnetization-prepared 2 rapid acquisition gradient-echo sequence (repetition time = 4000 ms, echo time = 2.98 ms, inversion time 1/inversion time 2 = 700 ms/2500 ms, flip angle 1/flip angle 2 = 4°/5°, 160 slices, 1-mm slice thickness) (41). Interleaved iTBS-fMRI was performed continuously for 3 minutes and 32 seconds (including a 12-second dummy scan) using a multiband accelerated echo-planar imaging sequence (multiband factor of 4, repetition time = 2000 ms, echo time = 30 ms, 40 slices, and voxel size of 3.3 × 3.3 × 3 mm) (Figure 1C).

MRI Data Preprocessing and Statistical Analyses. The detailed preprocessing steps of MRI data are described in the Supplement. Additionally, we used independent component analysis (ICA) to regress out potential coil artifacts caused by eddy/leakage currents or mechanical vibrations in the fMRI data. We applied FSL's MELODIC algorithm (42) to run a single-subject ICA, constraining the output to 15 components. We then manually classified and removed ICs related to noise or artifacts (see Figure S2 for examples of ICA classification). After removing noise ICs, we conducted group analysis using an established block-design analysis pipeline (35).

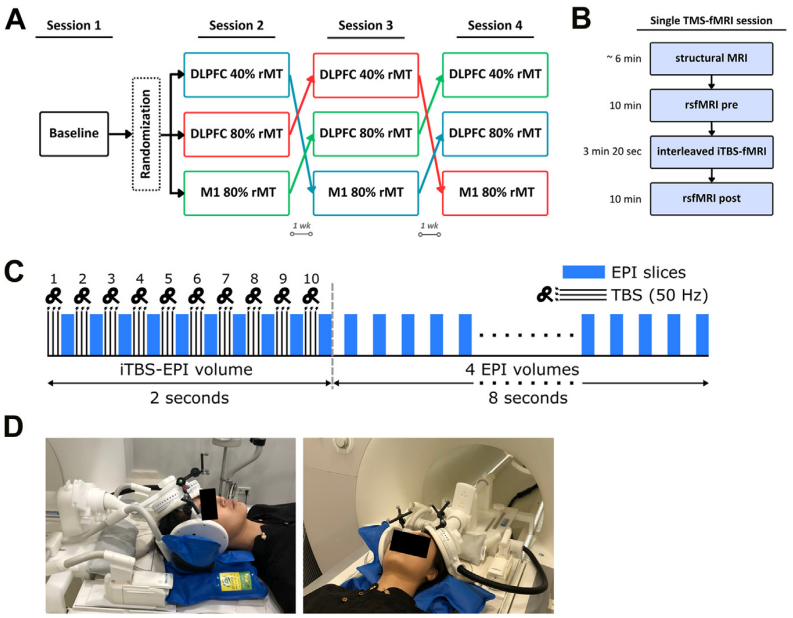

Figure 1. **(A)** The experimental design involved a baseline visit, followed by a randomized 3-way crossover design for interleaved intermittent theta burst stimulation–functional magnetic resonance imaging (iTBS-fMRI) sessions, with a minimum of 1 week washout between each session. **(B)** The MRI scan protocol was consistently used throughout transcranial magnetic stimulation–fMRI (TMS-fMRI) sessions. **(C)** Interleaved iTBS-fMRI sequence, which repeats 20 times, for a total of 3 minutes 20 seconds in the standard iTBS protocol. **(D)** Concurrent TMS-fMRI setup with two 7-channel radiofrequency coils. The MR-compatible TMS coil was mounted on the left radiofrequency coil. The images show (left panel) TMS-MRI coils targeting the left dorsolateral prefrontal cortex (DLPFC) and (right panel) primary motor cortex (M1). EPI, echo-planar imaging; rMT, resting motor threshold; rsfMRI, resting-state fMRI.

Correlation E-Field and BOLD Activation

To test for correlation between the simulated E-field strength and fMRI BOLD activation in each subject in the left DLPFC and left M1, we adopted predefined targets for the left DLPFC (−38, 44, 26 mm Montreal Neurological Institute [MNI]), in which we did the stimulation (16), and M1 (−37, −21, 58 mm MNI) (43). Data from only 16 subjects were included in the DLPFC 80% rMT condition, while 15 subjects were included in the DLPFC 40% rMT and M1 80% rMT conditions due to missing TMS trigger recordings. Subsequently, we calculated the mean E-field magnitude using SimNIBS 4.0 (https://simnibs.github.io/simnibs/build/html/index.html) and the mean HRF beta value from fMRI data within a 10-mm radius of our predefined targets as region of interest. Finally, the correlation coefficient was used to determine the relationship between the E-field magnitude and the fMRI beta value for the M1 and DLPFC conditions.

RESULTS

Immediate BOLD Changes During Interleaved iTBS-fMRI in Healthy Subjects

The 80% rMT iTBS over the left DLPFC represented the main focus of the experiment. The 40% rMT iTBS over the left DLPFC served as a low-intensity control condition, and the 80% rMT iTBS over the left M1 served as an active control condition at a different target region.

Effects of 40% rMT iTBS Over the Left DLPFC. The 40% rMT iTBS-DLPFC (Table 1) did not activate the underlying cortex but instead resulted in BOLD activity in the contralateral, right DLPFC (right superior frontal gyrus, t_{17} = 5.23) (Figure 2A). Similar to the 80% rMT left DLPFC data (see the following), we observed consistent peak BOLD activations in the bilateral auditory cortex (left superior temporal gyrus, t_{17} = 6.68; right superior temporal gyrus, t_{17} = 5.79) and anterior cingulate cortex (ACC) (right ACC, t_{17} = 4.13).

Effects of 80% rMT iTBS Over the Left DLPFC. In the 80% rMT iTBS-DLPFC condition (Table 1), significantly increased BOLD activation was observed locally under the TMS coil in the targeted region, with a focal cluster of BOLD activity localized at the stimulated left DLPFC (left superior frontal gyrus, t_{17}= 5.85) (Figure 2B). The BOLD activation also spread to the bilateral M1 (left precentral gyrus, t_{17} = 4.59; right precentral gyrus, t_{17} = 4.35) and ACC (left ACC, t_{17} = 4.84; right ACC, t_{17} = 4.06). Subcortically, BOLD activation was found in the anterior insula (left anterior insula, t_{17} = 4.66; right anterior insula, t_{17} = 4.72). Furthermore, significant BOLD activity peaks were also observed in the bilateral auditory cortex (left superior temporal gyrus, t_{17} = 6.64; right superior temporal gyrus, t_{17} = 3.85).

Effects of 80% rMT iTBS Over the Left M1. The 80% rMT iTBS-M1 (Table 1) elicited significant BOLD activity in the bilateral M1 (left precentral gyrus, t_{17} = 5.83; right precentral gyrus, t_{17} = 5.7) (Figure 2C), right DLPFC (right middle frontal gyrus, t_{17} = 6.22), right auditory cortex (right superior temporal gyrus, t_{17} = 8), and bilateral primary somatosensory cortex (left postcentral gyrus, t_{17} = 7.3; right postcentral gyrus, t_{17}= 5.83). In the subcortex, BOLD activations were found in the bilateral putamen (right putamen, t_{17} = 5.89; left putamen, t_{17} = 4.76) and left caudate (t_{17} = 4.45).

Table 1. Peak BOLD Activation in Interleaved iTBS-fMRI

Condition	Area	Peak MNI Coordinates, mm[a]	Cluster Size	*t* Value[b]	*z*
40% rMT Left DLPFC	Right superior frontal gyrus	22, 50, 28	354	5.23	3.98
	Right anterior cingulate gyrus	12, 36, 16	127	4.13	3.86
	Left superior temporal gyrus	−58, −12, 14	81	6.68	4.62
	Right superior temporal gyrus	68, −26, 14	72	5.79	4.91
80% rMT Left DLPFC	Left superior frontal gyrus	−22, 60, 24	388	5.85	4.27
	Left precentral gyrus	−60, 10, 28	57	4.59	3.65
	Right precentral gyrus	60, 8, 12	191	4.35	4.75
	Left anterior cingulate gyrus	−2, 30, 16	91	4.84	4.78
	Right anterior cingulate gyrus	4, 32, 16	41	4.06	4.21
	Left anterior insula	−32, 16, −4	45	4.66	3.69
	Right anterior insula	30, 18, 6	60	4.72	3.72
	Left superior temporal gyrus	−64, −18, 8	49	6.64	4.83
	Right superior temporal gyrus	68, −18, 8	40	3.85	4.44
80% rMT Left M1	Right middle frontal gyrus	26, 42, 26	203	6.22	4.43
	Left precentral gyrus	−32, −8, 52	130	5.83	4.26
	Right precentral gyrus	50, 2, 50	164	5.7	4.21
	Right superior temporal gyrus	62, −32, 20	75	8	5.59
	Left postcentral gyrus	−62, −18, 26	81	7.3	4.85
	Right postcentral gyrus	62, −16, 42	71	5.83	4.26
	Left putamen region	−24, 10, 2	44	4.76	3.74
	Right putamen region	26, 14, 2	73	5.89	4.29
	Left caudate region	−10, 4, 14	32	4.45	3.58

The 3 conditions were cluster corrected and thresholded at FWE $p < .05$.

BOLD, blood oxygen level–dependent; DLPFC, dorsolateral prefrontal cortex; fMRI, functional magnetic resonance imaging; FWE, familywise error; iTBS, intermittent theta burst stimulation; M1, primary motor cortex; MNI, Montreal Neurological Institute; rMT, resting motor threshold.

[a]Reported as x, y, z.

[b]*df* = 17.

Correlation of Mean E-Field Magnitude With fMRI in M1 and DLPFC iTBS

This correlation analysis aimed to estimate the relationship between E-field magnitude and fMRI beta values under 3 conditions (Figure 3). No correlation was observed in the 80% rMT or 40% rMT DLPFC condition, with correlation coefficients of $r = 0.30$ ($p = .24$) and $r = -0.14$ ($p = .6$), respectively. Strikingly, in the M1 condition, a strong positive correlation emerged with an $r = 0.65$ ($p = .008$). This suggests that the E-field magnitude was a good indicator of the BOLD response in M1, but no such relationship was observed in the DLPFC.

Individual Variability in Response to Low and High iTBS Intensity Over Bilateral DLPFC

To characterize the iTBS intensity response over the DLPFC in both the stimulated and remote DLPFC regions, and to investigate individual variability due to iTBS, we examined the HRF beta values in each interleaved iTBS-fMRI scan. Remarkably, high-intensity 80% rMT iTBS exhibited a significantly higher beta value in the left DLPFC than low-intensity 40% rMT iTBS ($t_{17} = 2.44$, $p = .03$). Additionally, in the 80% rMT DLPFC condition, the beta value in the left DLPFC was significantly higher than in the right DLPFC ($t_{17} = 2.57$, $p = .02$) (Figure 4B). At the same time, individual variability was apparent (Figure 4C), as some subjects did not demonstrate a strong difference in beta values between high-intensity and low-intensity iTBS. The remote effect of iTBS in the right DLPFC region exhibited considerable individual variability, with no clear evidence that higher intensity leads to a higher beta response in the remote DLPFC region.

DISCUSSION

This interleaved TMS-fMRI study investigated the effects of a full 600-stimuli iTBS protocol at 80% rMT intensity over the left DLPFC in healthy individuals. The iTBS form corresponds to the original iTBS protocol by Huang *et al.* (5), with the only difference that 80% rMT instead of 80% active MT intensity was applied. In the current study, iTBS of the left DLPFC at 80% rMT was compared intraindividually with 40% rMT intensity iTBS to show dose dependency and with 80% rMT M1 iTBS to demonstrate target specificity. We found that 80% rMT DLPFC iTBS led to a BOLD activation within the left DLPFC, with activation extending to a network including the M1 and other connected regions but not the contralateral DLPFC. In contrast, 40% rMT DLPFC iTBS did not show BOLD activation of the underlying cortex but did activate the contralateral prefrontal cortex. M1 iTBS was associated with bilateral BOLD activation in the M1 and extended networks but not in the left DLPFC. Interestingly, BOLD activation of the M1 was correlated with individual E-field strength, whereas this correlation was not observed for the left DLPFC target.

Main Effects of 80% rMT iTBS of the Left DLPFC: Left DLPFC TMS Affects the Left DLPFC

The 80% rMT iTBS left DLPFC condition (Figure 2B) showed BOLD activation of the cortical region at the target site. This

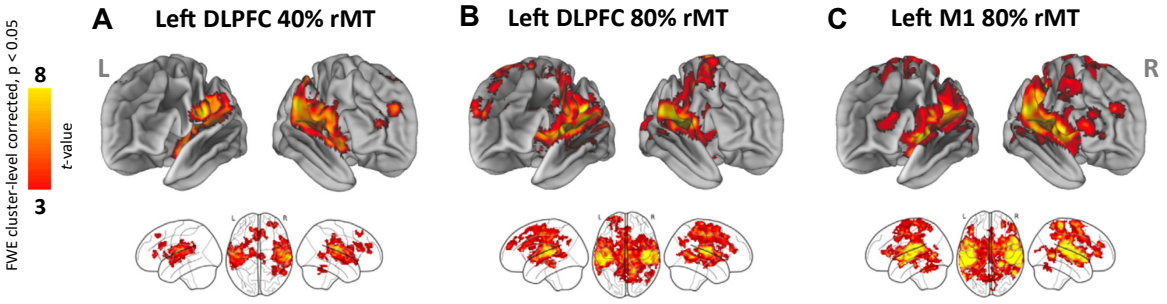

Figure 2. **(A)** Immediate blood oxygen level–dependent (BOLD) changes during 40% resting motor threshold (rMT) left dorsolateral prefrontal cortex (DLPFC) interleaved intermittent theta burst stimulation–functional magnetic resonance imaging (iTBS-fMRI) in healthy subjects. The peak activation in the prefrontal region was found at the right superior frontal gyrus, with $t_{17} = 5.23$. **(B)** Immediate BOLD changes during 80% rMT left DLPFC interleaved iTBS-fMRI in healthy subjects. The peak activation in the prefrontal region was found at the left superior frontal gyrus, with $t_{17} = 5.85$. **(C)** Immediate BOLD changes during 80% rMT left primary motor cortex (M1) interleaved iTBS-fMRI in healthy subjects. The peak BOLD activation was found at the right superior temporal gyrus, with $t_{17} = 8$. FWE, familywise error.

finding aligns with previous concurrent TMS-fMRI studies targeting the DLPFC with various rTMS protocols (31,32). Of note, our data also confirm that TMS not only modulates local neural activity, but also affects distant brain regions, as shown in many prior studies (31,32,36,44,45). We observed increased BOLD signals also in the M1, ACC, anterior insula, and auditory regions. Notably, activation in the ACC and anterior insula is indicative of salience network activity, consistent with Hawco *et al.* (36), who found that targeting the DLPFC with rTMS activates salience nodes, potentially leading to improved treatment outcomes (46). Importantly, while previous studies observed effects through functional connectivity analysis, our study detected effects using a block-design analysis.

Comparison With Low-Intensity and M1 Control Conditions: Target and Dose Specificity

Due to the technical and methodological limitations of iTBS sham conditions (47,48), rather than including a suboptimal sham control condition, our study used 2 well-established active control conditions: 1) low-intensity iTBS at 40% rMT and 2) a second target site, i.e., the M1 region, a target investigated in the majority of previous interleaved TMS-fMRI studies (23,24,26–28,39,49–53).

Applying 40% rMT iTBS to the left DLPFC, we observed fewer voxels showing BOLD activation throughout the brain (Figure 2A). Notably, no significant neural activation was observed at the primary target region, but significant BOLD activation was observed in the contralateral DLPFC. This observation may suggest a potential compensatory mechanism, a phenomenon consistent with findings observed when TMS was applied to other targets and only affected distal sites (51,54). BOLD activation of ACC and auditory regions was weaker than that observed with 80% rMT stimulation, which could be explained by reduced levels of noise and pain during iTBS at 40% intensity. This aligns with our subjects' pain ratings during interleaved iTBS-fMRI (Figure S1); 80% rMT iTBS-DLPFC induced significantly greater pain compared with the

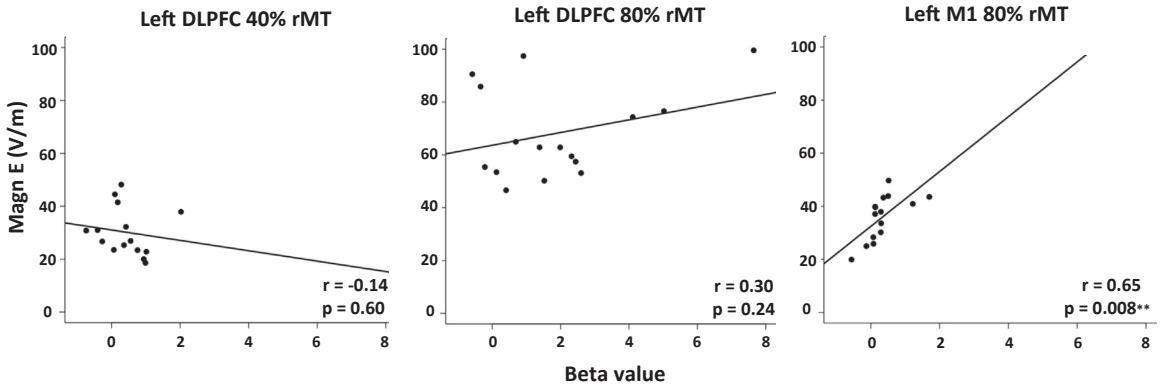

Figure 3. Correlation analysis of electric field magnitude (Magn E) and functional magnetic resonance imaging beta values in 40% resting motor threshold (rMT) dorsolateral prefrontal cortex (DLPFC), 80% rMT DLPFC, and 80% rMT primary motor cortex (M1) conditions. The 40% rMT DLPFC condition showed no correlation, with $r = -0.14$ ($p = .6$), and neither did the 80% rMT DLPFC condition, with $r = 0.3$ ($p = .24$), while in the M1 condition, a strong positive correlation was observed, with $r = 0.65$ ($p = .008$). $^{**}p < .01$.

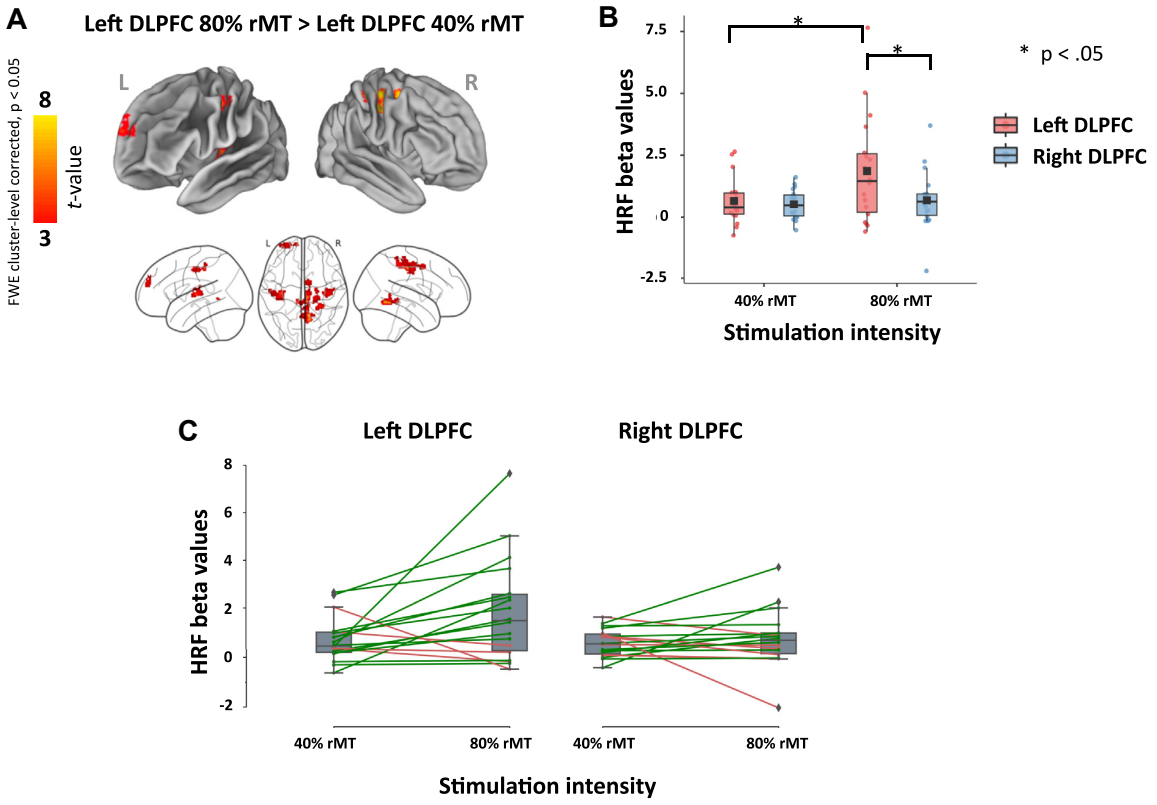

Figure 4. **(A)** For 80% resting motor threshold (rMT) stimulation intensity, there was a stronger activation in the left (L) dorsolateral prefrontal cortex (DLPFC) and a slightly stronger activation in auditory regions compared to 40% rMT stimulation intensity. **(B)** Average hemodynamic response function (HRF) beta values in the left and right (R) DLPFC regions of interest, demonstrating significant differences between low and high stimulation intensities in the left DLPFC. **(C)** Individual variability of HRF beta values for 40% and 80% rMT stimulation intensity over the left and right DLPFC regions of interest, respectively. The green lines indicate individuals who showed a stronger activation with 80% rMT intensity, while the red lines indicate individuals who showed a stronger activation with 40% rMT intensity. FWE, familywise error.

other two conditions. Recent findings in a sham condition by Tik *et al.* (31) showed intensity-dependent effects on somatosensory and auditory cortex regions but no effects on the ACC. Overall, our findings support the hypotheses that decreasing the strength of stimulation results in changes in remote areas as well (36,55,56). While demonstrating dose-dependent effects of iTBS, there is no established lower threshold for neurophysiological effects of iTBS. Thus, iTBS protocols with intensities below 80% rMT may depolarize subpopulations of interneurons and modulate cortex excitability (9).

As a second control condition, we included 80% rMT iTBS-M1 to identify regions that are activated by iTBS of the left DLPFC but not activated by 80% rMT iTBS of M1. As expected, we observed activation in the bilateral M1 and somatosensory cortex regions during iTBS-M1, consistent with previous research (57,58). However, we observed that the iTBS-M1 neural activity extended widely to the right DLPFC, contradicting a prior study that suggested that the effects of iTBS-M1 do not spread rostrally to the PFC (37). Nonetheless, our results align with previous findings indicating that M1 TMS can indeed propagate through anatomical projections to affect more distant regions such as the putamen (37,44,57).

Dose-Dependent Target Engagement and Interindividual Variability of E-Field With fMRI

To compare the interindividual dose-response relationship between M1 and DLPFC iTBS, MR-based E-field modeling was applied for both target sites and tested for a correlation with the fMRI beta value during iTBS. Only for the M1 was a significant positive correlation between fMRI BOLD activation and E-field magnitude found across subjects, while we did not observe such a correlation in the DLPFC conditions at either intensity. This finding was even more surprising because iTBS intensities are already personalized to the individual rMT. The most likely explanation for the difference between the M1 and left DLPFC targets in this respect is that the M1 target is functionally established (i.e., as a hotspot with the largest MEP amplitudes for the contralateral abductor pollicis brevis muscle), whereas the TMS coil position over the left DLPFC

followed anatomical landmarks (i.e., predefined MNI target). Thus, both factors, i.e., more variable positioning in relation to individual cortical structures and higher variability of functional connectivity in prefrontal as compared with motor networks (59), may contribute to the larger variation of BOLD activation in relation to E-field intensities for the 80% rMT iTBS-DLPFC condition. To reduce this variance in DLPFC targeting procedures, it is crucial to identify common biomarkers for rTMS therapeutic protocols and optimize personalized DLPFC targeting for clinical treatment. Several studies have shown that using fMRI to localize the DLPFC target region based on its anticorrelation with the subgenual ACC may represent an individualized target site for rTMS, resulting in improved psychiatric treatment outcomes (60–62). In addition, previous research has highlighted the variation in brain area depths (63), which our data also indicate with differences in coil-to-cortex distance between the DLPFC and M1 (see Figure S7). This underscores the importance of employing E-field modeling to adjust the TMS intensity across different brain regions, thereby ensuring stimulation of brain areas with equivalent effective strength as estimated for the M1 (38,64,65).

Furthermore, our findings suggest a dose-response relationship in the left DLPFC between 40% rMT and 80% rMT iTBS, in which higher stimulation intensity correlates with higher beta values. However, this pattern was not found for distant effects in the right DLPFC. In addition, we observed interindividual variability for the left DLPFC effect, with activation patterns differing among subjects at both 80% rMT and 40% rMT TMS intensities. For instance, not all subjects demonstrated consistently higher beta values with increased TMS intensity (Figure 4C). Such variability may offer insights into the varied responses to prefrontal TMS, but the current sample was too small for further analyzing this variability to reach meaningful conclusions.

Current and Previous Findings With Interleaved TMS-fMRI

In the study, 3 conditions featuring different stimulation locations and intensities showed widespread BOLD activation across multiple brain regions. This concurs with previous interleaved TMS-fMRI studies, with single pulses of TMS over the DLPFC leading to changes in BOLD signal across multiple brain areas, including the stimulated target and its contralateral region, subcortical regions, and auditory cortex (66,67). Furthermore, previous interleaved TMS-fMRI studies have also demonstrated a dose-response relationship between stimulation intensity and BOLD signals for M1 and DLPFC targets (26,32,44,51), aligning with our findings.

In addition, we assessed the feasibility of an ICA denoising strategy and compared it with our previous study without ICA denoising (35). Our observations revealed that 80% rMT iTBS-DLPFC had less extensive BOLD activation in stimulated and remote regions after implementing ICA denoising. ICA denoising has also been recommended as an essential step in concurrent TMS-fMRI (37). Various potential MRI artifacts can arise during data acquisition due to interactions with concurrent TMS. These artifacts may be attributed to factors such as magnetic susceptibility, vibration, thermal drift, leakage current originating from the TMS coil, coupling effects between the TMS device and the MRI hardware, and the echo-planar imaging sequence (27,28,68). These effects can be apparent as a reduced signal-to-noise ratio under the TMS coil. In some cases, image artifacts can occur, affecting data quality for durations ranging from milliseconds to minutes, and in extreme cases, even permanently (37). Here, we highlight a significant concern within the concurrent TMS-fMRI field that the potential data analysis method may induce a high type II error (false negatives), primarily attributable to factors such as motion artifacts or interaction between TMS and fMRI acquisition.

Limitations

We are aware that the current study has limitations: First, our findings may not be generalizable to other iTBS protocols, e.g., the Food and Drug Administration–cleared protocol for major depressive disorder, in which 120% rMT intensity (16) or longer iTBS sessions with 1800 stimuli were used. Second, the sample is small, and the study has limited power for conducting further secondary analyses. Thus, we may regard many of our findings as preliminary and hypothesis-generating. Third, it would be extremely challenging to disentangle direct neural activation by iTBS versus activation by sensory stimulation (e.g., noise from TMS and MRI or somatosensory artifacts and pain), novelty experience, or expectation, which might result, e.g., in large-scale activation observed in the ACC, putamen, and insula. Fourth, other potential sources of interindividual variability in our results may arise from biological differences between our healthy participants, such as gender, age, and brain state and structure, and furthermore, technical variability during the TMS-fMRI setup, e.g., TMS targeting, coil-to-cortex distance, and artificial induction between TMS and MRI. Additionally, heterogeneity in brain anatomy might be relevant as well, as indicated by interindividual differences in the coil-to-cortex distance (see Figure S7). At the analysis level, the inclusion of ICA denoising may introduce bias in removing ICs, potentially leading to variability in the sources detected. However, we still emphasize the importance of establishing an appropriate fMRI data preprocessing and analysis pipeline for future concurrent TMS-fMRI studies. Our study underscores the distinctive challenges presented by concurrent TMS-fMRI, e.g., the use of low-channel birdcage or thin-film surface coils during concurrent TMS-fMRI imaging sessions can lead to inferior MR image quality and incomplete coverage of the brain. Moreover, the interaction between TMS pulses and the MRI coil, particularly the high magnetic field and current leakage from TMS coil, can cause image distortion in milliseconds to seconds. This requires thorough attention to configuring concurrent TMS-fMRI sequences and during both pre- and postprocessing stages of data analysis.

Future Directions and Perspectives

The common challenges encountered in concurrent TMS-fMRI studies, including target engagement, complex setups, technical constraints, and the absence of an optimal sham condition, are also applicable to our study, as highlighted previously (28,35). At all levels, there is space for refining current interleaved TMS-fMRI methodology. The findings of the current study may therefore guide future development of experimental TMS-fMRI setups to investigate clinical iTBS protocols in

transdiagnostic samples and healthy subjects, with the overarching goal to better understand effects and mechanisms of therapeutic iTBS in relation to the individual brain connectivity and function. Concurrent TMS-fMRI represents a promising research area, as it holds the potential to identify biomarkers for therapeutic rTMS protocols and to leverage personalized treatment approaches.

Conclusions

This interleaved TMS-fMRI study revealed acute BOLD activation in DLPFC and M1 regions during a 600-stimuli iTBS session in healthy subjects, which was target and dose specific. Compared with iTBS over the M1, in which BOLD activation and iTBS E-field intensity were correlated, high interindividual variability was observed in this respect for iTBS of the left DLPFC. In addition, large-scale BOLD effects were found across all iTBS conditions, which not only may be due to nonspecific activation within the complex experimental setup, but also may be partially due to remote effects of the iTBS protocol. However, the differential impact of these factors cannot be further disentangled with the current study design. Our findings provide guidance for future studies to develop the TMS-fMRI approach toward a paradigm that enables mechanistic research on therapeutic rTMS protocols and a deeper understanding of the rTMS-brain interplay.

ACKNOWLEDGMENTS AND DISCLOSURES

This project was funded by the Federal Ministry of Education and Research within the ERA-NET NEURON program (Grant No. FKZ: 01EW1903: DisCoVeR) and the German Center for Mental Health (Grant No. 01EE2303, project MUC6). The procurement of the Prisma 3T MRI scanner was supported by the Deutsche Forschungsgemeinschaft (Grant No. INST 86/1739-1 FUGG). LB's work was part of the funding program of the Medical Faculty of LMU (FöFöLe Plus, Munich Clinician Scientist Program). MT's travel costs and research stays were supported by the visiting scholarship artificial intelligence programme (BaCaTeC 2022/01, Machine learning-based optimization for personalized brain stimulation therapy). PT's work was funded by the Deutsche Forschungsgemeinschaft (Grant No. TA 857/3-2).

K-YC: conceptualization, formal analysis, investigation, methodology, project administration, visualization, writing – original draft. MT: conceptualization, methodology, supervision, validation. YM-T: conceptualization, investigation, methodology, project administration. PT: writing – review & editing. TvH: visualization, writing – review & editing. PF: funding acquisition, supervision. FP: conceptualization, funding acquisition, methodology, project administration, resources, supervision, validation, writing – review & editing. LB: conceptualization, funding acquisition, methodology, project administration, resources, supervision, writing – review & editing. DK: conceptualization, formal analysis, funding acquisition, methodology, project administration, resources, supervision, validation, visualization, writing – review & editing.

We thank Linda Schuster, Zane Wilkinson, and Cuici Voon for assisting TMS-fMRI data collection and Larissa Behnke for E-field simulation data preprocessing. We thank Christian Windischberger (Center for Medical Physics and Biomedical Engineering at the Medical University of Vienna, Austria) for providing his comprehensive expertise in concurrent TMS-MRI, as well as Patrik Kunz (Localite GmbH, Bonn, Germany) and Matthias Kienle (MagVenture A/S, Farum, Denmark) for their kind support with the technical setup.

Access to the completed MRI data is available upon request. The data can be obtained upon formalizing a data sharing agreement, though not publicly accessible due to challenges in achieving complete anonymization. Unthresholded statistical maps of MRI data are provided on NeuroSynth.

This work is a part of K-YC's Ph.D. program at Munich Medical Research School. YM-T received remuneration from neuroCare Group AG as a part-time office worker. FP is a member of the European Scientific Advisory Board of BrainsWay Inc. (Jerusalem, Israel), and the International Scientific Advisory Board of Sooma (Helsinki, Finland); he has received speaker honoraria from Mag&More GmbH, the neuroCare Group (Munich, Germany), and BrainsWay Inc.; his lab has received support with equipment from neuroConn GmbH (Ilmenau, Germany), Mag&More GmbH, and BrainsWay Inc. PF has received grants and served as consultant, advisor, or continuing medical education speaker for Abbott, GlaxoSmithKline, Janssen, Essex, Lundbeck, Otsuka, Gedeon Richter, Servier, Takeda, the German Ministry of Science, and the German Ministry of Health. All other authors report no biomedical financial interests or potential conflicts of interest.

ARTICLE INFORMATION

From the Department of Psychiatry and Psychotherapy, LMU University Hospital, LMU Munich, Munich, Germany (K-YC, YM-T, TvH, PF, FP, LB, DK); Neuroimaging Core Unit Munich, LMU University Hospital, LMU Munich, Munich, Germany (K-YC, YM-T, TvH, PF, FP, LB, DK); German Center for Mental Health, Partner Site Munich-Augsburg, Germany (K-YC, YM-T, TvH, PF, FP, LB, DK); High Field MR Center, Center for Medical Physics and Biomedical Engineering, Medical University of Vienna, Vienna, Austria (MT); Brain Stimulation Lab, Department of Psychiatry and Behavioral Sciences, Stanford University, Stanford, California (MT); and Department of Psychology, LMU Munich, Munich, Germany (PT).

LB and DK contributed equally to this work.

Address correspondence to Frank Padberg, M.D., at frank.padberg@med.uni-muenchen.de.

Received Apr 29, 2024; revised Aug 8, 2024; accepted Aug 12, 2024.

Supplementary material cited in this article is available online at https://doi.org/10.1016/j.bpsc.2024.08.009.

REFERENCES

1. Larson J, Lynch G (1986): Induction of synaptic potentiation in hippocampus by patterned stimulation involves two events. Science 232:985–988.
2. Larson J, Lynch G (1989): Theta pattern stimulation and the induction of LTP: The sequence in which synapses are stimulated determines the degree to which they potentiate. Brain Res 489:49–58.
3. Capocchi G, Zampolini M, Larson J (1992): Theta burst stimulation is optimal for induction of LTP at both apical and basal dendritic synapses on hippocampal CA1 neurons. Brain Res 591:332–336.
4. Huang YZ, Rothwell JC (2004): The effect of short-duration bursts of high-frequency, low-intensity transcranial magnetic stimulation on the human motor cortex. Clin Neurophysiol 115:1069–1075.
5. Huang YZ, Edwards MJ, Rounis E, Bhatia KP, Rothwell JC (2005): Theta burst stimulation of the human motor cortex. Neuron 45: 201–206.
6. Huang YZ, Chen RS, Rothwell JC, Wen HY (2007): The after-effect of human theta burst stimulation is NMDA receptor dependent. Clin Neurophysiol 118:1028–1032.
7. Ishikawa S, Matsunaga K, Nakanishi R, Kawahira K, Murayama N, Tsuji S, *et al.* (2007): Effect of theta burst stimulation over the human sensorimotor cortex on motor and somatosensory evoked potentials. Clin Neurophysiol 118:1033–1043.
8. Labedi A, Benali A, Mix A, Neubacher U, Funke K (2014): Modulation of inhibitory activity markers by intermittent theta-burst stimulation in rat cortex is NMDA-receptor dependent. Brain Stimul 7:394–400.
9. Suppa A, Huang YZ, Funke K, Ridding MC, Cheeran B, Di Lazzaro V, *et al.* (2016): Ten years of theta burst stimulation in humans: Established knowledge, unknowns and prospects. Brain Stimul 9:323–335.
10. Schilberg L, Schuhmann T, Sack AT (2017): Interindividual variability and intraindividual reliability of intermittent theta burst stimulation-induced neuroplasticity mechanisms in the healthy brain. J Cogn Neurosci 29:1022–1032.
11. Li C, Huang Y, Bai Y, Tsai S, Su T, Cheng C (2019): Critical role of glutamatergic and GABAergic neurotransmission in the central mechanisms of theta-burst stimulation. Hum Brain Mapp 40:2001–2009.

12. Rounis E, Huang YZ (2020): Theta burst stimulation in humans: A need for better understanding effects of brain stimulation in health and disease. Exp Brain Res 238:1707–1714.
13. Neuteboom D, Zantvoord JB, Goya-Maldonado R, Wilkening J, Dols A, Van Exel E, *et al.* (2023): Accelerated intermittent theta burst stimulation in major depressive disorder: A systematic review. Psychiatry Res 327:115429.
14. Haiyang C, Liuqing S, Mei L, Chuntong Z, Mingjie L, Junjing M, *et al.* (2024): Reflections on "Theta burst stimulation for depression: A systematic review and network and pairwise meta-analysis" [published online Jul 23]. Mol Psychiatry.
15. Holzer M, Padberg F (2010): Intermittent theta burst stimulation (iTBS) ameliorates therapy-resistant depression: A case series. Brain Stimul 3:181–183.
16. Blumberger DM, Vila-Rodriguez F, Thorpe KE, Feffer K, Noda Y, Giacobbe P, *et al.* (2018): Effectiveness of theta burst versus high-frequency repetitive transcranial magnetic stimulation in patients with depression (THREE-D): A randomised non-inferiority trial. Lancet 391:1683–1692.
17. Chen L, Thomas EHX, Kaewpijit P, Miljevic A, Hughes R, Hahn L, *et al.* (2021): Accelerated theta burst stimulation for the treatment of depression: A randomised controlled trial. Brain Stimul 14:1095–1105.
18. Bulteau S, Laurin A, Pere M, Fayet G, Thomas-Ollivier V, Deschamps T, *et al.* (2022): Intermittent theta burst stimulation (iTBS) versus 10 Hz high-frequency repetitive transcranial magnetic stimulation (rTMS) to alleviate treatment-resistant unipolar depression: A randomized controlled trial (THETA-DEP). Brain Stimul 15:870–880.
19. Morriss R, Briley PM, Webster L, Abdelghani M, Barber S, Bates P, *et al.* (2024): Connectivity-guided intermittent theta burst versus repetitive transcranial magnetic stimulation for treatment-resistant depression: A randomized controlled trial. Nat Med 30:403–413.
20. Cash RFH, Cocchi L, Lv J, Wu Y, Fitzgerald PB, Zalesky A (2021): Personalized connectivity-guided DLPFC-TMS for depression: Advancing computational feasibility, precision and reproducibility. Hum Brain Mapp 42:4155–4172.
21. Elbau IG, Lynch CJ, Downar J, Vila-Rodriguez F, Power JD, Solomonov N, *et al.* (2023): Functional connectivity mapping for rTMS target selection in depression. Am J Psychiatry 180:230–240.
22. Cash RFH, Zalesky A (2024): Personalized and circuit-based transcranial magnetic stimulation: Evidence, controversies, and opportunities. Biol Psychiatry 95:510–522.
23. Bohning DE, Shastri A, McConnell K, Nahas Z, Lorberbaum J, Roberts D, *et al.* (1999): A combined TMS/fMRI study of intensity-dependent TMS over motor cortex. Biol Psychiatry 45:385–394.
24. Hanakawa T, Mima T, Matsumoto R, Abe M, Inouchi M, Urayama S i, *et al.* (2009): Stimulus-response profile during single-pulse transcranial magnetic stimulation to the primary motor cortex. Cereb Cortex 19:2605–2615.
25. Shitara H, Shinozaki T, Takagishi K, Honda M, Hanakawa T (2013): Movement and afferent representations in human motor areas: A simultaneous neuroimaging and transcranial magnetic/peripheral nerve-stimulation study. Front Hum Neurosci 7:554.
26. Navarro de Lara LI, Tik M, Woletz M, Frass-Kriegl R, Moser E, Laistler E, *et al.* (2017): High-sensitivity TMS/fMRI of the human motor cortex using a dedicated multichannel MR coil. NeuroImage 150:262–269.
27. Bergmann TO, Varatheeswaran R, Hanlon CA, Madsen KH, Thielscher A, Siebner HR (2021): Concurrent TMS-fMRI for causal network perturbation and proof of target engagement. NeuroImage 237:118093.
28. Mizutani-Tiebel Y, Tik M, Chang KY, Padberg F, Soldini A, Wilkinson Z, *et al.* (2022): Concurrent TMS-fMRI: Technical challenges, developments, and overview of previous studies. Front Psychiatry 13:825205.
29. Hawco C, Armony JL, Daskalakis ZJ, Berlim MT, Chakravarty MM, Pike GB, *et al.* (2017): Differing time of onset of concurrent TMS-fMRI during associative memory encoding: A measure of dynamic connectivity. Front Hum Neurosci 11:404.
30. Webler RD, Hamady C, Molnar C, Johnson K, Bonilha L, Anderson BS, *et al.* (2020): Decreased interhemispheric connectivity and increased cortical excitability in unmedicated schizophrenia: A prefrontal interleaved TMS fMRI study. Brain Stimul 13:1467–1475.
31. Tik M, Woletz M, Schuler AL, Vasileiadi M, Cash RFH, Zalesky A, *et al.* (2023): Acute TMS/fMRI response explains offline TMS network effects – An interleaved TMS-fMRI study. NeuroImage 267:119833.
32. Tik M, Vasileiadi M, Woletz M, Linhardt D, Schuler AL, Williams N, *et al.* (2023): Concurrent TMS/fMRI reveals individual DLPFC dose-response pattern. NeuroImage 282:120394.
33. Ge R, Humaira A, Gregory E, Alamian G, MacMillan EL, Barlow L, *et al.* (2022): Predictive value of acute neuroplastic response to rTMS in treatment outcome in depression: A concurrent TMS-fMRI trial. Am J Psychiatry 179:500–508.
34. Grosshagauer S, Woletz M, Vasileiadi M, Linhardt D, Nohava L, Schuler AL, *et al.* (2024): Chronometric TMS-fMRI of personalized left dorsolateral prefrontal target reveals state-dependency of subgenual anterior cingulate cortex effects [published online Mar 26]. Mol Psychiatry.
35. Chang KY, Tik M, Mizutani-Tiebel Y, Schuler AL, Taylor P, Campana M, *et al.* (2024): Neural response during prefrontal theta burst stimulation: Interleaved TMS-fMRI of full iTBS protocols. NeuroImage 291:120596.
36. Hawco C, Voineskos AN, Steeves JKE, Dickie EW, Viviano JD, Downar J, *et al.* (2018): Spread of activity following TMS is related to intrinsic resting connectivity to the salience network: A concurrent TMS-fMRI study. Cortex 108:160–172.
37. Riddle J, Scimeca JM, Pagnotta MF, Inglis B, Sheltraw D, Muse-Fisher C, *et al.* (2022): A guide for concurrent TMS-fMRI to investigate functional brain networks. Front Hum Neurosci 16:1050605.
38. Dannhauer M, Gomez LJ, Robins PL, Wang D, Hasan NI, Thielscher A, *et al.* (2024): Electric field modeling in personalizing transcranial magnetic stimulation interventions. Biol Psychiatry 95:494–501.
39. Navarro de Lara LI, Windischberger C, Kuehne A, Woletz M, Sieg J, Bestmann S, *et al.* (2015): A novel coil array for combined TMS/fMRI experiments at 3 T. Magn Reson Med 74:1492–1501.
40. Rossini PM, Burke D, Chen R, Cohen LG, Daskalakis Z, Di Iorio R, *et al.* (2015): Non-invasive electrical and magnetic stimulation of the brain, spinal cord, roots and peripheral nerves: Basic principles and procedures for routine clinical and research application. An updated report from an I.F.C.N. Committee. Clin Neurophysiol 126:1071–1107.
41. Marques JP, Kober T, Krueger G, van der Zwaag W, Van de Moortele PF, Gruetter R (2010): MP2RAGE, a self bias-field corrected sequence for improved segmentation and T1-mapping at high field. NeuroImage 49:1271–1281.
42. Jenkinson M, Beckmann CF, Behrens TEJ, Woolrich MW, Smith SM (2012): FSL. NeuroImage 62:782–790.
43. Mayka MA, Corcos DM, Leurgans SE, Vaillancourt DE (2006): Three-dimensional locations and boundaries of motor and premotor cortices as defined by functional brain imaging: A meta-analysis. NeuroImage 31:1453–1474.
44. Bestmann S, Baudewig J, Siebner HR, Rothwell JC, Frahm J (2004): Functional MRI of the immediate impact of transcranial magnetic stimulation on cortical and subcortical motor circuits. Eur J Neurosci 19:1950–1962.
45. Beynel L, Powers JP, Appelbaum LG (2020): Effects of repetitive transcranial magnetic stimulation on resting-state connectivity: A systematic review. NeuroImage 211:116596.
46. Downar J, Blumberger DM, Daskalakis ZJ (2016): The neural crossroads of psychiatric illness: An emerging target for brain stimulation. Trends Cogn Sci 20:107–120.
47. Duecker F, Sack AT (2015): Rethinking the role of sham TMS. Front Psychol 6:210.
48. Bagali K, Sreeraj VS, Mehta UM, Venkatasubramanian G, Thirthalli J (2023): Feasibility of intermediate theta burst stimulation as sham control in therapeutic transcranial magnetic stimulation studies. Asian J Psychiatry 79:103390.
49. Bohning DE, Shastri A, Nahas Z, Lorberbaum JP, Andersen SW, Dannels WR, *et al.* (1998): Echoplanar BOLD fMRI of brain activation induced by concurrent transcranial magnetic stimulation. Invest Radiol 33:336–340.
50. Baudewig J, Siebner HR, Bestmann S, Tergau F, Tings T, Paulus W, *et al.* (2001): Functional MRI of cortical activations induced by transcranial magnetic stimulation (TMS). Neuroreport 12:3543–3548.

51. Bestmann S, Baudewig J, Siebner HR, Rothwell JC, Frahm J (2003): Subthreshold high-frequency TMS of human primary motor cortex modulates interconnected frontal motor areas as detected by interleaved fMRI-TMS. NeuroImage 20:1685–1696.
52. Denslow S, Lomarev M, George MS, Bohning DE (2005): Cortical and subcortical brain effects of transcranial magnetic stimulation (TMS)-induced movement: An interleaved TMS/functional magnetic resonance imaging study. Biol Psychiatry 57:752–760.
53. Shitara H, Shinozaki T, Takagishi K, Honda M, Hanakawa T (2011): Time course and spatial distribution of fMRI signal changes during single-pulse transcranial magnetic stimulation to the primary motor cortex. NeuroImage 56:1469–1479.
54. Lee TG, D'Esposito M (2012): The dynamic nature of top-down signals originating from prefrontal cortex: A combined fMRI–TMS study. J Neurosci 32(44):15458–15466.
55. Nahas Z, Lomarev M, Roberts DR, Shastri A, Lorberbaum JP, Teneback C, *et al.* (2001): Unilateral left prefrontal transcranial magnetic stimulation (TMS) produces intensity-dependent bilateral effects as measured by interleaved BOLD fMRI. Biol Psychiatry 50:712–720.
56. Nettekoven C, Volz LJ, Kutscha M, Pool EM, Rehme AK, Eickhoff SB, *et al.* (2014): Dose-dependent effects of theta burst rTMS on cortical excitability and resting-state connectivity of the human motor system. J Neurosci 34:6849–6859.
57. Bestmann S, Baudewig J, Siebner HR, Rothwell JC, Frahm J (2005): BOLD MRI responses to repetitive TMS over human dorsal premotor cortex. NeuroImage 28:22–29.
58. Bestmann S, Swayne O, Blankenburg F, Ruff CC, Haggard P, Weiskopf N, *et al.* (2008): Dorsal premotor cortex exerts state-dependent causal influences on activity in contralateral primary motor and dorsal premotor cortex. Cereb Cortex 18:1281–1291.
59. Mueller S, Wang D, Fox MD, Yeo BTT, Sepulcre J, Sabuncu MR, *et al.* (2013): Individual variability in functional connectivity architecture of the human brain. Neuron 77:586–595.
60. Fox MD, Buckner RL, White MP, Greicius MD, Pascual-Leone A (2012): Efficacy of transcranial magnetic stimulation targets for depression is related to intrinsic functional connectivity with the subgenual cingulate. Biol Psychiatry 72:595–603.
61. Weigand A, Horn A, Caballero R, Cooke D, Stern AP, Taylor SF, *et al.* (2018): Prospective validation that subgenual connectivity predicts antidepressant efficacy of transcranial magnetic stimulation sites. Biol Psychiatry 84:28–37.
62. Cash RFH, Zalesky A, Thomson RH, Tian Y, Cocchi L, Fitzgerald PB (2019): Subgenual functional connectivity predicts antidepressant treatment response to transcranial magnetic stimulation: Independent validation and evaluation of personalization. Biol Psychiatry 86:e5–e7.
63. Stokes MG, Chambers CD, Gould IC, English T, McNaught E, McDonald O, *et al.* (2007): Distance-adjusted motor threshold for transcranial magnetic stimulation. Clin Neurophysiol 118:1617–1625.
64. Caulfield KA, Li X, George MS (2021): Four electric field modeling methods of dosing prefrontal transcranial magnetic stimulation (TMS): Introducing APEX MT dosimetry. Brain Stimul 14:1032–1034.
65. Numssen O, Kuhnke P, Weise K, Hartwigsen G (2024): Electric-field-based dosing for TMS. Imaging Neurosci 2:1–12.
66. Hanlon CA, Canterberry M, Taylor JJ, DeVries W, Li X, Brown TR, *et al.* (2013): Probing the frontostriatal loops involved in executive and limbic processing via interleaved tms and functional MRI at two prefrontal locations: A pilot study. PLoS One 8:e67917.
67. Dowdle LT, Brown TR, George MS, Hanlon CA (2018): Single pulse TMS to the DLPFC, compared to a matched sham control, induces a direct, causal increase in caudate, cingulate, and thalamic BOLD signal. Brain Stimul 11:789–796.
68. Weiskopf N, Josephs O, Ruff CC, Blankenburg F, Featherstone E, Thomas A, *et al.* (2009): Image artifacts in concurrent transcranial magnetic stimulation (TMS) and fMRI caused by leakage currents: Modeling and compensation. J Magn Reson Imaging 29:1211–1217.

References

Anderson, M. L., Kinnison, J., & Pessoa, L. (2013). Describing functional diversity of brain regions and brain networks. *NeuroImage*, *73*, 50–58. https://doi.org/10.1016/j.neuroimage.2013.01.071

Baeken, C., Duprat, R., Wu, G.-R., De Raedt, R., & Van Heeringen, K. (2017). Subgenual Anterior Cingulate–Medial Orbitofrontal Functional Connectivity in Medication-Resistant Major Depression: A Neurobiological Marker for Accelerated Intermittent Theta Burst Stimulation Treatment? *Biological Psychiatry: Cognitive Neuroscience and Neuroimaging*, *2*(7), 556–565. https://doi.org/10.1016/j.bpsc.2017.01.001

Baeken, C., Marinazzo, D., Wu, G.-R., Van Schuerbeek, P., De Mey, J., Marchetti, I., Vanderhasselt, M.-A., Remue, J., Luypaert, R., & De Raedt, R. (2014). Accelerated HF-rTMS in treatment-resistant unipolar depression: Insights from subgenual anterior cingulate functional connectivity. *The World Journal of Biological Psychiatry*, *15*(4), 286–297. https://doi.org/10.3109/15622975.2013.872295

Barker, A. T., Jalinous, R., & Freeston, I. L. (1985). Non-invasive magnetic stimulation of human motor cortex. *Lancet*, *1*(8437), 1106–1107. https://doi.org/10.1016/s0140-6736(85)92413-4

Bergmann, T. O., Varatheeswaran, R., Hanlon, C. A., Madsen, K. H., Thielscher, A., & Siebner, H. R. (2021). Concurrent TMS-fMRI for causal network perturbation and proof of target engagement. *NeuroImage*, *237*, 118093. https://doi.org/10.1016/j.neuroimage.2021.118093

Bestmann, S., Baudewig, J., Siebner, H. R., Rothwell, J. C., & Frahm, J. (2003). Subthreshold high-frequency TMS of human primary motor cortex modulates interconnected frontal motor areas as detected by interleaved fMRI-TMS. *NeuroImage*, *20*(3), 1685–1696. https://doi.org/10.1016/j.neuroimage.2003.07.028

Bestmann, S., Baudewig, J., Siebner, H. R., Rothwell, J. C., & Frahm, J. (2004). Functional MRI of the immediate impact of transcranial magnetic stimulation on cortical and subcortical motor circuits. *European Journal of Neuroscience*, *19*(7), 1950–1962. https://doi.org/10.1111/j.1460-9568.2004.03277.x

Blumberger, D. M., Vila-Rodriguez, F., Thorpe, K. E., Feffer, K., Noda, Y., Giacobbe, P., Knyahnytska, Y., Kennedy, S. H., Lam, R. W., Daskalakis, Z. J., & Downar, J. (2018). Effectiveness of theta burst versus high-frequency repetitive transcranial magnetic stimulation in patients with depression (THREE-D): A randomised non-inferiority trial. *The Lancet*, *391*(10131), 1683–1692. https://doi.org/10.1016/S0140-6736(18)30295-2

Bohning, D. E., Shastri, A., McConnell, K., Nahas, Z., Lorberbaum, J., Roberts, D., Teneback, C., Vincent, D., & George, M. (1999). A combined TMS/fMRI study of intensity-dependent TMS over motor cortex. *Biological Psychiatry*, *45*(4), 385–394. https://doi.org/10.1016/S0006-3223(98)00368-0

Bohning, D. E., Shastri, A., Nahas, Z., Lorberbaum, J. P., Andersen, S. W., Dannels, W. R., Haxthausen, E.-U., Vincent, D. J., & George, M. S. (1998). Echoplanar BOLD fMRI of Brain Activation Induced by Concurrent Transcranial Magnetic Stimulation. *Investigative Radiology*, *33*(6), 336–340.

Boroojerdi, B., Battaglia, F., Muellbacher, W., & Cohen, L. G. (2001). Mechanisms inØuencing stimulus-response properties of the human corticospinal system. *Clinical Neurophysiology*.

Brunoni, A. R., Chaimani, A., Moffa, A. H., Razza, L. B., Gattaz, W. F., Daskalakis, Z. J., & Carvalho, A. F. (2017). Repetitive Transcranial Magnetic Stimulation for the Acute Treatment of Major Depressive Episodes: A Systematic Review With Network Meta-analysis. *JAMA Psychiatry*, *74*(2), 143. https://doi.org/10.1001/jamapsychiatry.2016.3644

Cajavilca, C., Varon, J., & Sternbach, G. L. (2009). Luigi Galvani and the foundations of electrophysiology. *Resuscitation*, *80*(2), 159–162. https://doi.org/10.1016/j.resuscitation.2008.09.020

Chang, K.-Y., Tik, M., Mizutani-Tiebel, Y., Schuler, A.-L., Taylor, P., Campana, M., Vogelmann, U., Huber, B., Dechantsreiter, E., Thielscher, A., Bulubas, L., Padberg, F., & Keeser, D. (2024). Neural response during prefrontal theta burst stimulation: Interleaved TMS-fMRI of full iTBS protocols. *NeuroImage*, *291*, 120596. https://doi.org/10.1016/j.neuroimage.2024.120596

Chang, K.-Y., Tik, M., Mizutani-Tiebel, Y., Taylor, P., Van Hattem, T., Falkai, P., Padberg, F., Bulubas, L., & Keeser, D. (2024). Dose-dependent target engagement of a clinical iTBS protocol: An interleaved TMS-fMRI study in healthy subjects. *Biological Psychiatry: Cognitive Neuroscience and Neuroimaging*, S2451902224002441. https://doi.org/10.1016/j.bpsc.2024.08.009

Chistyakov, A. V., Kreinin, B., Marmor, S., Kaplan, B., Khatib, A., Darawsheh, N., Koren, D., Zaaroor, M., & Klein, E. (2015). Preliminary assessment of the therapeutic efficacy of continuous theta-burst magnetic stimulation (cTBS) in major depression: A double-blind sham-controlled study. *Journal of Affective Disorders*, *170*, 225–229. https://doi.org/10.1016/j.jad.2014.08.035

Cole, E. J., Phillips, A. L., Bentzley, B. S., Stimpson, K. H., Nejad, R., Barmak, F., Veerapal, C., Khan, N., Cherian, K., Felber, E., Brown, R., Choi, E., King, S., Pankow, H., Bishop, J. H., Azeez, A., Coetzee, J., Rapier, R., Odenwald, N., … Williams, N. R. (2022). Stanford Neuromodulation Therapy (SNT): A Double-Blind Randomized Controlled Trial. *American Journal of Psychiatry*, *179*(2), 132–141. https://doi.org/10.1176/appi.ajp.2021.20101429

Cole, E. J., Stimpson, K. H., Bentzley, B. S., Gulser, M., Cherian, K., Tischler, C., Nejad, R., Pankow, H., Choi, E., Aaron, H., Espil, F. M., Pannu, J., Xiao, X., Duvio, D., Solvason, H. B., Hawkins, J., Guerra, A., Jo, B., Raj, K. S., … Williams, N. R. (2020). Stanford Accelerated Intelligent Neuromodulation Therapy for Treatment-Resistant Depression. *American Journal of Psychiatry*, *177*(8), 716–726. https://doi.org/10.1176/appi.ajp.2019.19070720

Di Lazzaro, V., Dileone, M., Pilato, F., Capone, F., Musumeci, G., Ranieri, F., Ricci, V., Bria, P., Di Iorio, R., De Waure, C., Pasqualetti, P., & Profice, P. (2011). Modulation of motor cortex neuronal networks by rTMS: Comparison of local and remote effects of six different protocols of stimulation. *Journal of Neurophysiology*, *105*(5), 2150–2156. https://doi.org/10.1152/jn.00781.2010

Dowdle, L. T., Brown, T. R., George, M. S., & Hanlon, C. A. (2018). Single pulse TMS to the DLPFC, compared to a matched sham control, induces a direct, causal increase in caudate, cingulate, and thalamic BOLD signal. *Brain Stimulation*, *11*(4), 789–796. https://doi.org/10.1016/j.brs.2018.02.014

Eshel, N., Keller, C. J., Wu, W., Jiang, J., Mills-Finnerty, C., Huemer, J., Wright, R., Fonzo, G. A., Ichikawa, N., Carreon, D., Wong, M., Yee, A., Shpigel, E., Guo, Y., McTeague, L., Maron-Katz, A., & Etkin, A. (2020). Global connectivity and local excitability changes underlie antidepressant effects of repetitive transcranial magnetic stimulation. *Neuropsychopharmacology*, *45*(6), Article 6. https://doi.org/10.1038/s41386-020-0633-z

Fox, M. D., Buckner, R. L., White, M. P., Greicius, M. D., & Pascual-Leone, A. (2012). Efficacy of Transcranial Magnetic Stimulation Targets for Depression Is Related to Intrinsic Functional Connectivity with the Subgenual Cingulate. *Biological Psychiatry*, *72*(7), 595–603. https://doi.org/10.1016/j.biopsych.2012.04.028

Frith, C., & Dolan, R. (1996). The role of the prefrontal cortex in higher cognitive functions. *Cognitive Brain Research*, *5*(1–2), 175–181. https://doi.org/10.1016/S0926-6410(96)00054-7

Ge, R., Downar, J., Blumberger, D. M., Daskalakis, Z. J., & Vila-Rodriguez, F. (2020). Functional connectivity of the anterior cingulate cortex predicts treatment outcome for rTMS in treatment-resistant depression at 3-month follow-up. *Brain Stimulation*, *13*(1), 206–214. https://doi.org/10.1016/j.brs.2019.10.012

George, M. S., Lisanby, S. H., Avery, D., McDonald, W. M., Durkalski, V., Pavlicova, M., Anderson, B., Nahas, Z., Bulow, P., Zarkowski, P., Holtzheimer, P. E., Schwartz, T., & Sackeim, H. A. (2010). Daily Left Prefrontal Transcranial Magnetic Stimulation Therapy for Major Depressive Disorder: A Sham-Controlled Randomized Trial. *Archives of General Psychiatry*, *67*(5), 507. https://doi.org/10.1001/archgenpsychiatry.2010.46

George, M. S., Wassermann, E. M., Williams, W. A., Callahan, A., Ketter, T. A., Basser, P., Hallett, M., & Post, R. M. (1995). Daily repetitive transcranial magnetic stimulation (rTMS) improves mood in depression. *Neuroreport: An International Journal for the Rapid Communication of Research in Neuroscience*, *6*(14), 1853–1856. https://doi.org/10.1097/00001756-199510020-00008

Hanlon, C. A., Canterberry, M., Taylor, J. J., DeVries, W., Li, X., Brown, T. R., & George, M. S. (2013). Probing the Frontostriatal Loops Involved in Executive and Limbic Processing via Interleaved TMS and Functional MRI at Two Prefrontal Locations: A Pilot Study. *PLoS ONE*, *8*(7), e67917. https://doi.org/10.1371/journal.pone.0067917

Holzer, M., & Padberg, F. (2010). Intermittent theta burst stimulation (iTBS) ameliorates therapy-resistant depression: A case series. *Brain Stimulation*, *3*(3), 181–183. https://doi.org/10.1016/j.brs.2009.10.004

Hoogendam, J. M., Ramakers, G. M. J., & Di Lazzaro, V. (2010). Physiology of repetitive transcranial magnetic stimulation of the human brain. *Brain Stimulation*, *3*(2), 95–118. https://doi.org/10.1016/j.brs.2009.10.005

Huang, Y.-Z., Edwards, M. J., Rounis, E., Bhatia, K. P., & Rothwell, J. C. (2005). Theta Burst Stimulation of the Human Motor Cortex. *Neuron*, *45*(2), 201–206. https://doi.org/10.1016/j.neuron.2004.12.033

Klomjai, W., Katz, R., & Lackmy-Vallée, A. (2015). Basic principles of transcranial magnetic stimulation (TMS) and repetitive TMS (rTMS). *Annals of Physical and Rehabilitation Medicine*, *58*(4), 208–213. https://doi.org/10.1016/j.rehab.2015.05.005

Lee, L., Siebner, H., & Bestmann, S. (2006). Rapid Modulation of Distributed Brain Activity by Transcranial Magnetic Stimulation of Human Motor Cortex. *Behavioural Neurology*, *17*(3–4), 135–148. https://doi.org/10.1155/2006/287276

Li, X., Nahas, Z., Kozel, F. A., Anderson, B., Bohning, D. E., & George, M. S. (2004). Acute left prefrontal transcranial magnetic stimulation in depressed patients is associated with immediately increased activity in prefrontal cortical as well as subcortical regions. *Biological Psychiatry*, *55*(9), 882–890. https://doi.org/10.1016/j.biopsych.2004.01.017

Liston, C., Chen, A. C., Zebley, B. D., Drysdale, A. T., Gordon, R., Leuchter, B., Voss, H. U., Casey, B. J., Etkin, A., & Dubin, M. J. (2014). Default Mode Network Mechanisms of Transcranial Magnetic Stimulation in Depression. *Biological Psychiatry*, *76*(7), 517–526. https://doi.org/10.1016/j.biopsych.2014.01.023

Mizutani-Tiebel, Y., Tik, M., Chang, K.-Y., Padberg, F., Soldini, A., Wilkinson, Z., Voon, C. C., Bulubas, L., Windischberger, C., & Keeser, D. (2022). Concurrent TMS-fMRI: Technical Challenges, Developments, and Overview of Previous Studies. *Frontiers in Psychiatry*, *13*, 825205. https://doi.org/10.3389/fpsyt.2022.825205

Nahas, Z., Lomarev, M., Roberts, D. R., Shastri, A., Lorberbaum, J. P., Teneback, C., McConnell, K., Vincent, D. J., Li, X., George, M. S., & Bohning, D. E. (2001). Unilateral left prefrontal transcranial magnetic stimulation (TMS) produces intensity-dependent bilateral effects as measured by interleaved BOLD fMRI. *Biological Psychiatry*, *50*(9), 712–720. https://doi.org/10.1016/S0006-3223(01)01199-4

Navarro de Lara, L. I., Tik, M., Woletz, M., Frass-Kriegl, R., Moser, E., Laistler, E., & Windischberger, C. (2017). High-sensitivity TMS/fMRI of the Human Motor Cortex Using a Dedicated Multichannel MR Coil. *NeuroImage*, *150*, 262–269. https://doi.org/10.1016/j.neuroimage.2017.02.062

Navarro de Lara, L. I., Windischberger, C., Kuehne, A., Woletz, M., Sieg, J., Bestmann, S., Weiskopf, N., Strasser, B., Moser, E., & Laistler, E. (2015). A novel coil array for combined TMS/fMRI experiments at 3 T. *Magnetic Resonance in Medicine*, *74*(5), 1492–1501. https://doi.org/10.1002/mrm.25535

O'Reardon, J. P., Solvason, H. B., Janicak, P. G., Sampson, S., Isenberg, K. E., Nahas, Z., McDonald, W. M., Avery, D., Fitzgerald, P. B., Loo, C., Demitrack, M. A., George, M. S., & Sackeim, H. A. (2007). Efficacy and safety of transcranial magnetic stimulation in the acute treatment of major depression: A multisite randomized controlled trial. *Biological Psychiatry*, *62*(11), 1208–1216. https://doi.org/10.1016/j.biopsych.2007.01.018

Padberg, F., & George, M. S. (2009). Repetitive transcranial magnetic stimulation of the prefrontal cortex in depression. *Experimental Neurology*, *219*(1), 2–13. https://doi.org/10.1016/j.expneurol.2009.04.020

Pridmore, S., Fernandes Filho, J. A., Nahas, Z., Liberatos, C., & George, M. S. *. (1998). Motor Threshold in Transcranial Magnetic Stimulation A Comparison of a Neurophysiological Method and a Visualization of Movement Method. *The Journal of ECT*, *14*(1), p25-27.

Riddle, J., Scimeca, J. M., Pagnotta, M. F., Inglis, B., Sheltraw, D., Muse-Fisher, C., & D'Esposito, M. (2022). A guide for concurrent TMS-fMRI to investigate functional brain networks. *Frontiers in Human Neuroscience*, *16*, 1050605. https://doi.org/10.3389/fnhum.2022.1050605

Robertson, E. M., Théoret, H., & Pascual-Leone, A. (2003). Studies in Cognition: The Problems Solved and Created by Transcranial Magnetic Stimulation. *Journal of Cognitive Neuroscience*, *15*(7), 948–960. https://doi.org/10.1162/089892903770007344

Rossi, S., Hallett, M., Rossini, P. M., & Pascual-Leone, A. (2009). Safety, ethical considerations, and application guidelines for the use of transcranial magnetic stimulation in clinical practice and research. *Clinical Neurophysiology*, *120*(12), 2008–2039. https://doi.org/10.1016/j.clinph.2009.08.016

Rossini, P. M., Barker, A. T., Berardelli, A., Caramia, M. D., Caruso, G., Cracco, R. Q., Dimitrijević, M. R., Hallett, M., Katayama, Y., & Lücking, C. H. (1994). Non-invasive electrical and magnetic stimulation of the brain, spinal cord and roots: Basic principles and procedures for routine clinical application. Report of an IFCN committee. *Electroencephalography and Clinical Neurophysiology*, *91*(2), 79–92. https://doi.org/10.1016/0013-4694(94)90029-9

Salomons, T. V., Dunlop, K., Kennedy, S. H., Flint, A., Geraci, J., Giacobbe, P., & Downar, J. (2014). Resting-State Cortico-Thalamic-Striatal Connectivity Predicts Response to Dorsomedial Prefrontal rTMS in Major Depressive Disorder. *Neuropsychopharmacology*, *39*(2), 488–498. https://doi.org/10.1038/npp.2013.222

Suppa, A., Huang, Y.-Z., Funke, K., Ridding, M. C., Cheeran, B., Di Lazzaro, V., Ziemann, U., & Rothwell, J. C. (2016). Ten Years of Theta Burst Stimulation in Humans: Established Knowledge, Unknowns and Prospects. *Brain Stimulation*, *9*(3), 323–335. https://doi.org/10.1016/j.brs.2016.01.006

Tik, M., Hoffmann, A., Sladky, R., Tomova, L., Hummer, A., Navarro de Lara, L., Bukowski, H., Pripfl, J., Biswal, B., Lamm, C., & Windischberger, C. (2017). Towards understanding rTMS mechanism of action: Stimulation of the DLPFC causes network-specific increase in functional connectivity. *NeuroImage*, *162*, 289–296. https://doi.org/10.1016/j.neuroimage.2017.09.022

Tik, M., Vasileiadi, M., Woletz, M., Linhardt, D., Schuler, A.-L., Williams, N., & Windischberger, C. (2023). Concurrent TMS/fMRI reveals individual DLPFC dose-response pattern. *NeuroImage*, 120394. https://doi.org/10.1016/j.neuroimage.2023.120394

Tik, M., Woletz, M., Schuler, A.-L., Vasileiadi, M., Cash, R. F. H., Zalesky, A., Lamm, C., & Windischberger, C. (2023). Acute TMS/fMRI response explains offline TMS network effects – An interleaved TMS-fMRI study. *NeuroImage*, *267*, 119833. https://doi.org/10.1016/j.neuroimage.2022.119833

Tsoucalas, G., Karamanou, M., Lymperi, M., Gennimata, V., & Androutsos, G. (2014). The “torpedo” effect in medicine. *International Maritime Health*, *65*(2), 65–67. https://doi.org/10.5603/IMH.2014.0015

Tura, A., & Goya-Maldonado, R. (2023). Brain connectivity in major depressive disorder: A precision component of treatment modalities? *Translational Psychiatry*, *13*(1), 196. https://doi.org/10.1038/s41398-023-02499-y

Vidal-Dourado, M., Conforto, A. B., Caboclo, L. O. S. F., Scaff, M., Guilhoto, L. M. D. F. F., & Yacubian, E. M. T. (2014). Magnetic Fields in Noninvasive Brain Stimulation. *The Neuroscientist*, *20*(2), 112–121. https://doi.org/10.1177/1073858413491145

Vink, J. J. T., Mandija, S., Petrov, P. I., van den Berg, C. A. T., Sommer, I. E. C., & Neggers, S. F. W. (2018). A novel concurrent TMS-fMRI method to reveal propagation patterns of prefrontal magnetic brain stimulation. *Human Brain Mapping*, *39*(11), 4580–4592. https://doi.org/10.1002/hbm.24307

Weigand, A., Horn, A., Caballero, R., Cooke, D., Stern, A. P., Taylor, S. F., Press, D., Pascual-Leone, A., & Fox, M. D. (2018). Prospective Validation That Subgenual Connectivity Predicts Antidepressant Efficacy of Transcranial Magnetic Stimulation Sites. *Biological Psychiatry*, *84*(1), 28–37. https://doi.org/10.1016/j.biopsych.2017.10.028

Westin, G. G., Bassi, B. D., Lisanby, S. H., & Luber, B. (2014). Determination of motor threshold using visual observation overestimates transcranial magnetic stimulation dosage: Safety implications. *Clinical Neurophysiology*, *125*(1), 142–147. https://doi.org/10.1016/j.clinph.2013.06.187

Appendix A: Paper III

Concurrent TMS-fMRI: Technical Challenges, Developments, and Overview of Previous Studies

frontiers | Frontiers in Psychiatry

REVIEW
published: 21 April 2022
doi: 10.3389/fpsyt.2022.825205

Concurrent TMS-fMRI: Technical Challenges, Developments, and Overview of Previous Studies

Yuki Mizutani-Tiebel[1,2]*, *Martin Tik*[3], *Kai-Yen Chang*[1,2], *Frank Padberg*[1,2], *Aldo Soldini*[1,2,4], *Zane Wilkinson*[1,2], *Cui Ci Voon*[1,2], *Lucia Bulubas*[1,2,4], *Christian Windischberger*[3] and *Daniel Keeser*[1,2,5]

[1] Department of Psychiatry and Psychotherapy, University Hospital LMU, Munich, Germany, [2] Neuroimaging Core Unit Munich - NICUM, University Hospital LMU, Munich, Germany, [3] High Field MR Center, Center for Medical Physics and Biomedical Engineering, Medical University of Vienna, Vienna, Austria, [4] International Max Planck Research School for Translational Psychiatry, Munich, Germany, [5] Department of Radiology, University Hospital LMU, Munich, Germany

OPEN ACCESS

Edited by:
Stefan Borgwardt,
University of Lübeck, Germany

Reviewed by:
Elisa Kallioniemi,
University of Texas Southwestern Medical Center, United States
Jade Buse Jackson,
University of Cambridge, United Kingdom
Anna-Lisa Schuler,
San Camillo Hospital (IRCCS), Italy

***Correspondence:**
Yuki Mizutani-Tiebel
yuki.tiebel@med.uni-muenchen.de

Specialty section:
This article was submitted to Neuroimaging and Stimulation, a section of the journal Frontiers in Psychiatry

Received: 30 November 2021
Accepted: 09 March 2022
Published: 21 April 2022

Citation:
Mizutani-Tiebel Y, Tik M, Chang K-Y, Padberg F, Soldini A, Wilkinson Z, Voon CC, Bulubas L, Windischberger C and Keeser D (2022) Concurrent TMS-fMRI: Technical Challenges, Developments, and Overview of Previous Studies. Front. Psychiatry 13:825205. doi: 10.3389/fpsyt.2022.825205

Transcranial magnetic stimulation (TMS) is a promising treatment modality for psychiatric and neurological disorders. Repetitive TMS (rTMS) is widely used for the treatment of psychiatric and neurological diseases, such as depression, motor stroke, and neuropathic pain. However, the underlying mechanisms of rTMS-mediated neuronal modulation are not fully understood. In this respect, concurrent or simultaneous TMS-fMRI, in which TMS is applied during functional magnetic resonance imaging (fMRI), is a viable tool to gain insights, as it enables an investigation of the immediate effects of TMS. Concurrent application of TMS during neuroimaging usually causes severe artifacts due to magnetic field inhomogeneities induced by TMS. However, by carefully interleaving the TMS pulses with MR signal acquisition in the way that these are far enough apart, we can avoid any image distortions. While the very first feasibility studies date back to the 1990s, recent developments in coil hardware and acquisition techniques have boosted the number of TMS-fMRI applications. As such, a concurrent application requires expertise in both TMS and MRI mechanisms and sequencing, and the hurdle of initial technical set up and maintenance remains high. This review gives a comprehensive overview of concurrent TMS-fMRI techniques by collecting (1) basic information, (2) technical challenges and developments, (3) an overview of findings reported so far using concurrent TMS-fMRI, and (4) current limitations and our suggestions for improvement. By sharing this review, we hope to attract the interest of researchers from various backgrounds and create an educational knowledge base.

Keywords: concurrent TMS-fMRI, interleaved TMS-fMRI, functional MRI (fMRI), transcranial magnetic stimulation (TMS), review

BASIC INFORMATION

Why Should TMS Be Combined With FMRI?

Transcranial magnetic stimulation (TMS) is a non-invasive transcranial brain stimulation (NIBS) technique, which modulates neuronal activity by applying electromagnetic pulses to the scalp. A unique strength of TMS is that it allows for an experimental *in-vivo* investigation by depolarizing neurons to induce action potentials. TMS can be applied either as single-pulse TMS (sTMS) or

repetitive TMS (rTMS). sTMS is often used to investigate the functional role of a particular region by interfering or otherwise modulating specific cortical activities. Various rTMS protocols can be administered; for example, low-frequency and high-frequency rTMS, which are commonly used to induce inhibitory or facilitatory effects, respectively (1). rTMS is frequently used as a treatment for neurological and psychiatric patients (2). The most recent guideline for the therapeutic usage of rTMS shows level A evidence for depression, motor stroke, and neuropathic pain, as well as level B evidence in fibromyalgia, Parkinson's disease, multiple sclerosis, and post-traumatic stress disorder (2). The U.S. Food and Drug Administration (FDA) has approved rTMS as a therapeutic intervention for pharmacotherapy-non-responsive major depressive disorder (MDD) (3–5), obsessive-compulsive disorder (OCD) (6), smoking cessation (7), and migraine (8). Recently, intermittent theta-burst stimulation (iTBS), an rTMS variant, has also been approved by the FDA for depression therapy. Theta-burst stimulation (TBS) replicates a typical firing pattern of hippocampal neurons during the learning process. Among the TBS protocols, iTBS is a very short (e.g., 3 min) and safe protocol that mimics hippocampal TBS patterns to induce long-term potentiation (LTP) in basic neurophysiology (9, 10), and exerts, presumably at least, equally robust post-stimulation effects compared to longer standard protocols (3, 11).

Although rTMS is already used in therapy, the mechanism of TMS-mediated neuronal modulation is not yet fully understood. Over the last decades, various neuroimaging techniques have been combined with TMS to investigate neuronal activation changes due to stimulation: electroencephalography (EEG), near-infrared spectroscopy (NIRS), positron emission tomography (PET), and functional magnetic resonance imaging (fMRI) (12, 13). However, despite the importance of fMRI for mapping neuronal activity, the majority of the studies to date involve concurrent TMS-EEG (14, 15). Nonetheless, compared to EEG, fMRI boasts superior spatial resolution, especially when functional connectivity is of interest. A combination of TMS and fMRI can provide us with meaningful information that helps us elucidate the underlying mechanisms of TMS-mediated neuronal modulation.

How Can TMS Be Concurrently Applied With FMRI?

As fMRI data quality heavily depends on magnetic field homogeneity, concurrent application of strong TMS pulses during imaging would cause severe artifacts. Hence, TMS is often applied offline, i.e., separately from the actual imaging procedure, and cerebral activation after the TMS session is compared to a pre-TMS baseline. Obviously, such approaches are limited in their sensitivity for capturing post-stimulation effects, and immediate stimulation effects are likely to be undetected.

To address this problem, MR-compatible TMS systems have been developed which enable online TMS experiments, where TMS is applied inside the MR-scanner during image acquisition. **Figure 1** shows an example of such a TMS-fMRI setting. The TMS stimulator typically stays outside the MR room. A long cable through the wall connects the TMS main unit with the TMS coil in the scanner bore. The MR head coil can be set up in various ways (discussed in section MR Head Coil and TMS Positioning System), but in this specific example, the thin MR coil is attached to the TMS coil. This TMS-fMRI setting allows subjects to remain in the MR bore for the entire duration of the MRI scan acquisition while receiving TMS inside the scanner bore.

Furthermore, careful interleaving of TMS pulses with MR signal acquisition enables continuous fMRI scanning. In the field of TMS research, this technique is referred to as either concurrent or simultaneous TMS-fMRI with off-/online block or interleaved designs. The feasibility of the concurrent TMS-fMRI method was first demonstrated in 1998 (17) when TMS pulses were successfully applied during the gap time between slice acquisitions. Currently, there are three possible methods of concurrent TMS-fMRI approach (**Figure 2**).

Figure 2A illustrates how to interfere with echo-planar imaging (EPI) slices using TMS. Perturbed EPI slices (indicated by orange crosses in **Figure 2A**) are sacrificed and replaced by interpolation of slices, typically from the volumes before and after the volume of interest (indicated by orange EPI slices in **Figure 2A**). The advantage of this method is the high flexibility for stimulating at any time regardless of EPI timing, whereas the disadvantage is that it requires a high level of post-processing capabilities to detect the damaged EPI slices and replace them.

Figure 2B illustrates how to insert a gap time between EPI slices and then apply TMS pulses during this time. The advantage of this method is that no EPI slices are sacrificed, whereas the disadvantage is that the number of stimulations is limited as it needs to fit within the gap time. By virtue of these gap times, the whole TMS-fMRI protocol tends to become longer.

Figure 2C illustrates how to interleave TMS pulses with EPI slices. The advantage of this method is that it allows for continuous stimulation, which is often used as a therapeutic protocol. On the other hand, the disadvantage is that reliable hardware and software are essential, as the pulses must be controlled precisely.

TECHNICAL CONSIDERATIONS

One of the most critical considerations in concurrent TMS-fMRI experiments concerns the TMS coil to be used in the MR scanner, particularly the materials used in its manufacturing. This is due to two reasons: (1) to guarantee the safety of the subjects by avoiding any attraction forces of ferromagnetic material in the magnetic field; (2) to withstand Lorentz forces during the stimulation within the high magnetic field inside the MR scanner. Therefore, coil composition is suggested to include a copper coil and a robust plastic housing to make the coil safe, durable in the magnetic field, and affordable (18, 19).

A further challenge with combining TMS and fMRI is to avoid artifacts in the image induced by TMS. The source of artifacts and noise caused by TMS can be categorized into three domains: (1) magnetic field, (2) radio frequency (RF) noise, and (3) leakage currents. These factors are critical for intra-individual test-retest reliability of fMRI data in response to TMS (20). In the

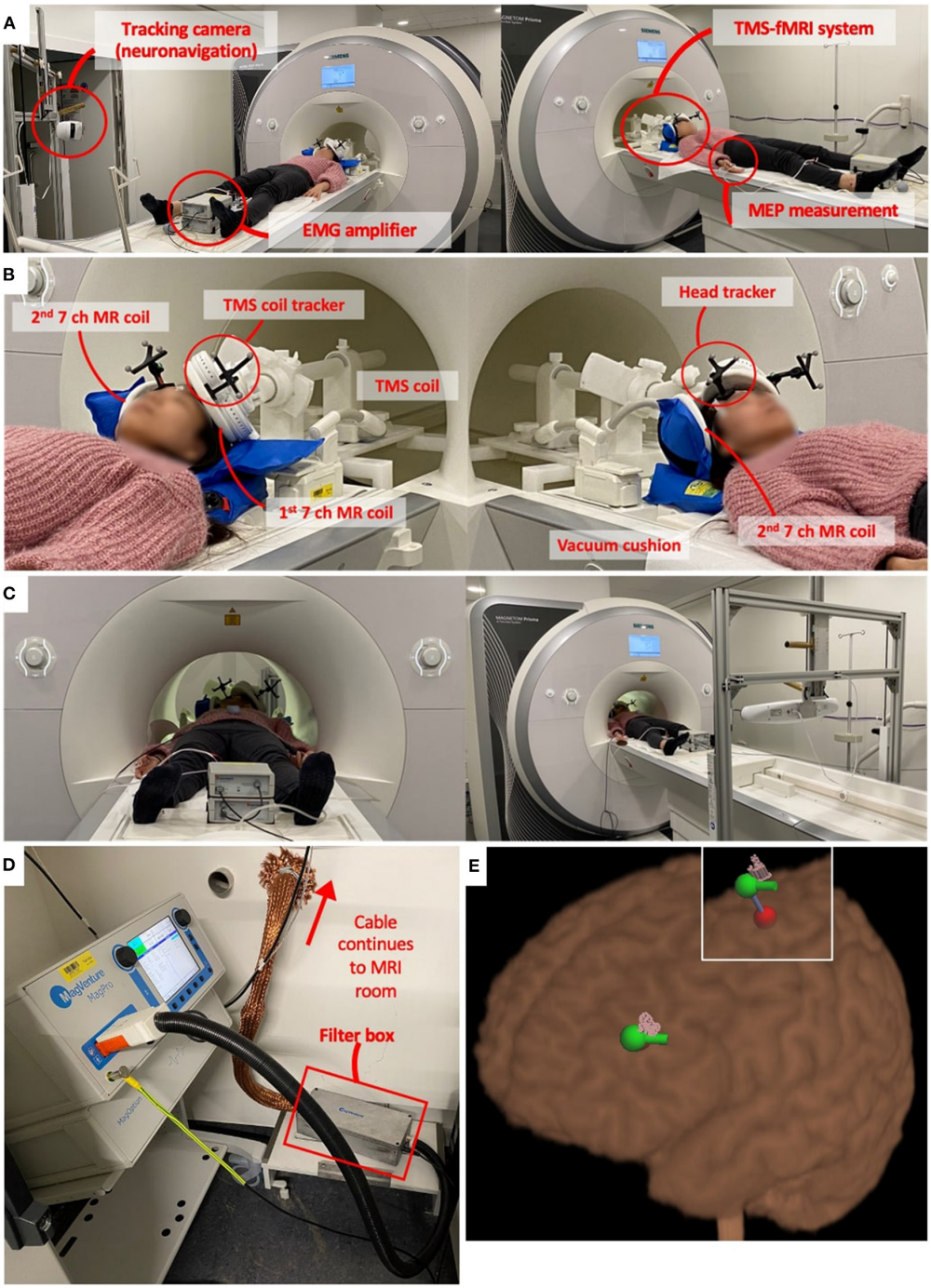

FIGURE 1 | Example of TMS-fMRI set up. **(A)** This particular example of TMS-fMRI set up includes MR compatible TMS coils (Magventure, Farum, Denmark), MR coils (16), neuronavigation system (Localite, Bonn, Germany), and a BrainAmp ExG MR amplifier (BrainProducts, Gilching, Germany) for electromyographic (EMG) measurements to determine motor threshold (MT). **(B)** TMS coil is mounted on a holder which goes in the bore of the scanner. The holder system is attached to the scanner bed so that it moves together. The MR head coil, in this example, is two thin and flat seven channel coils. One is attached below the TMS coil, and the

(Continued)

FIGURE 1 | other is stabilized on the other side of the head using a vacuum pillow. Two trackers on the forehead and coil enable neuronavigation. **(C)** EMG amplifier continues to record the motor evoked potential (MEP) and the neuronavigation system tracks the TMS coil location throughout the scanning session. **(D)** TMS device remains in the technical room as it is ferromagnetic. The TMS coil is connected to the MRI room by a 6-m cable through a hole in the wall. The cable is covered with a filter tube, and a filter box is installed along the cable. **(E)** Neuronavigation system shows the location of the stimulation. The red dot is calculated with a coordinate that defines the target point. By defining the coil orientation, it calculates the entering point which is the green dot with the green bar showing the coil handle orientation. The pink pins show the actual stimulation location, which is recorded each time a TMS pulse is applied during the TMS-fMRI session. These pink pins can be recorded during the concurrent TMS-fMRI session and can be used for the post-analysis as far as the head and coil trackers are visible in the MR bore as shown in panel **(C)**.

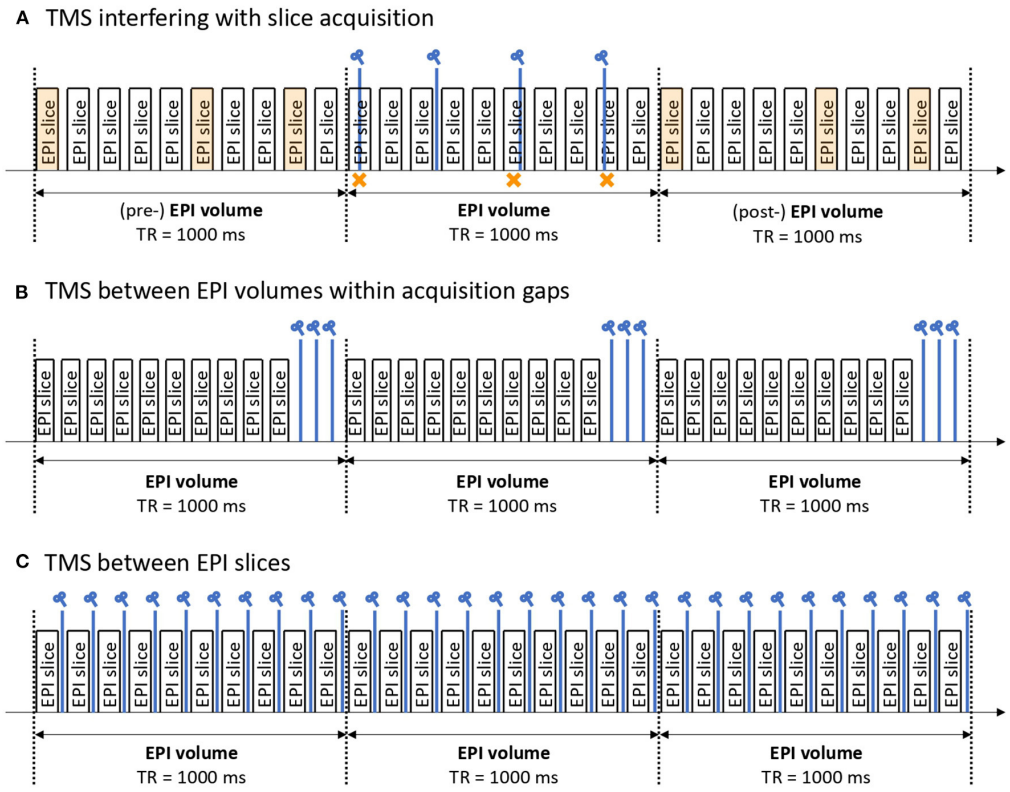

FIGURE 2 | Example of concurrent TMS-fMRI protocols. There are three possible ways to apply TMS pulses during fMRI simultaneously. **(A)** A method enabling TMS to interfere with EPI slices. Perturbed EPI slices (indicated by an orange cross) are sacrificed and replaced by slice interpolation, typically from the volumes before and after the volume of interest (indicated by orange EPI slices). Advantages: High flexibility to stimulate at any time regardless of EPI timing. Disadvantages: It requires a high level of post-processing capabilities to detect the damaged EPI slices and replace them. **(B)** A method to insert a gap time between EPI slices and apply TMS pulses meanwhile. Advantages: No EPI slices are sacrificed. Disadvantages: The number of stimulations is limited as it needs to fit in the gap time. Hence, the whole TMS-fMRI protocol tends to be longer. **(C)** A method to interleave TMS pulses with EPI slices. Advantages: It allows for continuous stimulation which is often used as a therapeutic protocol. Disadvantages: Reliable hardware and software are essential as the pulses must be controlled precisely.

following, appropriate technical suggestions and developments are discussed.

Controlling for Magnetic Field Interference

Data quality in functional MRI depends on a high homogeneity of the static magnetic field. As TMS coils are heavy metallic objects, field homogeneity is compromised by the TMS coil via susceptibility-related field changes. Field inhomogeneities lead not only to signal losses, via intra-voxel dephasing effects, but also to geometric distortions in the images acquired. Several recommendations have been made to control for these magnetic field interferences.

A straightforward approach is to increase the distance between the head and TMS coil. However, the effect of TMS measured by motor threshold (MT) is known to decline as a function of the coil-cortex distance (21, 22). Baudewig et al. (23) showed severe signal loss and geometric distortions when TMS-fMRI scans are performed on test objects, while no such artifacts

were seen in subject scans. They concluded that the distance between the head and cortical surface (typically 15–25 mm) is sufficient to minimize such artifacts. Hence, it is important to consider the optimal coil-cortex distance to preserve the TMS effect while minimizing artifacts.

Another essential factor to consider is the timing of the TMS pulse relative to fMRI data acquisition. Bestmann et al. (24) suggested that a period of at least 100 milliseconds (ms) before EPI onset is sufficient. However, the actual timing is a matter of the sequence and hardware used, and 100 ms spacing is not always required. Recently, due to newly developed protocols and the possibility of more precise timing, a shorter acquisition gap is allowed which improves the scanning quality. The important factors which could lead to a shorter delay include the sequence trigger configuration, stimulator model, software version, and any control units between scanner and stimulator, such as scripts used to control the stimulator based on received scanner triggers. Nevertheless, the most important factor for mitigating EPI distortions is the optimal delay length, which depends on various factors. Therefore, there is a degree of trial-and-error in the beginning when establishing the interleaved protocol for each TMS-fMRI setup.

It is also important to consider that the fMRI setting should suit the protocols employed. Baudewig et al. (23) suggested to keep the plane of the TMS coil parallel to the EPI section for a better signal-to-noise ratio (SNR). Bestmann et al. (24) recommended to keep it parallel to the frequency-encoding gradient. These suggestions from previous studies should be considered when planning the fMRI sequences. However, it is worth noting that these suggestions are not always feasible. For example, when the study protocol includes dorsolateral prefrontal cortex (DLPFC) stimulation and whole brain imaging, the above recommendations might not be advantageous. In reality, they may necessitate large volumes and significantly increase acquisition time. It is important to try different phase/frequency encoding directions, as well as EPI orientation, to see which configuration results in the best SNR and least artifacts at the same time.

Controlling Radio Frequency Noise

Noise signals from the control room can penetrate the scanner room via TMS coil cables. These coil cables can act as transmitting antennas for RF noise which causes artifacts and decreases the SNR (25). In principle, the best method to avoid outside RF noise is to locate the TMS stimulator within the MR scanner's Faraday cage, fit the TMS cable in ferrite cable traps, and channel the cable through an RF filter box (26–28). However, these approaches have potential danger due to the attractive forces of the scanner field on the stimulator and cable traps and should thus be avoided, particularly when high field systems (3T and above) are used (29). Instead, Bungert et al. (29) reported that using in-line RF-filters is sufficient for avoiding artifacts (only 3% SNR loss), though such a filter reduces the functional efficacy of TMS by around 7%. In recent TMS-fMRI settings, it is common to filter all the cables which are entering the MRI room to avoid RF noise propagating.

Controlling Leakage Currents

A TMS stimulator typically uses high-voltage capacitors that generate strong currents. These strong currents are delivered through the TMS coil when capacitors are discharged. However, small residual currents leak to the TMS coil even when the TMS coil is not discharged. These small leakage currents can cause magnetic field inhomogeneities resulting in spatial distortions in the EPI (30). Leakage currents need particular attention in TMS-fMRI experiments where TMS intensity is systematically varied, as this causes changes in the level of capacitor charges (31). To avoid these artifacts, Weiskopf et al. (31) suggested inserting a relay with minimal resistance in parallel, as well as two high-voltage diodes in series with the TMS coil. This relay-diode combination allows leakage current to flow through the relay and not through the TMS coil, thereby reducing artifacts considerably. Most current installations use a similar approach where a filter box is mounted at the filter plate. It includes a relay that redirects the leaking currents through the shorting box while the TMS coil is inactive, which mimics the effect of the relay-diode combination.

MR Head Coil and TMS Positioning System

The choice of MR coil and TMS holder are fundamental to the preparation of concurrent TMS-fMRI experiments. Regarding the MR coil, several approaches have been used including 12-channel head coils (32, 33), 8-channel head coils (34–36), 6-channel flexible coils (37, 38), FLEX-L coils (2 circular RF receive coils) (39, 40), standard circular-polarized (CP) head coils (26, 31, 41–43) and simple surface coils (28, 44, 45). Typically, excitation is accomplished with the standard transmitter body coil. In all these setups, the TMS coil is placed inside the RF coil. With birdcage coils, the flexibility of the TMS coil localization is limited. With FLEX coils, the localization is easier, but the SNR at the stimulation site tends to be poorer due to the increased distance and artifacts introduced by the presence of the TMS coil. Recently, a different approach has been suggested, where a thin RF coil is mounted underneath the TMS coil thereby avoiding signal loss at the stimulation site (16, 46). With this thin surface coil array, regions further away from the coil array show lower SNR. However, it can be compensated by using additional coil arrays to cover other regions of the brain (47). The technical feasibility of combining TMS and fMRI coils in a single element has been established (48).

As for the TMS coil positioning system, Bohning et al. (49) suggested a holder that can be used close to an MR scanner and enables a manual positioning of the TMS coil based on the anatomical scan. Moisa et al. (50) developed a new TMS positioning system to reduce the set up time and improve TMS coil positioning to accommodate subject movement. Other research groups attempted to make their own TMS fixing system (43, 45, 51, 52). Nowadays, the manufacturers of MR-compatible TMS coils develop their own coil positioning systems in collaboration with researchers (50). Therefore, this is no longer a major concern for those starting to establish a concurrent TMS-fMRI system.

OVERVIEW OF PREVIOUS CONCURRENT TMS-FMRI STUDIES

The literature search was conducted initially on April 23rd, 2020, followed by another search on April 16th, 2021, to cover more recently published studies. Both searches were conducted following the same method except that the time frame was specified for the second search. The search was performed using PubMed scientific database as well as MEDLINE and Embase via Ovid. On both databases, the search keywords were as follows: ("transcranial magnetic stimulation" OR "TMS" OR "rTMS") AND ("functional magnetic resonance imag*" OR "functional MRI" OR "fMRI" OR "functional connectivity" OR "fcMRI" OR "resting-state" OR "resting state" OR "rsMRI" OR "rsfMRI"). After deduplication, we identified 4,158 articles from the initial search and 715 articles from the second search. Through the screening and eligibility checks, we identified 73 and 5 concurrent TMS-fMRI articles with human subjects (sum of 78 articles) from the initial and second search, respectively (excluding one case study). This section focuses on providing an overview of the previous studies. The stimulation intensity and frequency (in the case of rTMS composed of more than 10 pulses per train) are indicated in the brackets. However, the parameters are very heterogeneous. For further detail of the study setup, it is recommended to look up the original publications.

Concurrent TMS-fMRI Studies With Healthy Subjects

Overview of Motor Cortex Studies

Does TMS Induce a BOLD Effect?

Motor cortex is the most often studied brain region because the TMS response is easily assessable as a movement of a body part, such as finger twitches. The first-ever interleaved TMS-fMRI study was published in 1998 which showed a statistically significant BOLD signal increase in the motor cortex (0.83 Hz, 110%MT) (17). A later follow-up study showed that TMS over the motor cortex at 120%MT induces activations in the contralateral motor cortex and the auditory cortex, with the latter caused by the noise from TMS discharge (53). From the same group, it was demonstrated that higher TMS intensity (1 Hz, 110%MT) caused higher BOLD response amplitudes compared to low-intensity TMS (1 Hz, 80%MT) (18).

For rTMS, a linear relationship between the number of stimuli and the BOLD responses was reported for train lengths of up to 24 pulses (1 Hz, 120%MT) using a simple impulse-response model (54). Furthermore, it was shown that thumb movement induced by suprathreshold rTMS (1 Hz, 110%MT) over the motor cortex generates a similar BOLD signal pattern as if the thumb was moved volitionally (55, 56), and this result was confirmed for high-frequency rTMS (10 Hz, 110%MT) as well (57). Early studies on subthreshold rTMS [3–4 Hz, 90% active MT (AMT)] in the motor cortex did not find motor cortex activity (58, 59). Using a modified RF coil setup with increased sensitivity at the cortical target, a recent study confirmed that subthreshold stimulation (1 Hz, 80, 90%AMT) does not yield statistically significant increases in BOLD responses at the primary motor cortex (M1) target site (46). Applying rTMS to adjacent cortical areas of the M1 hand area (where no motor response is provoked) showed no consistent signal changes under the stimulated area (4 Hz, 150%AMT) (60). Therefore, it can be concluded that BOLD signal changes observed in the M1 hand area is the re-afferent somatosensory feedback of TMS-evoked movements, rather than any direct effects induced by the stimulation itself (41, 58–60). In fact, Denslow et al. (61) reported no significant difference between 100% MT TMS- and volition-induced effects (1 Hz). Interestingly, however, the authors showed qualitative differences in the BOLD signal time courses between stimulation and volition trials. Shitara et al. (41) conducted a more detailed examination of the time courses and spatial distribution of sTMS-induced fMRI signal changes and reported that neither the BOLD activity time courses nor spatial distributions were distinguishable between TMS and voluntary hand movements. However, the undershoot of the usual hemodynamic response function (HRF) was not observed with TMS-induced activities, except at the direct area (directly under the TMS coil) when TMS was applied with subthreshold intensity (randomized frequency, 90%AMT,). The TMS-induced activity was more deeply investigated by Shitara et al. (42) by subtracting the muscle twitch signal [by subtracting median nerve stimulation [MNS] induced sensory-related signal from MNS-induced muscle twitch signal] from the suprathreshold M1 TMS signal [randomized frequency, 120% of resting MT (RMT)]. As a result, a significant effect of TMS was still observed in M1, which suggests that TMS-evoked neuronal activations are not only sensory re-afferent related.

The Intensity and State Dependency of TMS-Induced BOLD Signals

The intensity of the BOLD signal depends on the intensity of the stimulation (46, 58, 59). A deeper investigation into this relationship revealed that BOLD intensity increases approximately linearly with subthreshold TMS intensity but non-linearly with suprathreshold intensity [0.15 Hz, 30–110% of maximum output (MO)] (62). Additionally, remote effects were found both with sub- and suprathreshold intensities, while direct effects at the area under the coil are observed only with suprathreshold intensity (58, 62). Shitara et al. (41) showed that the HRF lacks the typical undershoot after the signal peak at both direct and remote areas with suprathreshold single-pulse stimulation (120%RMT), but with subthreshold stimulation (90%AMT), the lack of undershooting was observed only at remote areas. With the subthreshold stimulation, the standard form of HRF was observed, but only at the direct area.

Moreover, the fMRI signal is not only stimulation intensity-dependent but also state-dependent. When comparing the neuronal activity induced by TMS at the dorsal premotor cortex (PMd) and M1, the activity change was state-dependent between the hand gripping task and resting state. During the hand gripping task, TMS (5 pulses at 11 Hz, 110%RMT) increased hemodynamic response in PMd and M1, but during the rest period, it decreased activity in the same area (63). When 1 Hz M1 rTMS is applied (100, 120%RMT), Jung et al. (64) reported that deductions in motor network activity are state-dependent too;

rTMS decreases activity in motor networks during hand gripping, but it decreases even further during resting state. Furthermore, activations in the networks related to bodily self-consciousness were higher during resting state compared to task conditions.

The Network Effect of Motor Cortex TMS

TMS is known to produce a network effect—through the stimulated area, the effect of TMS can be observed at connected brain regions (65). This remote effect is observed with concurrent TMS-fMRI settings as well, which means that the propagation occurs immediately after the stimulation (61, 62, 66, 67). When TMS is given at the pre-motor cortex, the network effect is present with a subthreshold stimulation as well (3 Hz, 90%AMT), though the effect is smaller than with suprathreshold stimulation (3 Hz, 110%RMT) (66). Furthermore, the remote effect is present with both cortico-cortical and cortico-subcortical connections (66). Therefore, motor cortex stimulation can be administered to target deeper structures. For example, Hodkinson et al. (67) showed that TMS to M1 region (1 Hz, 100%RMT) modulates the connectivity between M1 and medial and lateral pain systems, which includes the insular cortex, anterior cingulate cortex (ACC), and parietal operculum cortex. This study presents credence to use M1 TMS for chronic pain patients.

Overview of Prefrontal Cortex Studies

Compared to the primary motor cortex, the effects of TMS over the prefrontal cortex are more difficult to observe. Despite this challenge, several researchers have targeted the prefrontal cortex with TMS to reveal the underlying mechanisms of neuronal modulation.

Intensity Dependency and Spatial Relationship

Studying prefrontal TMS with fMRI started by investigating the spatial relationship of prefrontal TMS with various intensities (68). They reported that 1 Hz rTMS to the prefrontal lobe at an intensity of 80%MT induces no significant activation except for the auditory cortex. At 100%MT stimulation, contralateral prefrontal activation was observed, and with 120%MT stimulation, bilateral prefrontal activation was observed with the contralateral side showing higher activation levels. These results were reported during the time when the motor cortex was heavily investigated and were in line with the result from the motor cortex stimulation, which showed BOLD signal reduction at the directly stimulated site (17). Twenty years later, Dowdle et al. (32) showed that sTMS to the dorsolateral prefrontal cortex (DLPFC) induces increased neuronal activity in the middle frontal gyri, insula, thalamus, and anterior cingulate cortex (ACC) with both active and sham (3 cm foam under TMS coil) stimulation (randomized frequency, 90–120%RMT). However, BOLD signal increases with active stimulation were greater in the ACC, caudate, and thalamus compared to sham control. Vink et al. (40) showed that sTMS to the DLPFC induces elevated activity in the prefrontal cortex, premotor cortex, primary somatosensory cortex, and subgenual ACC (sgACC), but not in the thalamus and insula (randomized frequency, 115%RMT). Furthermore, when sTMS was applied to the DLPFC, no linear relationship was observed between TMS and BOLD signal intensity (randomized frequency, 90–120%RMT) (32).

Prefrontal TMS-fMRI and Memory Function

Prefrontal regions, especially the DLPFC, are known to contribute to working memory (WM) function (69, 70). When TMS is applied to the DLPFC during memory encoding, it interferes with this function due to the virtual lesion effect (71). Feredoes et al. (72) used concurrent TMS-fMRI to show that DLPFC-TMS increases the activity in WM-related regions, such as the fusiform face area (FFA), which is related to face recognition, and the parahippocampal place area (PPA), related to environmental scene recognition (3 pulses at 11 Hz, 110%RMT). This effect, however, was only present when a distractor was present and was observed only in the region where current stimuli are represented (e.g., the effect is present in FFA only when a face is shown as a target and a house is shown as a distractor). This result provides valuable causal evidence that the DLPFC controls the stimuli-filtering function of the posterior area, which is consistent with previous studies (73–75).

In another TMS-fMRI study targeting semantic memory, Hawco et al. (76) showed that 10 Hz excitatory DLPFC-rTMS effects differ depending on the TMS onset timing (200, 600, or 1,000 ms post-stimulus) (3 pulses at 10 Hz, 100%RMT). These differences were observed at regions that are involved in higher-level cognitive processing (lateral frontal and anterior cingulate cortices) and semantic information processing (medial frontal and mid-temporal cortices), as well as at the visual cortex. This study provides another line of causal evidence that the DLPFC interacts with other WM process-related regions to control semantic memory encoding.

The Network Effect of Prefrontal TMS

Prefrontal TMS-fMRI studies also showed network effects. Hanlon et al. (20) reported that prefrontal sTMS (DLPFC and ventromedial PFC) activates the frontostriatal network, specifically in the prefrontal cortex, striatum, and thalamus (0.1 Hz, 100%RMT). This study showed that prefrontal TMS can also induce both cortico-cortical and cortico-subcortical network effects, as was the case for motor cortex stimulation (61, 62, 66). Thus, this network effect can be used to target a deeper structure. Oathes et al. (77) used a resting-state fMRI-guided sTMS system (randomized frequency, 120%RMT) to target an individual frontal area that is functionally connected with sgACC and amygdala. This study demonstrated that individually targeted TMS can modulate the sgACC distributed brain network, as well as the activity in the amygdala itself.

The prefrontal cortex has main nodes in three relatively well-studied networks that are known to be involved in higher cognitive functions: the central executive network (CEN) and the salience network (SN), which are less activated during the resting state (78, 79), and the default-mode network (DMN), which is reduced in activity whenever subjects attend to a specific task (80).

In a more recent study, the modulatory mechanisms between these networks were examined (51). It was shown that facilitatory sTMS (single pulses at 0.4 Hz, 120%RMT) to a CEN node

(the posterior middle frontal gyrus) elicits negative connectivity between the DMN and CEN, and between the DMN and SN. On the other hand, inhibitory rTMS induced upregulation of DMN activity, though this effect was observed with an offline experiment where EPI was acquired immediately after 20 min of 1 Hz rTMS (120%RMT). Nevertheless, these results support the causal relationship of CEN in regulating the DMN activity, as has been suggested previously (79). Hawco et al. (81) showed that when the DLPFC has a stronger interaction with the SN, the correlation between intrinsic resting connectivity and TMS-induced changes in neuronal activity become stronger (randomized frequency, 100%RMT). From these applications, it may be concluded that concurrent TMS-fMRI is not only useful for investigating the direct effect of TMS in a certain functional network but also for examining the relationship between different functional networks.

Other Studies Within the Frontal Lobe

Frontal Eye Field

Frontal eye fields (FEF) are involved in controlling saccadic eye movement which plays an important role in visual attention and visuomotor control (82). Concurrent TMS-fMRI studies have revealed a top-down effect of the FEF on the modulation of the visual cortex. sTMS to the *right* FEF induces BOLD signal decreases in the central visual representation field, as well as BOLD signal increases in the peripheral field in V1–V4 (note that TMS to the *left* FEF induces effects only for central visual representation) (5 pulses at 10 Hz, 40–85%MO) (45). Ruff et al. (45) observed that FEF modulate activity in the retinotopic visual cortex, regardless of the presence of visual stimuli. When visual stimuli are present, right FEF-TMS elicits feature-specific effects; when attending to moving dots, the visual motion area shows an increase in cortical activity, whereas when attention is toward a face, the increase is observed in the fusiform face area (FFA) (3 pulses at 11 Hz, 110%RMT) (83). These findings support the idea that visual saccade attention is modulated via FEF feature-based functions.

Overview of Parietal Lobe Studies

The parietal lobe contributes to a wide range of complex functions, such as visuospatial attention, sensory processing, body awareness, language-related functions (such as writing, recognition, and naming of objects), and arithmetic processing. TMS to the parietal lobe can facilitate or inhibit these functions, and researchers have attempted to understand the mechanisms underlying these modulations. Furthermore, parietal stimulation also shows a network effect.

Parietal TMS-fMRI and Visuospatial Function

The first parietal concurrent TMS-fMRI study was conducted by Sack et al. (84) exploring visuospatial judgments. Sack and his colleagues showed that right, but not left, parietal TMS (randomized frequency, 100%MO) interferes with visuospatial processing by modulating the right-hemispheric frontoparietal network, indicating that the parietal cortex interacts with frontal areas to regulate visuospatial attention. Consequently, Ricci et al. (36) confirmed with three subjects that right suprathreshold posterior parietal cortex (PPC) sTMS (115%RMT) induces rightward bias with the line bisection task due to neglect-like behavior produced in the left visual hemifield, and this effect was observed in frontoparietal regions. Additionally, Blankenburg et al. (44) found that the effect of the PPC stimulation intensity, which was observed in the occipital visual cortex during a visuospatial attention task, depends on the visually attended side; when visual attention is toward the contralateral side, a larger difference in BOLD signal between high (75%MO) and low (35%MO) TMS intensity condition was observed compared to ipsilateral visual attention (5 pulses at 10 Hz). Regarding visuospatial attention, the neuronal activity of the right angular gyrus (AG) is considered to play a crucial role when reorientation of visuospatial attention is required, for example, by receiving a wrong cue. The right AG TMS (three pulses at 11 Hz, 120%RMT) elicited a facilitatory effect when the target was on the right hemifield following the invalid cue, meaning that right AG TMS facilitates rightward spatial reorientation. The neuronal effect was observed in the left AG and left visual area, suggesting that there is interhemispheric interaction between the right AG and remote connected areas in the left hemisphere. Moreover, this study showed that the right AG also influences the neuronal activity of the visual cortex, in addition to the right PPC (27).

Parietal TMS-fMRI With Visual Stimuli

With regards to the interaction with the visual cortex, the intra-parietal sulcus (IPS) is a region that has been relatively well-investigated with concurrent TMS-fMRI. IPS is known to contribute to visual-motor coordination (such as saccade preparation and grasping objects) (85). IPS TMS increases activation in the parietal cortex during resting state without any visual stimuli (10 Hz, 69%MO) (86). However, when visual stimuli are present, IPS TMS increases cortical activation in the cuneus, and this activation at the cuneus decreases when no visual stimuli are shown (four pulses at 10 Hz, 66%MO) (87). For moving visual stimuli, Ruff et al. (28) showed that TMS over the right IPS interacts with the occipital visual cortex depending on the visual context (five pulses at 9 Hz). With higher intensity IPS TMS (tested with 40–85%MO), the BOLD signal increase was observed in visual motion areas but only when stimuli were present and moving. On the other hand, when stimuli were absent, the effect was observed in V1–V4 visual retinotopic areas. Furthermore, it was confirmed that TMS over the right IPS is more effective than over the left IPS; right TMS induced stronger BOLD signal modulation in the visual cortex but left TMS did not induce any significant difference (45) (five pulses at 9 Hz, tested with 40–85%MO).

As for low-salience visual stimuli, IPS TMS (four pulses at 10 Hz, 69%MO) modulates neuronal activation. In the no-TMS condition, detecting weak visual stimuli showed activation increases in the anterior insula, which is a crucial node of the ventral attentional network for salience detection, and decreases in the ventral visual area. However, with IPS TMS, the activation increased in the right temporoparietal junction (TPJ), which is also a node of the ventral attentional network, and decreased in the right fusiform area (86). This IPS function of low salience stimuli detection is useful for the brain to decide which visual

information is relevant from the sensorially noisy environment. IPS TMS did not improve accuracy in finding low saliency stimuli but did quicken response times following the error trials (88). Furthermore, IPS TMS attenuated activity increases in the left middle and superior frontal gyri, which was only observed in the missed visual stimuli case but not when correctly seen (four pulses at 10 Hz, 69%MO) (88). Hence, the IPS is considered to be involved in the post-decisional process by reflecting the decision accuracy and confidence (88).

Parietal TMS-fMRI and Sensorimotor Integration

Another important function of the parietal cortex is sensorimotor integration, such as assisting hand movements in line with the goal orientation (89). de Vries et al. (90) found that impaired function of the superior parietal cortex, which is related to the proprioceptive adjustment of spatial movement control (91), leads to an increase in BOLD signal in remote areas. Suprathreshold TMS at the frequency of 1 Hz (115%MT) was given over the left superior parietal cortex prior to hand movement execution. The result showed increased activity in bilateral prefrontal, right temporo-parietal, and left posterior parietal cortices. Therefore, these remote areas may compensate for any functional impairments of the superior parietal cortex (90).

Parietal TMS-fMRI With Somatosensory Function

TMS over the right parietal cortex was conducted to investigate the neural association of somatosensory function. Blankenburg et al. (43) demonstrated that TMS to the right parietal cortex (five pulses at 10 Hz, 110%RMT) modulates BOLD signals in the left primary somatosensory cortex (SI), but that this depends on whether the somatosensory input is present or not; with somatosensory input (MNS to the right wrist in this case), the neural activity in SI increases, whereas it decreases without somatosensory input. A similar effect was observed in the thalamus with the region of interest (ROI) analysis. This study suggests that the right parietal cortex is involved in the somatosensory processing in the left SI.

The Network Effect of Parietal Stimulation

Targeting the hippocampus enables us to investigate its role in episodic memory. Hermiller et al. (92) applied TBS to the lateral parietal cortex, which is a part of the hippocampal network, and demonstrated that the left hippocampus shows increased neuronal activity during scene encoding and the subsequent recollection was significantly better when performed after the TBS (80%RMT). This study suggests the ability of TBS to influence hippocampal memory function.

Overall, these parietal concurrent TMS-fMRI studies suggest heavy interaction between the parietal cortex and occipital visual cortex. It is considered that high-level adaptive behavior is processed as an integration of bottom-up sensory inputs and top-down control signals to adjust the current action to meet the task goal. In the case of visual control, the parietal cortex supports the visual function of the occipital lobe to fine-tune its visual actions. Moreover, these concurrent TMS-fMRI studies show that right hemispheric structures induce stronger effects in the visual cortex compared to the left.

Overview of Occipital Lobe Studies

Occipital TMS-fMRI and Phosphene

The occipital lobe is the central system of visual processing. TMS to the primary visual cortex in the occipital lobe is known to induce phosphenes, i.e., the perception of transient light. This phosphene threshold (PT) is another method to determine the TMS intensity. The neural correlates of the TMS-induced phosphene have been mostly studied with EEG (93–95), but also some have investigated this phenomenon with fMRI. Since phosphenes are subjective, it is difficult to find its neuronal correlates with small sample sizes. In fact, de Graaf et al. (96) reported no meaningful observation in cortical activity modulation associated with phosphenes, but this study included only four subjects (randomized frequency, 80–120% phosphene threshold; PT). However, consistent with previous research (97), Caparelli et al. (98) employed a concurrent TMS-fMRI paradigm and reported that considerable differences in activity are observed in the visual network between those who perceive phosphenes and those who do not (0.25 Hz, 100%PT). These studies imply that a functional distinction within visual networks separates subjects who experience phosphenes from those who do not, and this is possibly the origin of phosphene generation (98).

Concurrent TMS-fMRI Studies With Clinical Subjects

Psychiatric Disorders

DLPFC TMS-fMRI With Depression

In recent years, the number of concurrent TMS-fMRI studies with psychiatric patients has increased. With MDD patients, DLPFC stimulation has induced elevated local and global network effects, both directly under the coil and in connected subcortical regions, such as the thalamus, putamen, and insula (1 Hz, 100%MT) (99), which is in line with other studies involving healthy subjects (32, 68). Following these studies, Eshel et al. (100) conducted a DLPFC TMS-fMRI study with MDD and healthy controls, specifically targeting the DLPFC node of the frontoparietal control network. This study showed that DLPFC stimulation activates the right DLPFC in patients with MDD, but not in healthy controls. Eshel and colleagues also report that DLPFC stimulation inhibits amygdala activity in healthy controls, but not in patients with MDD (0.4 Hz, 120%RMT) (100).

DLPFC TMS-fMRI With PTSD

The efficacy of DLPFC stimulation for post-traumatic stress disorder (PTSD) is another avenue for TMS research. A concurrent TMS-fMRI study reported that right DLPFC stimulation to PTSD patients induces an inhibitory effect in the left amygdala. Furthermore, a positive correlation was reported between the degree of inhibition and the outcome of the typical exposure psychotherapy (101). Another study investigated PTSD patients with frontopolar stimulation and found that the ventromedial prefrontal cortex, which is related

to emotion regulation and is usually downregulated via the frontopolar cortex, can be deactivated with frontopolar TMS as well (102) (both studies: 0.4 Hz, 120%RMT).

Prefrontal TMS-fMRI With Substance Abuse

As for cocaine users, left DLPFC stimulation did not evoke a significant difference in BOLD signal compared to healthy controls (33). However, TMS over the medial PFC led to lower ventral striatal activation in cocaine users compared to healthy controls (0.08 Hz, 110%RMT) (33). rTMS applied to the frontal pole induces BOLD responses at the striatum and salience network in cocaine users (randomized frequency, 100%RMT) (103). Furthermore, Hanlon et al. (104) investigated the effects of TMS on BOLD signals before and after frontal pole continuous theta-burst stimulation (cTBS) with cocaine and alcohol users. Compared to the pre-cTBS fMRI scan, the post-cTBS scan revealed inhibition at the orbitofrontal cortex as well as at regions that are related to salience regulation, which are known to be activated by drug usage (0.1 Hz, 110%RMT).

Prefrontal TMS-fMRI With Schizophrenia

Guller et al. (105) showed that precentral gyrus TMS administered to schizophrenia patients evokes decreased BOLD responses in the thalamus and medial superior frontal cortex compared to healthy controls. Additionally, reduced connectivity between the thalamus and superior frontal gyrus, as well as between the thalamus and insula, was observed in this study (single pulse, 110%MR). Webler et al. (106) stimulated the left frontal cortex (Brodmann area 9; BA9) of schizophrenia patients with 10 Hz triplet pulses (80–120%RMT; cortical distance adjusted). This study reported stronger activity in left BA9 and neighboring BA46 compared to healthy controls. Furthermore, disrupted interhemispheric functional connectivity between left and right BA9 was demonstrated with schizophrenia patients.

Neurological Disorders

With neurological disorders, Bestmann et al. (26) conducted a concurrent TMS-fMRI study with post-stroke patients. The study showed a stronger BOLD signal effect in posterior regions of the ipsilesional sensorimotor cortex induced by contralesional dorsal premotor TMS during handgrip, which is associated with more severe clinical and neurophysiological post-stroke impairment (five pulses at 11 Hz, 110%RMT). With cervical dystonia patients, 1 Hz rTMS (115%RMT) to the left superior parietal cortex led to significantly less activation in the right angular gyrus compared to healthy controls (107).

As for epilepsy, no concurrent TMS-fMRI studies have been conducted yet. However, a series of concurrent TMS-fMRI studies from Li and colleagues investigated the psychopharmacological effect of two anticonvulsant drugs, lamotrigine and valproic acid, with healthy subjects. After lamotrigine intake, TMS to the motor cortex inhibited cortical activity overall compared to placebo (no detail of frequency, 100, 120%RMT). However, prefrontal TMS promoted activity in the orbitofrontal cortex and hippocampus, which indicates an effect of lamotrigine in corticolimbic circuits (108). With valproic acid, an inhibitory effect was observed with motor cortex TMS (five pulses at 1 Hz, 100,120%RMT). However, the facilitatory effect of prefrontal TMS was not observed (35). Further investigation indicated that both lamotrigine and valproic acid have an inhibitory effect in the connectivity between the M1 and pre-motor cortex, as well as between M1 and the supplementary motor area, after motor cortex TMS (five pulses at 1 Hz, 100,120%RMT). Moreover, lamotrigine, but not valproic acid, has a facilitatory effect in the network between the left DLPFC and ACC (34).

LIMITATION AND FUTURE DIRECTION

Although concurrent TMS-fMRI has helped us to understand the neural correlates of TMS in an unprecedented manner, there are still some technical limitations that should be considered. One of them is the temporal resolution of concurrent TMS-fMRI. For example, with the inter-volume protocol, where the TMS is applied during the gap time between EPI volumes, the stimulation protocol is limited to the length of the repetition time (TR) of the fMRI sequence, which is typically around 2 s. With the inter-slice protocols, where TMS pulses are interleaved with EPI slices, continuous image acquisition is possible with frequencies up to 10 Hz (109). However, a precise interleaving of EPI sequences and timing of TMS pulses remains complex.

Other challenges that need to be addressed in concurrent TMS-fMRI are (1) restricted spatial selection of the stimulation target due to spatial constraints within the MR coils, (2) subject movements that increase the distance between the TMS coil and stimulation target, (3) sham conditions. To overcome spatial constraints, recent approaches sometimes use flex-coils that can be dynamically placed around an area of interest (40), or a thin RF receiver coil on which the TMS coil can be mounted (16, 46).

Minimizing the subject's motion during a TMS-fMRI session is critical to ensure. Head movement can affect not only scanning quality but also TMS efficacy by accidentally increasing the coil-head distance. The spatial flexibility of coil localization and motion minimization are often inversely related, i.e., the birdcage MR coil is less flexible with TMS coil localization but easier to fixate the head [pictures of the actual setup can be found in Bestmann et al. (59) and Hodkinson et al. (67)]. When flexible MR coils are used, the head fixation becomes difficult as there is no frame where sponges can be inserted. It is recommended to create a wall around the head to minimize the head movement [for example, **Figure 1B** uses a deflatable pillow. For another example, see Vink et al. (40)]. Regarding the motion tracking in the scanner, it has recently been proposed to extract subject motion information from alignment parameters obtained from EPIs (110). However, this method is limited by spatial (about 1 mm) and temporal resolution (typically 1–2 s, defined by the TR). To control the motion effect, online visual feedback

procedures and online dose adjustment have also been proposed (111). The idea is to track the head and coil locations using a neuro-navigation camera throughout the TMS-fMRI sessions (**Figures 1C,E**). It requires a system that is both MR-compatible and detectable within the narrow scanner bore. Further development of motion minimization and tracking systems are required.

Regarding sham conditions, the recent approach is to increase the distance between the coil and the scalp by placing a plastic block between the TMS coil and the scalp, thereby avoiding effective stimulation (32, 40, 112), or between the MR receiver coil and the TMS stimulation coil when a 7-channel concurrent TMS-fMRI coil array is used (113). Tik et al. (113) showed that this approach resulted in an activation increase in somatosensory areas during sham and verum stimulation, with only the latter resulting in an increase in DLPFC activity during verum stimulation.

As the number of studies increases, the technical aspects of concurrent TMS-fMRI have dramatically improved over the past decades. However, setting up the concurrent TMS-fMRI environment still requires a considerable amount of time and knowledge. Due to its complexity, it often requires the study participants to stay still for a long time, which makes it even more difficult to employ patients. As shown in this review, most studies have been conducted with healthy subjects, while clinical populations are underrepresented. To lower the barrier of the TMS-fMRI system implementation for clinical researchers, knowledge should be pooled and shared for technical solutions. A systematic review of concurrent TMS-fMRI should be also referred to when a new study design is developed (114).

Furthermore, previous concurrent TMS-fMRI studies mainly investigated the effect of the motor cortex, while other brain regions are still underrepresented—especially posterior regions, such as the occipital cortex, where it is difficult to stimulate subjects in the supine position on the scanner bed. To date, ∼80% of concurrent TMS-fMRI studies have investigated the motor cortex. With the help of novel developments in TMS-fMRI hardware, future studies may extend TMS-fMRI research to other areas of the brain.

Last but not least, recent technological improvements showed the feasibility of concurrent TMS-EEG-fMRI (15, 115, 116). The combination of EEG and fMRI covers both temporal and spatial resolution. Therefore, concurrent TMS-EEG-fMRI allows for the investigation of TMS effects in a widely distributed network with higher accuracy over time.

Concurrent TMS-fMRI will contribute to increased biological validity. TMS can modulate neuronal activity at different cortical areas. However, the mechanism of cortical excitation and inhibition is not completely understood yet. Moreover, the relationship between neuronal modulation and behavioral consequences remains a black box. Clinical protocols can be better individualized to achieve a higher treatment efficacy when it becomes clearer how neuronal networks, hub regions, and read-outs such as inter- and intra-hemispheric connections are interacting. We strongly encourage all TMS-fMRI researchers to collaborate and share knowledge and experiences of this extremely complicated but powerful technique. An effective way to achieve this is to share data and exchange knowledge through Open Science platforms, such as OSF (https://osf.io/), zenodo (https://zenodo.org/), or Gitlab (https://gitlab.com/gitlab-org/gitlab).

AUTHOR CONTRIBUTIONS

YM-T and MT gathered the knowledge and wrote the review. CW, FP, and DK supervised and provided the corrections and feedback for improvements. K-YC and AS supported to make the list of previous studies. ZW, CV, and LB supported the set-up of TMS-fMRI system. All authors contributed and approved the final manuscript.

FUNDING

The study was done using the NICUM Siemens Prisma scanner supported by German Research Foundation (DFG; Deutsche Forschungsgemeinschaft) [grant number INST 86/1739-1 FUGG].

REFERENCES

1. Speer AM, Kimbrell TA, Wassermann EM, Repella JD, Willis MW, Herscovitch P, et al. Opposite effects of high and low frequency rTMS on regional brain activity in depressed patients. *Biol Psychiatry.* (2000) 48:1133–41. doi: 10.1016/S0006-3223(00)01065-9
2. Lefaucheur J-P, Aleman A, Baeken C, Benninger DH, Brunelin J, Di Lazzaro V, et al. Evidence-based guidelines on the therapeutic use of repetitive transcranial magnetic stimulation (rTMS): an update (2014-2018). *Clin Neurophysiol.* (2020) 131:474–528. doi: 10.1016/j.clinph.2019.11.002
3. Blumberger DM, Vila-Rodriguez F, Thorpe KE, Feffer K, Noda Y, Giacobbe P, et al. Effectiveness of theta burst versus high-frequency repetitive transcranial magnetic stimulation in patients with depression (THREE-D): a randomised non-inferiority trial. *Lancet.* (2018) 391:1683–92. doi: 10.1016/S0140-6736(18)30295-2
4. George MS, Lisanby SH, Avery D, McDonald WM, Durkalski V, Pavlicova M, et al. Daily left prefrontal transcranial magnetic stimulation therapy for major depressive disorder: a sham-controlled randomized trial. *Arch Gen Psychiatry.* (2010) 67:507–16. doi: 10.1001/archgenpsychiatry.2010.46
5. O'Reardon JP, Solvason HB, Janicak PG, Sampson S, Isenberg KE, Nahas Z, et al. Efficacy and safety of transcranial magnetic stimulation in the acute treatment of major depression: a multisite randomized controlled trial. *Biol Psychiatry.* (2007) 62:1208–16. doi: 10.1016/j.biopsych.2007.01.018
6. Carmi L, Alyagon U, Barnea-Ygael N, Zohar J, Dar R, Zangen A. Clinical and electrophysiological outcomes of deep TMS over the medial prefrontal and anterior cingulate cortices in OCD patients. *Brain Stimul.* (2018) 11:158–65. doi: 10.1016/j.brs.2017.09.004
7. Zangen A, Moshe H, Martinez D, Barnea-Ygael N, Vapnik T, Bystritsky A, et al. Repetitive transcranial magnetic stimulation for smoking cessation: a pivotal multicenter double-blind randomized controlled trial. *World Psychiatry.* (2021) 20:397–404. doi: 10.1002/wps.20905
8. Lipton RB, Dodick DW, Silberstein SD, Saper JR, Aurora SK, Pearlman SH, et al. Single-pulse transcranial magnetic stimulation for acute treatment of migraine with aura: a randomised, double-blind, parallel-group, sham-controlled trial. *Lancet Neurol.* (2010) 9:373–80. doi: 10.1016/S1474-4422(10)70054-5

9. Grossheinrich N, Rau A, Pogarell O, Hennig-Fast K, Reinl M, Karch S, et al. Theta burst stimulation of the prefrontal cortex: safety and impact on cognition, mood, resting electroencephalogram. *Biol Psychiatry.* (2009) 65:778–84. doi: 10.1016/j.biopsych.2008.10.029
10. Huang Y-Z, Edwards MJ, Rounis E, Bhatia KP, Rothwell JC. Theta burst stimulation of the human motor cortex. *Neuron.* (2005) 45:201–6. doi: 10.1016/j.neuron.2004.12.033
11. Cole EJ, Phillips AL, Bentzley BS, Stimpson KH, Nejad R, Barmak F, et al. Stanford Neuromodulation Therapy (SNT): A double-blind randomized controlled trial. *Am J Psychiatry.* (2022) 179:132–41. doi: 10.1176/appi.ajp.2021.20101429
12. Bergmann TO, Karabanov A, Hartwigsen G, Thielscher A, Siebner HR. Combining non-invasive transcranial brain stimulation with neuroimaging and electrophysiology: current approaches and future perspectives. *Neuroimage.* (2016) 140:4–19. doi: 10.1016/j.neuroimage.2016.02.012
13. Siebner HR, Bergmann TO, Bestmann S, Massimini M, Johansen-Berg H, Mochizuki H, et al. Consensus paper: combining transcranial stimulation with neuroimaging. *Brain Stimul.* (2009) 2:58–80. doi: 10.1016/j.brs.2008.11.002
14. Cao KX, Ma ML, Wang CZ, Iqbal J, Si JJ, Xue YX, et al. TMS-EEG: an emerging tool to study the neurophysiologic biomarkers of psychiatric disorders. *Neuropharmacology.* (2021) 197:108574. doi: 10.1016/j.neuropharm.2021.108574
15. Janssens SEW, Sack AT. Spontaneous fluctuations in oscillatory brain state cause differences in transcranial magnetic stimulation effects within and between individuals. *Front Hum Neurosci.* (2021) 15:802244. doi: 10.3389/fnhum.2021.802244
16. Navarro de Lara LI, Windischberger C, Kuehne A, Woletz M, Sieg J, Bestmann S, et al. A novel coil array for combined TMS/fMRI experiments at 3 T. *Magn Reson Med.* (2015) 74:1492–501. doi: 10.1002/mrm.25535
17. Bohning DE, Shastri A, Nahas Z, Lorberbaum JP, Andersen SW, Dannels WR, et al. Echoplanar BOLD fMRI of brain activation induced by concurrent transcranial magnetic stimulation. *Invest Radiol.* (1998) 33:336–40. doi: 10.1097/00004424-199806000-00004
18. Bohning D, Shastri A, McConnell K, Nahas Z, Lorberbaum J, Roberts D, et al. A combined TMS/fMRI study of intensity-dependent TMS over motor cortex. *Biol Psychiatry.* (1999) 45:385–94. doi: 10.1016/S0006-3223(98)00368-0
19. Bohning DE, Pecheny AP, Epstein CM, Speer AM, Vincent DJ, Dannels W, et al. Mapping transcranial magnetic stimulation (TMS) fields *in vivo* with MRI. *Neuroreport.* (1997) 8:2535–8. doi: 10.1097/00001756-199707280-00023
20. Hanlon CA, Canterberry M, Taylor JJ, DeVries W, Li X, Brown TR, et al. Probing the frontostriatal loops involved in executive and limbic processing via interleaved TMS and functional MRI at two prefrontal locations: a pilot study. *PLoS One.* (2013) 8:e67917. doi: 10.1371/journal.pone.0067917
21. Kozel FA, Nahas Z, Debrux C, Molloy M, Lorberbaum JP, Bohning D, et al. How coil-cortex distance relates to age, motor threshold, and antidepressant response to repetitive transcranial magnetic stimulation. *J Neuropsychiatry Clin Neurosci.* (2000) 12:376–84. doi: 10.1176/jnp.12.3.376
22. McConnell KA, Nahas Z, Shastri A, Lorberbaum JP, Kozel FA, Bohning DE, et al. The transcranial magnetic stimulation motor threshold depends on the distance from coil to underlying cortex: a replication in healthy adults comparing two methods of assessing the distance to cortex. *Biol Psychiatry.* (2001) 49:454–9. doi: 10.1016/S0006-3223(00)01039-8
23. Baudewig J, Paulus W, Frahm J. Artifacts caused by transcranial magnetic stimulation coils and EEG electrodes in T2∗-weighted echo-planar imaging. *Magn Reson Imaging.* (2000) 18:479–84. doi: 10.1016/S0730-725X(00)00122-3
24. Bestmann S, Baudewig J, Frahm J. On the synchronization of transcranial magnetic stimulation and functional echo-planar imaging. *J Magn Reson Imaging.* (2003) 17:309–16. doi: 10.1002/jmri.10260
25. Friedman L, Glover GH. Report on a multicenter fMRI quality assurance protocol. *J Magn Resonan Imaging.* (2006) 23:827–39. doi: 10.1002/jmri.20583
26. Bestmann S, Swayne O, Blankenburg F, Ruff CC, Teo J, Weiskopf N, et al. The role of contralesional dorsal premotor cortex after stroke as studied with concurrent TMS-fMRI. *J Neurosci.* (2010) 30:11926–37. doi: 10.1523/JNEUROSCI.5642-09.2010
27. Heinen K, Ruff CC, Bjoertomt O, Schenkluhn B, Bestmann S, Blankenburg F, et al. Concurrent TMS-fMRI reveals dynamic interhemispheric influences of the right parietal cortex during exogenously cued visuospatial attention. *Eur J Neurosci.* (2011) 33:991–1000. doi: 10.1111/j.1460-9568.2010.07580.x
28. Ruff CC, Bestmann S, Blankenburg F, Bjoertomt O, Josephs O, Weiskopf N, et al. Distinct causal influences of parietal versus frontal areas on human visual cortex: evidence from concurrent TMS-fMRI. *Cereb Cortex.* (2008) 18:817–27. doi: 10.1093/cercor/bhm128
29. Bungert A, Chambers CD, Long E, Evans CJ. On the importance of specialized radiofrequency filtering for concurrent TMS/MRI. *J Neurosci Methods.* (2012) 210:202–5. doi: 10.1016/j.jneumeth.2012.07.023
30. Jezzard P, Clare S. Sources of distortion in functional MRI data. *Hum Brain Mapp.* (1999) 8:80–5. doi: 10.1002/(SICI)1097-0193(1999)8:2/3<80::AID-HBM2>3.0.CO;2-C
31. Weiskopf N, Josephs O, Ruff CC, Blankenburg F, Featherstone E, Thomas A, et al. Image artifacts in concurrent transcranial magnetic stimulation (TMS) and fMRI caused by leakage currents: modeling and compensation. *J Magn Reson Imaging.* (2009) 29:1211–7. doi: 10.1002/jmri.21749
32. Dowdle LT, Brown TR, George MS, Hanlon CA. Single pulse TMS to the DLPFC compared to a matched sham control, induces a direct, causal increase in caudate, cingulate, and thalamic BOLD signal. *Brain Stimul.* (2018) 11:789–96. doi: 10.1016/j.brs.2018.02.014
33. Hanlon CA, Dowdle LT, Moss H, Canterberry M, George MS. Mobilization of medial and lateral frontal-striatal circuits in cocaine users and controls: an interleaved TMS/BOLD functional connectivity study. *Neuropsychopharmacology.* (2016) 41:3032–41. doi: 10.1038/npp.2016.114
34. Li X, Large CH, Ricci R, Taylor JJ, Nahas Z, Bohning DE, et al. Using interleaved transcranial magnetic stimulation/functional magnetic resonance imaging (fMRI) and dynamic causal modeling to understand the discrete circuit specific changes of medications: lamotrigine and valproic acid changes in motor or prefrontal effective connectivity. *Psychiatry Res.* (2011) 194:141–8. doi: 10.1016/j.pscychresns.2011.04.012
35. Li X, Ricci R, Large CH, Anderson B, Nahas Z, Bohning DE, et al. Interleaved transcranial magnetic stimulation and fMRI suggests that lamotrigine and valproic acid have different effects on corticolimbic activity. *Psychopharmacology (Berl).* (2010) 209:233–44. doi: 10.1007/s00213-010-1786-y
36. Ricci R, Salatino A, Li X, Funk AP, Logan SL, Mu Q, et al. Imaging the neural mechanisms of TMS neglect-like bias in healthy volunteers with the interleaved TMS/fMRI technique: preliminary evidence. *Front Hum Neurosci.* (2012) 6:326. doi: 10.3389/fnhum.2012.00326
37. Wang WT, Xu B, Butman JA. Improved SNR for combined TMS-fMRI: a support device for commercially available body array coil. *J Neurosci Methods.* (2017) 289:1–7. doi: 10.1016/j.jneumeth.2017.06.020
38. Yau JM, Hua J, Liao DA, Desmond JE. Efficient and robust identification of cortical targets in concurrent TMS-fMRI experiments. *Neuroimage.* (2013) 76:134–44. doi: 10.1016/j.neuroimage.2013.02.077
39. de Weijer AD, Sommer IE, Bakker EJ, Bloemendaal M, Bakker CJ, Klomp DW, et al. A setup for administering TMS to medial and lateral cortical areas during whole-brain FMRI recording. *J Clin Neurophysiol.* (2014) 31:474–87. doi: 10.1097/WNP.0000000000000075
40. Vink JJT, Mandija S, Petrov PI, van den Berg CAT, Sommer IEC, Neggers SFW. A novel concurrent TMS-fMRI method to reveal propagation patterns of prefrontal magnetic brain stimulation. *Hum Brain Mapp.* (2018) 39:4580–92. doi: 10.1002/hbm.24307
41. Shitara H, Shinozaki T, Takagishi K, Honda M, Hanakawa T. Time course and spatial distribution of fMRI signal changes during single-pulse transcranial magnetic stimulation to the primary motor cortex. *Neuroimage.* (2011) 56:1469–79. doi: 10.1016/j.neuroimage.2011.03.011
42. Shitara H, Shinozaki T, Takagishi K, Honda M, Hanakawa T. Movement and afferent representations in human motor areas: a simultaneous neuroimaging and transcranial magnetic/peripheral nerve-stimulation study. *Front Hum Neurosci.* (2013) 7:554. doi: 10.3389/fnhum.2013.00554

43. Blankenburg F, Ruff CC, Bestmann S, Bjoertomt O, Eshel N, Josephs O, et al. Interhemispheric effect of parietal TMS on somatosensory response confirmed directly with concurrent TMS-fMRI. *J Neurosci.* (2008) 28:13202–8. doi: 10.1523/JNEUROSCI.3043-08.2008
44. Blankenburg F, Ruff CC, Bestmann S, Bjoertomt O, Josephs O, Deichmann R, et al. Studying the role of human parietal cortex in visuospatial attention with concurrent TMS-fMRI. *Cereb Cortex.* (2010) 20:2702–11. doi: 10.1093/cercor/bhq015
45. Ruff CC, Blankenburg F, Bjoertomt O, Bestmann S, Weiskopf N, Driver J. Hemispheric differences in frontal and parietal influences on human occipital cortex: direct confirmation with concurrent TMS-fMRI. *J Cogn Neurosci.* (2009) 21:1146–61. doi: 10.1162/jocn.2009.21097
46. Navarro de Lara LI, Tik M, Woletz M, Frass-Kriegl R, Moser E, Laistler E, et al. High-sensitivity TMS/fMRI of the human motor cortex using a dedicated multichannel MR coil. *Neuroimage.* (2017) 150:262–9. doi: 10.1016/j.neuroimage.2017.02.062
47. Windischberger C, Vasileiadi M, Woletz M, Tik M. Concurrent TMS/fMRI with high sensitivity and accelerated image acquisition. *Brain Stimul.* (2021) 14:1723. doi: 10.1016/j.brs.2021.10.444
48. Lu H, Wang S. A 2-in-1 single-element coil design for transcranial magnetic stimulation and magnetic resonance imaging. *Magn Reson Med.* (2018) 79:582–7. doi: 10.1002/mrm.26640
49. Bohning DE, Denslow S, Bohning PA, Walker JA, George MS. A TMS coil positioning/holding system for MR image-guided TMS interleaved with fMRI. *Clin Neurophysiol.* (2003) 114:2210–9. doi: 10.1016/S1388-2457(03)00232-3
50. Moisa M, Pohmann R, Ewald L, Thielscher A. New coil positioning method for interleaved transcranial magnetic stimulation (TMS)/functional MRI (fMRI) and its validation in a motor cortex study. *J Magn Reson Imaging.* (2009) 29:189–97. doi: 10.1002/jmri.21611
51. Chen AC, Oathes DJ, Chang C, Bradley T, Zhou ZW, Williams LM, et al. Causal interactions between fronto-parietal central executive and default-mode networks in humans. *Proc Natl Acad Sci U S A.* (2013) 110:19944–9. doi: 10.1073/pnas.1311772110
52. Xu B, Sandrini M, Wang WT, Smith JF, Sarlls JE, Awosika O, et al. PreSMA stimulation changes task-free functional connectivity in the fronto-basal-ganglia that correlates with response inhibition efficiency. *Hum Brain Mapp.* (2016) 37:3236–49. doi: 10.1002/hbm.23236
53. Bohning DE, Shastri A, Wassermann EM, Ziemann U, Lorberbaum JP, Nahas Z, et al. BOLD-fMRI response to single-pulse transcranial magnetic stimulation (TMS). *J Magn Reson Imaging.* (2000) 11:569–74. doi: 10.1002/1522-2586(200006)11:6<569::AID-JMRI1>3.0.CO;2-3
54. Bohning DE, Shastri A, Lomarev MP, Lorberbaum JP, Nahas Z, George MS. BOLD-fMRI response vs. transcranial magnetic stimulation (TMS) pulse-train length: testing for linearity. *J Magn Reson Imaging.* (2003) 17:279–90. doi: 10.1002/jmri.10271
55. Bohning DE, Shastri A, McGavin L, McConnell KA, Nahas Z, Lorberbaum JP, et al. Motor cortex brain activity induced by 1-Hz transcranial magnetic stimulation is similar in location and level to that for volitional movement. *Invest Radiol.* (2000) 35:676–83. doi: 10.1097/00004424-200011000-00005
56. Denslow S, Lomarev M, Bohning DE, Mu Q, George MS. A high resolution assessment of the repeatability of relative location and intensity of transcranial magnetic stimulation-induced and volitionally induced blood oxygen level-dependent response in the motor cortex. *Cogn Behav Neurol.* (2004) 17:163–73. doi: 10.1097/01.wnn.0000117864.42205.6d
57. Baudewig J, Siebner HR, Bestmann S, Tergau F, Tings T, Paulus W, et al. Functional MRI of cortical activations induced by transcranial magnetic stimulation (TMS). *Neuroreport.* (2001) 12:3543–8. doi: 10.1097/00001756-200111160-00034
58. Bestmann S, Baudewig J, Siebner HR, Rothwell JC, Frahm J. Subthreshold high-frequency TMS of human primary motor cortex modulates interconnected frontal motor areas as detected by interleaved fMRI-TMS. *Neuroimage.* (2003) 20:1685–96. doi: 10.1016/j.neuroimage.2003.07.028
59. Bestmann S, Baudewig J, Siebner HR, Rothwell JC, Frahm J. Functional MRI of the immediate impact of transcranial magnetic stimulation on cortical and subcortical motor circuits. *Eur J Neurosci.* (2004) 19:1950–62. doi: 10.1111/j.1460-9568.2004.03277.x
60. Kemna LJ, Gembris D. Repetitive transcranial magnetic stimulation induces different responses in different cortical areas: a functional magnetic resonance study in humans. *Neurosci Lett.* (2003) 336:85–8. doi: 10.1016/S0304-3940(02)01195-3
61. Denslow S, Lomarev M, George MS, Bohning DE. Cortical and subcortical brain effects of transcranial magnetic stimulation (TMS)-induced movement: an interleaved TMS/functional magnetic resonance imaging study. *Biol Psychiatry.* (2005) 57:752–60. doi: 10.1016/j.biopsych.2004.12.017
62. Hanakawa T, Mima T, Matsumoto R, Abe M, Inouchi M, Urayama S, et al. Stimulus-response profile during single-pulse transcranial magnetic stimulation to the primary motor cortex. *Cereb Cortex.* (2009) 19:2605–15. doi: 10.1093/cercor/bhp013
63. Bestmann S, Swayne O, Blankenburg F, Ruff CC, Haggard P, Weiskopf N, et al. Dorsal premotor cortex exerts state-dependent causal influences on activity in contralateral primary motor and dorsal premotor cortex. *Cereb Cortex.* (2008) 18:1281–91. doi: 10.1093/cercor/bhm159
64. Jung J, Bungert A, Bowtell R, Jackson SR. Modulating brain networks with transcranial magnetic stimulation over the primary motor cortex: a concurrent TMS/fMRI study. *Front Hum Neurosci.* (2020) 14:31. doi: 10.3389/fnhum.2020.00031
65. Fox P, Ingham R, George MS, Mayberg H, Ingham J, Roby J, et al. Imaging human intra-cerebral connectivity by PET during TMS. *Neuroreport.* (1997) 8:2787–91. doi: 10.1097/00001756-199708180-00027
66. Bestmann S, Baudewig J, Siebner HR, Rothwell JC, Frahm J. BOLD MRI responses to repetitive TMS over human dorsal premotor cortex. *Neuroimage.* (2005) 28:22–9. doi: 10.1016/j.neuroimage.2005.05.027
67. Hodkinson DJ, Bungert A, Bowtell RW, Jackson SR, Jung J. Operculo-insular and anterior cingulate plasticity induced by transcranial magnetic stimulation in the human motor cortex: a dynamic casual modelling study. *J Neurophysiol.* (2021) 125:1180–90. doi: 10.1152/jn.00670.2020
68. Nahas Z, Lomarev M, Roberts DR, Shastri A, Lorberbaum JP, Teneback C, et al. Unilateral left prefrontal transcranial magnetic stimulation (TMS) produces intensity-dependent bilateral effects as measured by interleaved BOLD fMRI. *Biol Psychiatry.* (2001) 50:712–20. doi: 10.1016/S0006-3223(01)01199-4
69. Barbey AK, Koenigs M, Grafman J. Dorsolateral prefrontal contributions to human working memory. *Cortex.* (2013) 49:1195–205. doi: 10.1016/j.cortex.2012.05.022
70. Curtis CE, D'Esposito M. Persistent activity in the prefrontal cortex during working memory. *Trends Cogn Sci.* (2003) 7:415–23. doi: 10.1016/S1364-6613(03)00197-9
71. Mull BR, Seyal M. Transcranial magnetic stimulation of left prefrontal cortex impairs working memory. *Clin Neurophysiol.* (2001) 112:1672–5. doi: 10.1016/S1388-2457(01)00606-X
72. Feredoes E, Heinen K, Weiskopf N, Ruff C, Driver J. Causal evidence for frontal involvement in memory target maintenance by posterior brain areas during distracter interference of visual working memory. *Proc Natl Acad Sci U S A.* (2011) 108:17510–5. doi: 10.1073/pnas.1106439108
73. Chao LL, Knight RT. Contribution of human prefrontal cortex to delay performance. *J Cogn Neurosci.* (1998) 10:167–77. doi: 10.1162/089892998562636
74. Clapp WC, Rubens MT, Gazzaley A. Mechanisms of working memory disruption by external interference. *Cereb Cortex.* (2010) 20:859–72. doi: 10.1093/cercor/bhp150
75. Postle BR. Delay-period activity in the prefrontal cortex: one function is sensory gating. *J Cogn Neurosci.* (2005) 17:1679–90. doi: 10.1162/089892905774589208
76. Hawco C, Armony JL, Daskalakis ZJ, Berlim MT, Chakravarty MM, Pike GB, et al. Differing time of onset of concurrent TMS-fMRI during associative memory encoding: a measure of dynamic connectivity. *Front Hum Neurosci.* (2017) 11:404. doi: 10.3389/fnhum.2017.00404
77. Oathes DJ, Zimmerman JP, Duprat R, Japp SS, Scully M, Rosenberg BM, et al. Resting fMRI-guided TMS results in subcortical and brain network modulation indexed by interleaved TMS/fMRI. *Exp Brain Res.* (2021) 239:1165–78. doi: 10.1007/s00221-021-06036-5
78. Seeley WW, Menon V, Schatzberg AF, Keller J, Glover GH, Kenna H, et al. Dissociable intrinsic connectivity networks for salience

processing and executive control. *J Neurosci.* (2007) 27:2349–56. doi: 10.1523/JNEUROSCI.5587-06.2007

79. Sridharan D, Levitin DJ, Menon V. A critical role for the right fronto-insular cortex in switching between central-executive and default-mode networks. *Proc Nat Acad Sci U S A.* (2008) 105:12569–74. doi: 10.1073/pnas.0800005105
80. Shulman GL, Fiez JA, Corbetta M, Buckner RL, Miezin FM, Raichle ME, et al. Common blood flow changes across visual tasks: II. Decreases in Cerebral Cortex. *J Cogn Neurosci.* (1997) 9:648–63. doi: 10.1162/jocn.1997.9.5.648
81. Hawco C, Voineskos AN, Steeves JKE, Dickie EW, Viviano JD, Downar J, et al. Spread of activity following TMS is related to intrinsic resting connectivity to the salience network: a concurrent TMS-fMRI study. *Cortex.* (2018) 108:160–72. doi: 10.1016/j.cortex.2018.07.010
82. Paus T. Location and function of the human frontal eye-field: a selective review. *Neuropsychologia.* (1996) 34:475–83. doi: 10.1016/0028-3932(95)00134-4
83. Heinen K, Feredoes E, Weiskopf N, Ruff CC, Driver J. Direct evidence for attention-dependent influences of the frontal eye-fields on feature-responsive visual cortex. *Cereb Cortex.* (2014) 24:2815–21. doi: 10.1093/cercor/bht157
84. Sack AT, Kohler A, Bestmann S, Linden DE, Dechent P, Goebel R, et al. Imaging the brain activity changes underlying impaired visuospatial judgments: simultaneous FMRI, TMS, behavioral studies. *Cereb Cortex.* (2007) 17:2841–52. doi: 10.1093/cercor/bhm013
85. Swisher JD, Halko MA, Merabet LB, McMains SA, Somers DC. Visual topography of human intraparietal sulcus. *J Neurosci.* (2007) 27:5326–37. doi: 10.1523/JNEUROSCI.0991-07.2007
86. Leitao J, Thielscher A, Tunnerhoff J, Noppeney U. Concurrent TMS-fMRI reveals interactions between dorsal and ventral attentional systems. *J Neurosci.* (2015) 35:11445–57. doi: 10.1523/JNEUROSCI.0939-15.2015
87. Leitao J, Thielscher A, Werner S, Pohmann R, Noppeney U. Effects of parietal TMS on visual and auditory processing at the primary cortical level – a concurrent TMS-fMRI study. *Cereb Cortex.* (2013) 23:873–84. doi: 10.1093/cercor/bhs078
88. Leitao J, Thielscher A, Lee H, Tuennerhoff J, Noppeney U. Transcranial magnetic stimulation of right inferior parietal cortex causally influences prefrontal activation for visual detection. *Eur J Neurosci.* (2017) 46:2807–16. doi: 10.1111/ejn.13743
89. Pisella L, Grea H, Tilikete C, Vighetto A, Desmurget M, Rode G, et al. An 'automatic pilot' for the hand in human posterior parietal cortex: toward reinterpreting optic ataxia. *Nat Neurosci.* (2000) 3:729–36. doi: 10.1038/76694
90. de Vries PM, de Jong BM, Bohning DE, Walker JA, George MS, Leenders KL. Changes in cerebral activations during movement execution and imagery after parietal cortex TMS interleaved with 3T MRI. *Brain Res.* (2009) 1285:58–68. doi: 10.1016/j.brainres.2009.06.006
91. de Jong BM, van der Graaf FHCE, Paans AMJ. Brain activation related to the representations of external space and body scheme in visuomotor control. *Neuroimage.* (2001) 14:1128–35. doi: 10.1006/nimg.2001.0911
92. Hermiller MS, Chen YF, Parrish TB, Voss JL. Evidence for immediate enhancement of hippocampal memory encoding by network-targeted theta-burst stimulation during concurrent fMRI. *J Neurosci.* (2020) 40:7155–68. doi: 10.1523/JNEUROSCI.0486-20.2020
93. Bagattini C, Mazzi C, Savazzi S. Waves of awareness for occipital and parietal phosphenes perception. *Neuropsychologia.* (2015) 70:114–25. doi: 10.1016/j.neuropsychologia.2015.02.021
94. Romei V, Brodbeck V, Michel C, Amedi A, Pascual-Leone A, Thut G. Spontaneous fluctuations in posterior α-band EEG activity reflect variability in excitability of human visual areas. *Cereb Cortex.* (2008) 18:2010–8. doi: 10.1093/cercor/bhm229
95. Taylor PCJ, Walsh V, Eimer M. The neural signature of phosphene perception. *Hum Brain Mapp.* (2010) 31:1408–17. doi: 10.1002/hbm.20941
96. de Graaf TA, van den Hurk J, Duecker F, Sack AT. Where are the fMRI correlates of phosphene perception? *Front Neurosci.* (2018) 12:883. doi: 10.3389/fnins.2018.00883
97. Meister IG, Weidemann J, Dambeck N, Foltys H, Sparing R, Krings T, et al. Neural correlates of phosphene perception. *Suppl Clin Neurophysiol.* (2003) 56:305–311. doi: 10.1016/S1567-424X(09)70234-X
98. Caparelli E, Backus W, Telang F, Wang G, Maloney T, Goldstein R, et al. Simultaneous TMS-fMRI of the visual cortex reveals functional network, even in absence of phosphene sensation. *Open Neuroimag J.* (2010) 4:100. doi: 10.2174/1874440001004010100
99. Li X, Nahas Z, Kozel FA, Anderson B, Bohning DE, George MS. Acute left prefrontal transcranial magnetic stimulation in depressed patients is associated with immediately increased activity in prefrontal cortical as well as subcortical regions. *Biol Psychiatry.* (2004) 55:882–90. doi: 10.1016/j.biopsych.2004.01.017
100. Eshel N, Keller CJ, Wu W, Jiang J, Mills-Finnerty C, Huemer J, et al. Global connectivity and local excitability changes underlie antidepressant effects of repetitive transcranial magnetic stimulation. *Neuropsychopharmacology.* (2020) 45:1018–25. doi: 10.1038/s41386-020-0633-z
101. Fonzo GA, Goodkind MS, Oathes DJ, Zaiko YV, Harvey M, Peng KK, et al. PTSD psychotherapy outcome predicted by brain activation during emotional reactivity and regulation. *Am J Psychiatry.* (2017) 174:1163–74. doi: 10.1176/appi.ajp.2017.16091072
102. Fonzo GA, Goodkind MS, Oathes DJ, Zaiko YV, Harvey M, Peng KK, et al. Selective effects of psychotherapy on frontopolar cortical function in PTSD. *Am J Psychiatry.* (2017) 174:1175–84. doi: 10.1176/appi.ajp.2017.16091073
103. Kearney-Ramos TE, Lench DH, Hoffman M, Correia B, Dowdle LT, Hanlon CA. Gray and white matter integrity influence TMS signal propagation: a multimodal evaluation in cocaine-dependent individuals. *Sci Rep.* (2018) 8:3253. doi: 10.1038/s41598-018-21634-0
104. Hanlon CA, Dowdle LT, Correia B, Mithoefer O, Kearney-Ramos T, Lench D, et al. Left frontal pole theta burst stimulation decreases orbitofrontal and insula activity in cocaine users and alcohol users. *Drug Alcohol Depend.* (2017) 178:310–17. doi: 10.1016/j.drugalcdep.2017.03.039
105. Guller Y, Ferrarelli F, Shackman AJ, Sarasso S, Peterson MJ, Langheim FJ, et al. Probing thalamic integrity in schizophrenia using concurrent transcranial magnetic stimulation and functional magnetic resonance imaging. *Arch Gen Psychiatry.* (2012) 69:662–71. doi: 10.1001/archgenpsychiatry.2012.23
106. Webler RD, Hamady C, Molnar C, Johnson K, Bonilha L, Anderson BS, et al. Decreased interhemispheric connectivity and increased cortical excitability in unmedicated schizophrenia: a prefrontal interleaved TMS fMRI study. *Brain Stimul.* (2020) 13:1467–75. doi: 10.1016/j.brs.2020.06.017
107. de Vries PM, de Jong BM, Bohning DE, Hinson VK, George MS, Leenders KL. Reduced parietal activation in cervical dystonia after parietal TMS interleaved with fMRI. *Clin Neurol Neurosurg.* (2012) 114:914–21. doi: 10.1016/j.clineuro.2012.02.006
108. Li X, Teneback CC, Nahas Z, Kozel FA, Large C, Cohn J, et al. Interleaved transcranial magnetic stimulation/functional MRI confirms that lamotrigine inhibits cortical excitability in healthy young men. *Neuropsychopharmacology.* (2004) 29:1395–407. doi: 10.1038/sj.npp.1300452
109. Tik M, Woletz M, Schuler A, Linhardt D, Princic M, Hummer A, et al. Multiband accelerated TMS/fMRI for continuous EPI during stimulation shows acute 10Hz TMS effects. In: *Annual Meeting of the Organization for Human Brain Mapping*, QC (2020).
110. Woletz M, Tik M, Prinčič M, Schuler A, Windischberger C. EPI-based target tracking in concurrent TMS-fMRI. *Brain Stimul.* (2019) 12:486. doi: 10.1016/j.brs.2018.12.589
111. Woletz M, Tik M, Pratapa N, Prinčič M, Schuler A, Windischberger C. Real-time neuronavigation feedback in concurrent TMS-fMRI. *Brain Stimul.* (2019) 12:574–5. doi: 10.1016/j.brs.2018.12.904
112. Leitao J, Thielscher A, Tuennerhoff J, Noppeney U. Comparing TMS perturbations to occipital and parietal cortices in concurrent TMS-fMRI studies-Methodological considerations. *PLoS One.* (2017) 12:e0181438. doi: 10.1371/journal.pone.0181438

113. Tik M, Woletz M, Princic M, Schuler A, Geissberger N, Hummer A, et al. Individualizing brainstimulation through concurrent TMS/fMRI. *Brain Stimul.* (2019) 12:425–7. doi: 10.1016/j.brs.2018.12.381
114. Bergmann TO, Varatheeswaran R, Hanlon CA, Madsen KH, Thielscher A, Siebner HR. Concurrent TMS-fMRI for causal network perturbation and proof of target engagement. *Neuroimage.* (2021) 237:118093. doi: 10.1016/j.neuroimage.2021.118093
115. Peters JC, Reithler J, de Graaf TA, Schuhmann T, Goebel R, Sack AT. Concurrent human TMS-EEG-fMRI enables monitoring of oscillatory brain state-dependent gating of cortico-subcortical network activity. *Commun Biol.* (2020) 3:1. doi: 10.1038/s42003-020-0764-0
116. Peters JC, Reithler J, Schuhmann T, de Graaf T, Uludag K, Goebel R, et al. On the feasibility of concurrent human TMS-EEG-fMRI measurements. *J Neurophysiol.* (2013) 109:1214–27. doi: 10.1152/jn.00071.2012

Conflict of Interest: FP was a member of the European Scientific Advisory Board of Brainsway Inc., Jerusalem, Israel and has received speaker's honoraria from MagandMore GmbH and the neuroCare Group. His lab has received support with equipment from neuroConn GmbH, Ilmenau, Germany, MagandMore GmbH, and Brainsway Inc., Jerusalem, Israel. YM-T was a half-time employee of neuroCare Group and this work is a part of her Ph.D. program at Munich Medical Research School.

The remaining authors declare that the research was conducted in the absence of any commercial or financial relationships that could be construed as a potential conflict of interest.

Publisher's Note: All claims expressed in this article are solely those of the authors and do not necessarily represent those of their affiliated organizations, or those of the publisher, the editors and the reviewers. Any product that may be evaluated in this article, or claim that may be made by its manufacturer, is not guaranteed or endorsed by the publisher.

Acknowledgements

I would like to express my deepest gratitude to everyone who has supported and contributed to the successful completion of this thesis.

First and foremost, I am profoundly thankful to my supervisors, Prof. Dr. Frank Padberg and Dr. Daniel Keeser, for their invaluable guidance, insightful discussions, and unwavering support throughout this project and beyond. Their encouragement and trust, which allowed me to explore various possibilities in my studies, have been crucial in shaping the direction and outcome of this research. I also extend my special thanks to Dr. Paul Taylor for being a member of my Ph.D. thesis advisory committee.

I am immensely grateful to Dr. Martin Tik for his collaboration and for sharing his extensive knowledge of concurrent TMS-fMRI setup and analysis. His pivotal role in assisting with the setup of the interleaved iTBS-fMRI sequence at our center was essential; without his expertise, this project would not have been successful.

Special thanks to Yuki Mizutani-Tiebel and Dr. Lucia Blulubas for their significant contributions to the MRstim project, particularly in the initial planning and data collection stages. Their meticulous work and dedication were essential to the smooth execution of the project.

I would also like to extend my heartfelt thanks to all the research assistants and master's students, including Linda Schuster, Cuici Voon, Zane Wilkinson, Larissa Behnke, and Timo van Hattem, for their assistance with data collection and setup testing. I thoroughly enjoyed working with them and deeply appreciated their company throughout this often lonely and seemingly endless Ph.D. journey.

I am also grateful to all the lab members in our team, including the medical students and research doctors, for making me feel like part of a big family in Munich. Special thanks to Dr. Ulrike Vogelmann, Dr. Mattia Campana, and Esther Dechantsreiter for their support from the clinical side.

Finally, I wish to thank my family and friends for their endless support, patience, and encouragement throughout this journey. Your belief in me has been a constant source of strength and motivation.

Thank you all for your invaluable contributions. This thesis would not have been possible without you.